A Combined Experimental and Computational Study to Decipher Complexity in the Asymmetric Hydrogenation of Imines with Ru Catalysts Bearing Atropisomerizable Ligands

Félix León,[a] Aleix Comas-Vives,[b] Eleuterio Álvarez,[a] and Antonio Pizzano[a,*]

[a]Instituto de Investigaciones Químicas and Centro de Innovación en Química Avanzada (ORFEO-CINQA), CSIC and Universidad de Sevilla, Avda Américo Vespucio 49, 41092 Sevilla, Spain.

[b]Department of Chemistry, Universitat Autònoma de Barcelona, 08193, Cerdanyola del Vallès, Catalonia, Spain.

SUPPLEMENTARY MATERIAL

General Experimental Procedures. Manipulations with air sensitive compounds were performed under an atmosphere of dry nitrogen either using standard Schlenk techniques or a glove-box. The reagents were obtained from commercial suppliers and used without further purification. Solvents were dried by standard methods and distilled under nitrogen before use. Imines **5** were prepared as described previously.[S1a] Complex **1d** and its enantiomer **1e** were prepared as described previously.[S1a] The C, H, N analyses were carried out with a LECO CHNS-TruSpec microanalyzer. NMR spectra were recorded on Bruker DPX-300, DRX-400, AV-400 or DRX-500 spectrometers. The values of chemical shifts are given in parts per million (ppm) and referenced to TMS or 85 % H_3PO_4 as standards. The values for coupling constants (*J*) are given in Hz. Assignment of some ^1H NMR spectra was aided by the use of 2D ^1H-^{13}C HSQC experiments. HPLC analyses were performed by using a Waters 2690 chromatograph, these analyses were performed at 303 K. HRMS data were obtained on a Thermo Scientific Q Exactive hybrid quadrupole-Orbitrap mass spectrometer in the General Services of Universidad de Sevilla (CITIUS). Optical rotations were measured on a PerkinElmer Model 341 polarimeter.

$Ru(Cl)_2$(**2a**)(**3a**) (**1a**). This complex was prepared before by reaction of Ru(2-Me-$C_3H_4)_2$(P-OP) with HCl and (*S,S*)-DPEN albeit in low yield (25 %).[S1b] Following the procedure described for **1f** it was obtained as a yellow solid in better yield (0.200 g, 60 %). For the sake of completeness spectroscopic data are also provided here,[S2] while a full characterization of its enantiomer **1b** is also provided below. ^1H NMR (CD_2Cl_2, 500 MHz): δ = 7.71 (m, 4H, Ar-H), 7.33 (m, 7H, H arom), 7.13 (m, 6H, H arom), 7.07 (m, 4H, H arom), 6.94 (m, 3H, H arom), 4.93 (m, 2H, PCH_2), 4.40 (dt, *J*(H-H) = 11.8, 4.5 Hz, 1H, NCH), 4.26 (dt, *J*(H-H) = 11.8, 4.3 Hz, 1H, NCH), 4.12 (m, 1H, N*H*H), 3.96 (m, 1H, N*H*H), 3.16 (m, 1H, N*H*H), 2.99 (m, 1H, N*H*H), 1.36 (s, 9H, $C(CH_3)_3$), 1.30 (s, 9H,

$C(CH_3)_3$), 1.12 (s, 9H, $C(CH_3)_3$), 1.07 (s, 9H, $C(CH_3)_3$); $^{31}P\{^1H\}$ NMR (CD_2Cl_2, 162 MHz): δ = 172.7 (d, *J*(P-P) = 47 Hz, P-O), 70.4 (d, *J*(P-P) = 47 Hz, P-C).

$Ru(Cl)_2$(**2a**)(**3b**) (**1b**). Obtained as a yellow solid following the procedure described for **1f** (0.220 g, 65 %). ^1H NMR (CD_2Cl_2, 400 MHz): δ = 7.76 (m, 4H, Ar-H), 7.38 (m, 8H, H arom), 7.16 (m, 7H, H arom), 7.12 (m, 3H, H arom), 6.99 (m, 2H, H arom), 4.97 (m, 2H, PCH_2), 4.45 (dt, *J*(H-H) = 11.7, 4.3 Hz, 1H, NCH), 4.31 (dt, *J*(H-H) = 11.7, 4.5 Hz, 1H, NCH), 4.18 (m, 1H, N*H*H), 4.00 (m, 1H, N*H*H), 3.22 (m, 1H, N*H*H), 3.04 (m, 1H, N*H*H), 1.42 (s, 9H, $C(CH_3)_3$), 1.35 (s, 9H, $C(CH_3)_3$), 1.17 (s, 9H, $C(CH_3)_3$), 1.12 (s, 9H, $C(CH_3)_3$); $^{31}P\{^1H\}$ NMR (CD_2Cl_2, 162 MHz): δ = 172.7 (d, *J*(P-P) = 47 Hz, P-O), 70.4 (d, *J*(P-P) = 47 Hz, P-C); $^{13}C\{^1H\}$ NMR (CD_2Cl_2, 100 MHz): δ = 146.4 (C_q arom), 146.1 (C_q arom), 140.0 (2 C_q arom), 139.7 (2 C_q arom), 134.5 (d, *J*(C-P) = 40 Hz, C_q arom), 134.3 (d, *J*(C-P) = 40 Hz, C_q arom), 133.2 (d, *J*(C-P) = 9 Hz, 2 CH arom), 133.1 (d, *J*(C-P) = 9 Hz, 2 CH arom), 131.3 (C_q arom), 130.7 (C_q arom), 129.8 (2 C_q arom), 128.9 (CH arom), 128.8 (CH arom), 128.2 (2 CH arom), 128.1 (2 CH arom), 128.0 (2 CH arom), 127.4 (2 CH arom), 127.3 (2 CH arom), 127.2 (2 CH arom), 126.9 (2 CH arom), 125.7 (2 CH arom), 125.5 (2 CH arom). Elem. Anal. (%): C 63.50 %, H 6.85 %, N 2.84 (calcd for $C_{55}H_{68}Cl_2N_2O_3P_2Ru$: C 63.58, H 6.60, N 2.70).

$Ru(Cl)_2$(**2b**)(**3b**) (**1c**). Obtained as a yellow solid following the procedure described for **1f** (0.062 g, 56 %). ^1H NMR (CD_2Cl_2, 400 MHz): δ = 7.68 (m, 4H, Ar-H), 7.36 (m, 6H, Ar-H), 7.18 (m, 8H, Ar-H), 6.98 (m, 2H, Ar-H), 6.88 (d, *J*(H-H) = 3.2 Hz, 1H, Ar-H), 6.86 (d, *J*(H-H) = 3.2 Hz, 1H, Ar-H), 6.62 (d, *J*(H-H) = 3.5 Hz, 1H, Ar-H), 6.58 (d, *J*(H-H) = 3.5 Hz, 1H, Ar-H), 4.89 (m, 2H, CH_2), 4.46 (dt, *J*(H-H) = 11.8, 4.5 Hz, 1H, NCH), 4.28 (m, 1H, NCH), 4.22 (m, 1H, NH*H*), 3.98 (dt, *J*(H-H) = 11.8, 4.8 Hz, 1H, NCH), 3.52 (s, 3H, OCH_3), 3.41 (s, 3H, OCH_3), 3.06 (brm, 2H, NH*H*), 1.36 (s, 9H, $C(CH_3)_3$), 1.32 (s, 9H, $C(CH_3)_3$); $^{31}P\{^1H\}$ NMR (CD_2Cl_2, 162 MHz): δ = 170.0 (d, *J*(P-

P) = 48 Hz, P-O), 70.0 (d, *J*(P-P) = 48 Hz, P-C); $^{13}C\{^{1}H\}$ NMR (CD_2Cl_2, 100 MHz): δ = 155.5 (C_q arom), 155.1 (C_q arom), 142.8 (d, *J*(C-P) = 10 Hz, C_q arom), 142.4 (C_q arom), 142.4 (d, *J*(C-P) = 10 Hz, C_q arom), 142.0 (d, *J*(C-P) = 4 Hz, C_q arom), 139.9 (d, *J*(C-P) = 4 Hz, C_q arom), 139.5 (d, *J*(C-P) = 4 Hz, C_q arom), 134.3 (d, *J*(C-P) = 6 Hz, C_q arom), 133.9 (d, *J*(C-P) = 6 Hz, C_q arom), 132.7 (d, *J*(C-P) = 9 Hz, 2 CH arom), 132.5 (d, *J*(C-P) = 9 Hz, 2 CH arom), 131.7 (d, *J*(C-P) = 2 Hz, C_q arom), 131.0 (d, *J*(C-P) = 3 Hz, C_q arom), 129.8 (d, *J*(C-P) = 2 Hz, CH arom), 129.7 (d, *J*(C-P) = 2 Hz, CH arom), 128.8 (2 CH arom), 128.8 (2 CH arom), 128.1 (d, *J*(C-P) = 10 Hz, 2 CH arom), 128.1 (CH arom), 128.0 (d, *J*(C-P) = 10 Hz, 2 CH arom), 128.0 (CH arom), 127.4 (2 CH arom), 127.1 (2 CH arom), 115.3 (CH arom), 114.9 (CH arom), 113.5 (CH arom), 112.8 (CH arom), 67.9 (dd, *J*(C-P) = 33, 14 Hz, OCH_2), 62.4 (2 NCH), 55.4 (OCH_3), 55.3 (OCH_3), 36.5 ($C(CH_3)_3$), 36.1 ($C(CH_3)_3$), 31.4 ($C(CH_3)_3$), 31.0 ($C(CH_3)_3$). Elem. Anal. (%): C 59.75 %, H 6.02 %, N 2.45 (calcd for $C_{49}H_{56}Cl_2N_2O_5P_2Ru$: C 59.63, H 5.72, N 2.84).

$Ru(Cl)_2$(**2d**)(**3b**) (**1f**). Over a solution of $RuCl_2(PPh_3)_3$ (0.288 g, 0.297 mmol) in DCM (10 mL) was added dropwise a solution of phosphine-phosphite ligand **2d** (0.239 g, 0.360 mmol) in DCM (4 mL). The mixture was stirred for 16 h and then a solution of diamine **3b** (0.073 g, 0.30 mmol) in DCM (3 mL) was added and the resulting mixture stirred for 2 h. After this time the reaction was evaporated under reduced pressure and the resulting solid prepurified through a short pad of sílica first using a Et_2O/*n*-hexane (1:99) mixture to remove PPh_3 and then with Et_2O toe lute the complex. The solution obtained was evaporated and the solid purify by column chromatography on sílica using an Et_2O/*n*-hexane (30:70) mixture, yielding **1f** as a yellow solid (0.240 g, 76%). ^{1}H NMR (CD_2Cl_2, 400 MHz): δ = 7.76 (t, *J*(H-H) = 8.5 Hz, 2H, Ar-H), 7.68 (t, *J*(H-H) = 8.5 Hz, 2H, Ar-H), 7.47 (t, *J*(H-H) = 7.8 Hz, 2H, Ar-H), 7.39 (m, 5H, Ar-H), 7.16 (m, 8H, Ar-H), 7.01 (m, 2H, Ar-H), 6.94 (m, 2H, Ar-H), 6.85 (ddd, *J*(H-P) = 9.3, *J*(H-H) = 7.7, 1.6 Hz, 1H, Ar-

H), 6.79 (d, *J*(H-H) = 2.1 Hz, 1H, Ar-H), 6.78 (d, *J*(H-H) = 2.1 Hz, 1H, Ar-H), 6.61 (m, 2H, Ar-H), 4.35 (dt, *J*(H-H) = 11.8, 4.5 Hz, 1H, NCH), 4.18 (dt, *J*(H-H) = 11.8, 4.6 Hz, 1H, NCH), 3.68 (brm, 1H, NH*H*), 3.46 (m, 1H, N*H*H), 3.45 (s, 3H, OCH_3), 3.44 (s, 3H, OCH_3), 2.98 (dt, *J*(H-H) = 11.8, 3.2 Hz, 1H, NH*H*), 2.81 (m, 1H, N*H*H), 1.20 (s, 9H, $C(CH_3)_3$, 1.19 (s, 9H, $C(CH_3)_3$); $^{31}P\{^1H\}$ NMR (CD_2Cl_2, 162 MHz): δ = 147.4 (d, *J*(P-P) = 72 Hz, P-O), 39.7 (d, *J*(P-P) = 73 Hz, P-C); $^{13}C\{^1H\}$ NMR (CD_2Cl_2, 100 MHz): δ = 155.8 (2 C_q arom), 155.6 (d, *J*(C-P) = 10 Hz, 2 C_q arom), 142.5 (dd, *J*(C-P) = 10, 4 Hz, C_q arom),, 140.2 (d, *J*(C-P) = 3 Hz, C_q arom), 140.0 (d, *J*(C-P) = 2 Hz, C_q arom), 134.7 (d, *J*(C-P) = 10 Hz, 2 CH arom), 134.5 (d, *J*(C-P) = 10 Hz, 2 CH arom), 133.1 (d, *J*(C-P) = 15 Hz, C_q arom), 132.7 (d, *J*(C-P) = 15 Hz, C_q arom), 132.7 (C_q arom), 132.3 (C_q arom),130.5 (d, *J*(C-P) = 3 Hz, CH arom), 130.4 (d, *J*(C-P) = 3 Hz, CH arom), 129.2 (CH arom), 129.2 (d, *J*(C-P) = 9 Hz, 4 CH arom), 128.8 (CH arom), 128.7 (2 CH arom), 128.6 (2 CH arom), 128.5 (CH arom), 128.4 (CH arom), 128.3 (2 Cq arom), 127.4 (4 CH arom), 125.4 (d, *J*(C-P) = 50 Hz, C_q arom), 123.6 (d, *J*(C-P) = 7 Hz, CH arom), 121.8 (CH arom), 115.7 (CH arom), 115.3 (CH arom), 114.3 (CH arom), 114.1 (CH arom), 63.7 (NCH), 62.2 (NCH), 55.8 (2 OCH_3), 36.6 (2 *C*$(CH_3)_3$), 31.6 (2 (C(*C*$H_3)_3$). Elem. Anal. (%):C 61.77, H 5.83, N 2.61 (calcd for $C_{54}H_{58}Cl_2N_2O_5P_2Ru$: C 61.83, H 5.57, N 2.67).

$Ru(Cl)_2$(**2e**)(**3a**) (**1g**). Obtained as a yellow solid as described for **1f** (0.105 g, 68 %). ^1H NMR ($CDCl_3$, 400 MHz): δ = 8.07 (t, *J*(H-H) = 8.4 Hz, 2H, Ar-H), 7.58 (t, *J*(H-H) = 8.4 Hz, 2H, Ar-H), 7.42 (m, 4H, Ar-H), 7.28 (m, 4H, Ar-H), 7.22 (d, 1H, *J*(H-H) = 2.5 Hz, Ar-H), 7.10 (d, *J*(H-H) = 2.5 Hz, 1H, Ar-H), 7.05 (m, 3H, Ar-H), 6.99 (m, 2H, Ar-H), 6.88 (d, *J*(H-H) = 2.5 Hz, 1H, Ar-H), 6.81 (m, 2H, Ar-H), 6.67 (m, 2H, Ar-H), 4.30 (m, 2H, OCH_2), 4.05 (m, 2H, 2NCH), 3.61 (m, 1H, CHP), 3.47 (m, 1H, N*H*H), 3.27 (m, 1H, NH*H*), 3.11 (m, 1H, N*H*H), 2.65 (m, 1H, NH*H*), 1.63 (s, 9H, $C(CH_3)_3$), 1.53 (s, 9H, $C(CH_3)_3$), 1.27 (s, 9H, $C(CH_3)_3$), 1.02 (dd, *J*(H-P) = 11.0 Hz, *J*(H-H) = 7.3 Hz, 3H,

CH_3), 0.94 (s, 9H, $C(CH_3)_3$); $^{31}P\{^1H\}$ NMR ($CDCl_3$, 162 MHz): δ = 147.7 (d, *J*(P-P) = 66 Hz, P-O), 50.4 (d, *J*(P-P) = 66 Hz, P-C); $^{13}C\{^1H\}$ NMR ($CDCl_3$, 100 MHz): δ =148.0 (d, *J*(C-P) = 16 Hz, C_q arom), 146.6 (C_q arom), 145.2 (C_q arom), 145.0 (d, *J*(C-P) = 3 Hz, C_q arom), 139.7 (C_q arom), 139.6 (d, *J*(C-P) = 3 Hz, C_q arom), 139.4 (C_q arom), 137.4 (d, *J*(C-P)= 10 Hz, 2 CH arom), 133.4 (d, *J*(C-P) = 24 Hz, C_q arom), 133.1 (d, *J*(C-P) = 15 Hz, C_q arom), 133.0 (d, *J*(C-P) = 8 Hz, 2 CH arom), 131.3 (C_q arom), 130.5 (C_q arom), 129.7 (C_q arom), 129.3 (C_q arom), 129.1 (CH arom), 128.9 (2 CH arom), 128.5 (2 CH arom), 128.4 (CH arom), 128.2 (CH arom), 127.8 (CH arom), 127.7, (d, *J*(C-P) = 9 Hz, 2 CH arom), 127.5 (d, *J*(C-P) = 9 Hz, 2 CH arom), 127.1 (2 CH arom), 126.7 (2 CH arom), 126.5 (CH arom), 126.4 (CH arom), 124.5 (CH arom), 69.0 (CH_2O), 64.2 (NCH), 62.1 (NCH), 37.2 ($C(CH_3)_3$), 36.0 ($C(CH_3)_3$), 34.5 ($C(CH_3)_3$), 34.1 ($C(CH_3)_3$), 32.9 ($C(CH_3)_3$), 31.5 ($C(CH_3)_3$), 31.5 ($C(CH_3)_3$), 31.2 ($C(CH_3)_3$), 29.5 (d, *J*(C-P) = 31 Hz, P*C*H(CH_3)), 14.1 (d, *J*(C-P) = 6 Hz, PCH(*C*H_3)). Elem. Anal. (%): C 64.31, H 6.99, N 2.36 (calcd for $C_{57}H_{72}Cl_2N_2O_3P_2Ru$: C 64.16, H 6.80, N 2.63).

$Ru(Cl)_2$(**2e**)(**3b**) (**1h**). Obtained as a yellow solid as described for **1f** (0.098 g, 65 %). ^1H NMR ($CDCl_3$, 400 MHz): δ = 8.09 (t, *J*(H-H) = 8.4 Hz, 2H, Ar-H), 7.61 (t, *J*(H-H) = 8.4 Hz, 2H, Ar-H), 7.46 (m, 4H, Ar-H), 7.32 (m, 4H, Ar-H), 7.22 (d, *J*(H-H) = 3.0 Hz, 1H, Ar-H), 7.13 (d, *J*(H-H) = 3.0 Hz, 1H, Ar-H), 7.09 (m, 3H, Ar-H), 7.01 (m, 2H, Ar-H), 6.90 (d, *J*(H-H) = 3.0 Hz, 1H, Ar-H), 6.83 (m, 2H, Ar-H), 6.69 (m, 2H, Ar-H), 4.30 (m, 2H, OCH_2), 4.08 (m, 2H, 2NCH), 3.63 (m, 1H, CHP), 3.49 (m, 1H, N*H*H), 3.29 (m, 1H, NH*H*), 3.16 (m, 1H, N*H*H), 2.65 (m, 1H, NH*H*), 1.66 (s, 9H, $C(CH_3)_3$), 1.56 (s, 9H, $C(CH_3)_3$), 1.30 (s, 9H, $C(CH_3)_3$), 1.02 (m, 3H, CH_3), 0.97 (s, 9H, $C(CH_3)_3$); $^{31}P\{^1H\}$ NMR ($CDCl_3$, 162 MHz): δ = 147.7 (d, *J*(P-P) = 66 Hz, P-O), 50.4 (d, *J*(P-P) = 66 Hz, P-C); $^{13}C\{^1H\}$ NMR ($CDCl_3$, 100 MHz): δ = 147.9 (d, *J*(C-P) = 15 Hz, C_q arom), 146.6 (C_q arom), 145.1 (C_q arom), 144.9 (d, *J*(C-P) = 3 Hz, C_q arom), 139.6 (C_q arom), 139.5 (d,

J(C-P) = 3 Hz, C_q arom), 139.3 (C_q arom), 137.3 (d, *J*(C-P) = 10 Hz, 2 CH arom), 133.3 (d, *J*(C-P) = 25 Hz, C_q arom), 133.1 (d, *J*(C-P) = 14 Hz, C_q arom), 133.0 (d, *J*(C-P) = 7 Hz, 2 CH arom), 131.1 (C_q arom), 130.4 (CH arom), 129.6 (C_q arom), 129.2 (C_q arom), 129.1 (CH arom), 128.9 (2 CH arom), 128.5 (2 CH arom), 128.3 (CH arom), 128.1 (CH arom), 127.7 (CH arom), 127.6, (d, *J*(C-P) = 9 Hz, 2 CH arom), 127.3 (d, *J*(C-P) = 9 Hz, 2 CH arom), 127.0 (2 CH arom), 126.7 (2 CH arom), 126.4 (CH arom), 126.3 (CH arom), 124.4 (CH arom), 68.9 (CH_2O), 64.1 (NCH), 62.0 (NCH), 37.0 ($C(CH_3)_3$), 35.9 ($C(CH_3)_3$), 34.4 ($C(CH_3)_3$), 34.0 ($C(CH_3)_3$), 32.8 ($C(CH_3)_3$), 31.4 ($C(CH_3)_3$), 31.3 ($C(CH_3)_3$), 31.0 ($C(CH_3)_3$), 29.4 (d, *J*(C-P) = 30 Hz, $PCH(CH_3)$), 14.0 (d, *J*(C-P)= 6 Hz, $PCH(CH_3)$). Elem. Anal. (%): C 64.35, H 7.03, N 2.32 (calcd for $C_{57}H_{72}Cl_2N_2O_3P_2Ru$: C 64.16, H 6.80, N 2.63).

$Ru(Cl)_2$(**2c**)(**3c**) (**1i**). Obtained as a yellow solid as described for **1j** (0.200 g, 72 %). ^{1}H NMR (CD_2Cl_2, 400 MHz): δ = 7.78 (t, *J*(H-H) = 8.5 Hz, 2H, Ar-H), 7.70 (t, *J*(H-H) = 8.5 Hz, 2H, Ar-H), 7.48 (t, *J*(H-H) = 7.8 Hz, 1H, Ar-H), 7.38 (m, 6H, Ar-H), 7.30 (d, *J*(H-H) = 2.1 Hz, 2H, Ar-H), 7.18 (dd, *J*(H-H) = 7.9 Hz, *J*(H-P) = 4.8 Hz, 1H, Ar-H), 7.11 (m, 3H, Ar-H), 6.87 (m, 9H, Ar-H), 4.28 (dt, *J*(H-H) = 11.7, 4.3 Hz, 1H, NCH), 4.16 (dt, *J*(H-H) = 11.7, 4.5 Hz, 1H, NCH), 3.68 (brm, 1H, NH*H*), 3.43 (brm, 1H, N*H*H), 3.01 (brt, *J*(H-H) = 11.7 Hz, 1H, NH*H*), 2.80 (m, 1H, N*H*H), 1.23 (s, 9H, $C(CH_3)_3$), 1.22 (s, 9H, $C(CH_3)_3$), 1.11 (s, 9H, $C(CH_3)_3$), 1.10 (s, 9H, $C(CH_3)_3$); ^{31}P{^{1}H} NMR (CD_2Cl_2, 162 MHz): δ = 146.8 (d, *J*(P-P) = 72 Hz, P-O), 39.5 (d, *J*(P-P) = 73 Hz, P-C); ^{13}C{^{1}H} NMR (CD_2Cl_2, 100 MHz): δ = 162.4 (d, *J*(C-F) = 246 Hz, C_q arom), 162.1 (d, *J*(C-F) = 246 Hz, C_q arom), 155.2 (d, *J*(C-P) = 10 Hz, C_q arom), 146.4 (2 C_q arom), 145.9 (C_q arom), 145.8 (C_q arom), 139.7 (2 C_q arom), 135.5 (2 C_q arom), 134.4 (d, *J*(C-P) = 10 Hz, 2 CH arom), 134.1 (d, *J*(C-P) = 10 Hz, 2 CH arom), 132.8 (d, *J*(C-P) = 15 Hz, C_q arom), 132.3 (d, *J*(C-P) = 12 Hz, C_q arom), 132.3 (CH arom), 131.9 (CH arom), 131.4 (CH arom), 131.2 (CH

arom), 130.1 (d, *J*(C-P) = 9 Hz, 2 CH arom), 128.8 (d, *J*(C-F) = 22 Hz, 2 CH arom), 128.8 (d, *J*(C-F) = 22 Hz, 2 CH arom), 128.4 (d, *J*(C-P) = 9 Hz, 2 CH arom) 128.2 (d, *J*(C-P) = 9 Hz, 2 CH arom), 127.3 (2 CH arom), 125.7 (2 C_q arom), 124.3 (dd, *J*(C-P) = 55, 5Hz, C_q arom), 123.2 (d, *J*(C-P) = 6 Hz, CH arom), 121.5 (CH arom), 116.0 (CH arom), 115.8 (CH arom), 115.7 (CH arom), 115.5 (CH arom), 63.0 (NCH), 61.7 (NCH), 36.2 ($C(CH_3)_3$), 36.1 ($C(CH_3)_3$), 34.1 (2 $C(CH_3)_3$), 31.5 ($C(CH_3)_3$), 31.4 ($C(CH_3)_3$), 30.9 (2 ($C(CH_3)_3$); $^{19}F\{^1H\}$ NMR ($CDCl_3$, 380 MHz): δ = -114.3, -114.4. Elem. Anal. (%): C 63.03, H 6.14, N 2.31 (calcd for $C_{60}H_{68}Cl_2F_2N_2O_3P_2Ru$: C 63.38, H 6.03, N 2.46).

Ru(Cl)$_2$(**2c**)(**3d**) (**1j**). Over a solution of $RuCl_2(PPh_3)_3$ (0.122 g, 0.126 mmol) in DCM (5 mL) was added dropwise a solution of **2c** (0.100 g, 0.14 mmol) in DCM (2 mL). The mixture was stirred for 16 h after which a suspensión of the dihydrochloride of diamine **3d** (0.023 g, 0.084 mmol) in DCM (2 mL) and NEt_3 (0.043 mL, 0.336 mmol) were added. The resulting mixture was stirred for 2 h and evaporated under reduced pressure to give a yellow residue which was dissolved in a Et_2O/*n*-hexane (1:99) mixture, passed through a short pad of sílica to remove PPh_3 and the compound finally eluted with Et_2O. The solution obtained was evaporated and the residue purified by column chromatography on sílica using a Et_2O/*n*-hexane (20:80) mixture as eluent. Complex **1j** was finally obtained as a yellow solid (0.095 g, 65%). ^1H NMR (CD_2Cl_2, 400 MHz): δ = 8.07 (t, *J*(H-H) = 8.5 Hz, 2H, Ar-H), 7.99 (t, *J*(H-H) = 8.5 Hz, 2H, Ar-H), 7.77 (t, *J*(H-H) = 7.7 Hz, 1H, Ar-H), 7.66 (m, 6H, Ar-H), 7.58 (brs, 2H, Ar-H), 7.47 (dd, *J*(H-H) = 7.7 Hz, *J*(H-P) = 4.5 Hz, 1H, Ar-H), 7.39 (m, 3H, Ar-H), 7.19 (m, 3H, Ar-H), 7.13 (d, *J*(H-H) = 8.5 Hz, 2H, Ar-H), 6.95 (t, *J*(H-H) = 8.8 Hz, 4H, Ar-H), 4.54 (dt, *J*(H-H) = 11.9, 4.6 Hz, 1H, NCH), 4.41 (dt, *J*(H-H) = 11.9, 4.5 Hz, 1H, NCH), 4.00 (s, 3H, OCH_3), 3.96 (s, 3H, OCH_3), 3.90 (m, 1H, NH*H*), 3.68 (brm, 1H, N*H*H), 3.23 (brt, *J*(H-H) = 10.8 Hz 1H, NH*H*), 3.07 (m, 1H, N*H*H), 1.51 (s, 18H, $C(CH_3)_3$, 1.39 (s, 18H, $C(CH_3)_3$); $^{31}P\{^1H\}$ NMR

(CD_2Cl_2, 162 MHz): δ = 146.6 (d, *J*(P-P) = 72 Hz, P-O), 39.3 (d, *J*(P-P) = 72 Hz, P-C); $^{13}C\{^1H\}$ NMR (CD_2Cl_2, 100 MHz): δ = 159.4 (C_q arom), 159.0 (C_q arom), 155.2 (d, *J*(C-P) = 10 Hz, C_q arom), 146.3 (d, *J*(C-P) = 4 Hz, C_q arom), 145.9 (d, *J*(C-P) = 7 Hz C_q arom), 139.6 (2 C_q arom), 134.4 (d, *J*(C-P) = 10 Hz, 2 CH arom), 134.1 (d, *J*(C-P) = 10 Hz, 2 CH arom), 132.9 (d, *J*(C-P) = 15 Hz, C_q arom), 132.5 (d, *J*(C-P) = 15 Hz, C_q arom), 132.3 (CH arom), 132.0 (d, *J*(C-P) = 7 Hz, 2 CH arom), 131.8 (CH arom), 131.3 (C_q arom), 131.3 (C_q arom), 130.1 (d, *J*(C-P) = 11 Hz, 2 CH arom), 128.3 (CH arom), 128.2 (4 CH arom), 128.1 (CH arom), 128.0 (4 CH arom), 127.3 (C_q arom), 127.3 (C_q arom), 125.7 (2 C_q arom), 124.4 (d, *J*(C-P) = 55 Hz, C_q arom), 123.1 (d, *J*(C-P) = 6 Hz, CH arom), 121.4 (CH arom), 114.2 (2 CH arom), 114.0 (2 CH arom), 62.9 (NCH), 61.5 (NCH), 55.1 (OCH_3), 55.0 (OCH_3), 36.1 (2 *C*$(CH_3)_3$), 34.1 (2 *C*$(CH_3)_3$), 31.4 (2 C(*C*$H_3)_3$), 30.9 (2 C(*C*$H_3)_3$). Elem. Anal. (%): C 64.31, H 6.56, N 2.16 (calcd for $C_{62}H_{74}Cl_2N_2O_5P_2Ru$: C 64.13, H 6.42, N 2.41).

Ru(Cl)$_2$(**2c**)(**4**) (**1k**). Obtained as described for **1f** as a yellow solid (0.095 g, 71 %). ^1H NMR (CD_2Cl_2, 400 MHz): δ = 7.90 (t, *J*(H-H) = 8.5 Hz, 2H, Ar-H), 7.75 (t, *J*(H-H) = 8.5 Hz, 2H, Ar-H), 7.42 (m, 9H, Ar-H), 7.22 (d, *J*(H-H) = 2.5 Hz, 1H, Ar-H), 7.19 (m, 1H, Ar-H), 7.14 (m, 2H, Ar-H), 7.10 (d, *J*(H-H) = 2.5 Hz, 1H, Ar-H), 2.76 (m, 3H, 2 NCH+N*H*H), 2.60 (brm, 2H, N*H*H), 2.45 (brm, 1H, NH*H*), 1.70 (m, 2H, C*H*(CH3)$_2$) 1.38 (s, 9H, C$(CH_3)_3$), 1.34 (s, 9H, C$(CH_3)_3$), 1.30 (s, 9H, C$(CH_3)_3$), 1.17 (s, 9H, C$(CH_3)_3$), 0.79 (d, *J*(H-H) = 7.0 Hz, 3H, CH(C*H*$_3)_2$), 0.64 (d, *J*(H-H) = 7.0 Hz, 3H, CH(C*H*$_3)_2$), 0.62 (d, *J*(H-H) = 7.0 Hz, 3H, CH(C*H*$_3)_2$), 0.61 (d, *J*(H-H) = 7.0 Hz, 3H, CH(C*H*$_3)_2$); $^{31}P\{^1H\}$ NMR (CD_2Cl_2, 162 MHz): δ = 144.8 (d, *J*(P-P) = 72 Hz, P-O), 38.9 (d, *J*(P-P) = 72 Hz, P-C); $^{13}C\{^1H\}$ NMR (CD_2Cl_2, 100 MHz): δ 155.7 (d, *J*(C-P) = 10 Hz, C_q arom), 146.8 (d, *J*(C-P) = 12 Hz, C_q arom), 145.8 (d, *J*(C-P) = 9 Hz, C_q arom), 145.6 (C_q arom), 145.4 (C_q arom), 140.0 (d, *J*(C-P) = 3 Hz, C_q arom), 139.4 (d, *J*(C-P) = 3 Hz, C_q arom), 134.7

(d, *J*(C-P) = 10 Hz, 2 CH arom), 133.8 (d, *J*(C-P) = 10 Hz, 2 CH arom), 133.6 (d, *J*(C-P) = 4 Hz, C_q arom), 133.2 (d, *J*(C-P) = 3 Hz, C_q arom), 132.4 (d, *J*(C-P) = 3 Hz, CH arom), 132.3 (CH arom), 131.9 (CH arom), 131.4 (d, *J*(C-P) = 3 Hz, CH arom), 129.9 (d, *J*(C-P) = 2 Hz, C_q arom), 129.7 (d, *J*(C-P) = 2 Hz, C_q arom), 128.2 (d, *J*(C-P) = 10 Hz, 2 CH arom), 128.0 (d, *J*(C-P) = 10 Hz, 2 CH arom), 127.7 (CH arom), 127.5 (CH arom), 126.0 (CH arom), 125.3 (CH arom), 123.1 (dd, *J*(C-P) = 56, 5 Hz, C_q arom) 122.9 (d, *J*(C-P) = 7 Hz, CH arom), 121.8 (t, *J*(C-P) = 4 Hz, CH arom), 59.9 (NCH), 57.8 (NCH), 36.5 (*C*$(CH_3)_3$), 35.8 (*C*$(CH_3)_3$), 34.6 (*C*$(CH_3)_3$), 34.5 (*C*$(CH_3)_3$), 32.1 (C(*C*$H_3)_3$), 31.5 (2 C(*C*$H_3)_3$), 31.3 (C(*C*$H_3)_3$), 27.3 (*C*H(CH_3)), 26.9 (*C*H(CH_3)), 20.9 (CH(*C*H_3)), 19.9 (CH(*C*H_3)), 13.8 (CH(*C*H_3)), 13.5 (CH(*C*H_3). Elem. Anal. (%): C 63.02, H 7.36, N 2.41 (calcd for $C_{54}H_{74}Cl_2N_2O_3P_2Ru$: C 62.78, H 7.22, N 2.71).

Isomerization of 1a. A sample of **1a** (0.068 g, 0.062 mmol) was added EtOH (0.6 mL) and the mixture heated at 60 ºC for 18 h. After this time, conversion over 95 % was observed by $^{31}P\{^1H\}$ NMR. The solution was evaporated under reduced pressure, extracted in a Et_2O:*n*-hexane (1:2) mixture and the mixture passed through a short pad of silica. Evaporation of the solution obtained yielded a mixture of *cis*-**1a** and *cis*-**1a'** in a 2.5:1 ratio as a very pale yellow solid (0.057 g, 84 %). *cis*-**1a**: ^1H NMR ($CDCl_3$, 400 MHz): δ = 8.23 (brm, 2H, H arom), 7.71 (t, *J*(H-H) = 7.7 Hz, 2H, H arom), 7.59 (brm, 1H, H arom), 7.51 (brm, 1H, H arom), 7.41 (brm, 3H, H arom), 7.33 (brm, 3H, H arom), 7.28 (brm, 2H, H arom), 7.09 (brm, 3H, H arom), 7.00 (t, *J*(H-H) = 7.1 Hz, 1H, H arom), 6.83 (brm, 4H, H arom), 6.34 (d, *J*(H-H) = 7.3 Hz, 2H, H arom), 5.31 (dt, *J*(H-P) = 37.2, 9.5 Hz, *J*(H-H) = 11.9 Hz, 1H, PC*H*H), 4.35 (m, 2H, PC*H*H and NCH), 4.19 (brm, 1H, N*H*H), 3.64 (brm, 1H, NCH), 2.52 (brm, 2H, 2 N*H*H), 2.03 (brm, 1H, N*H*H), 1.51 (s, 9H, C$(CH_3)_3$, 1.43 (s, 9H, C$(CH_3)_3$, 1.39 (s, 9H, C$(CH_3)_3$, 0.96 (s, 9H, C$(CH_3)_3$; $^{31}P\{^1H\}$ NMR ($CDCl_3$, 162 MHz): δ = 169.3 (d, *J*(P-P) = 44 Hz, P-O), 75.3 (d, *J*(P-P) = 44 Hz, P-C);

$^{13}C\{^1H\}$ NMR ($CDCl_3$, 100 MHz): δ = 147.4 (C_q arom), 146.2 (C_q arom), 145.0 (C_q arom), 142.2 (C_q arom), 139.2 (C_q arom), 138.9 (C_q arom), 138.6 (C_q arom), 138.6 (d, *J*(C-P) = 40 Hz, C_q arom), 138.6 (C_q arom), 135.8 (d, *J*(C-P) = 39 Hz, C_q arom), 135.3 (d, *J*(C-P) = 9 Hz, 2 CH arom), 131.0 (C_q arom), 130.6 (C_q arom), 129.8 (d, *J*(C-P) = 9 Hz, 2 CH arom), 129.3 (2 CH arom), 128.9 (CH arom), 128.8 (CH arom), 128.7 (CH arom), 128.7 (CH arom), 128.5 (d, *J*(C-P) = 11 Hz, 2 CH arom), 128.3 (2 CH arom), 128.2 (2 CH arom), 127.0 (2 CH arom), 127.0 (2 CH arom), 124.9 (2 CH arom), 123.3 (2 CH arom), 66.6 (dd, *J*(C-P) = 31, 10 Hz, PCH_2), 66.3 (NCH), 65.3 (NCH), 37.7 ($C(CH_3)_3$), 35.7 ($C(CH_3)_3$), 34.7 ($C(CH_3)_3$), 34.3 ($C(CH_3)_3$), 32.9 ($C(CH_3)_3$), 31.5 ($C(CH_3)_3$), 31.1 ($C(CH_3)_3$), 30.8 ($C(CH_3)_3$). *Selected signals for cis*-**1a'**: ^1H NMR ($CDCl_3$, 400 MHz): δ = 8.22 (m, 2H, H arom), 7.68 (m, 3H, H arom), 7.49 (m, 2H, H arom), 7.34 (m, 8H , H arom), 7.12 (m, 2H, H arom), 7.07 (m, 1H, H arom), 6.99 (m, 2H, H arom), 6.82 (m, 1H, H arom), 6.72 (m, 3H, H arom), 5.29 (m, PC*H*H), 4.88 (dt, *J*(H-H) = 11.7, 5.9 Hz, 1H, NCH), 4.29 (m, 1H, PC*H*H), 3.75 (m, 1H, NCH), 3.42 (m, 1H, N*H*H), 3.30 (m, 2H, N*H*H), 2.11 (m, 1H, N*H*H), 1.49 (s, 9H, $C(CH_3)_3$, 1.27 (s, 9H, $C(CH_3)_3$, 1.19 (s, 9H, $C(CH_3)_3$, 1.10 (s, 9H, $C(CH_3)_3$. $^{31}P\{^1H\}$ NMR ($CDCl_3$, 162 MHz): δ = 169.9 (d, *J*(P-P) = 45 Hz, P-O), 73.9 (d, *J*(P-P) = 45 Hz, P-C). Elem. Anal. (%): C 63.27 %, H 6.16 %, N 2.81 (calcd for $C_{55}H_{68}Cl_2N_2O_3P_2Ru$: C 63.58, H 6.60, N 2.70).

Ru(H)(BH_4)(**2c**)(**3b**) (**7**). A mixture of **1e** (0.110 g, 0.100 mmol) and $NaBH_4$ (0.038 g, 1.00 mmol) in a toluene:EtOH 1:1 mixture (2 mL) was heated at 60 ºC for 1 h. After this time the mixture was evaporated under reduced pressure and the residue was extracted in *n*-pentane (3 × 3 mL). The solution was filtered through Celite and evaporated, yielding **7** as a beige solid (0.120 g, 86 %). The product is obtained as a mixture of two isomers in a 2:1 ratio. Below are given spectroscopic data for the major isomer. ^1H NMR (C_6D_6, 400 MHz): δ = 8.53 (dd, *J*(H-H) = 10.9, 8.1 Hz, 2H, Ar-H), 7.77

(s, 1H, CH arom), 7.70 (m, 3H, CH arom), 7.50 (3H, CH arom), 7.38 (d, *J*(H-H) = 2.5 Hz, 1H, CH arom), 7.33 (d, *J*(H-H) = 2.4 Hz, 1H, CH arom), 7.28 (d, *J*(H-H) = 2.4 Hz, 1H, CH arom), 7.06 (m, 3H, CH arom), 6.91 (m, 9H, CH arom), 4.52 (m, 1H, NH*H*), 4.45 (m, 1H, CH), 4.05 (m, 2H, CH + N*H*H), 2.75 (d, *J*(H-H) = 2.1 Hz, 1H, NH*H*), 2.60 (t, *J*(H-H) = 8.3 Hz, 1H, N*H*H), 1.76 (s, 9H, $C(CH_3)_3$), 1.72 (s, 9H, $C(CH_3)_3$), 1.38 (s, 9H, $C(CH_3)_3$), 0.96 (s, 9H, $C(CH_3)_3$), -0.43 (bs, 4H, BH_4), -13.45 (t, *J*(H-P) = 26.6 Hz, 1H, Ru-H); $^{31}P\{^1H\}$ NMR (C_6D_6 , 162 MHz): δ = 177.5 (d, *J*(P-P) = 77 Hz, P-O), 58.2 (d, *J*(P-P) = 77 Hz, P-C); $^{13}C\{^1H\}$ NMR (C_6D_6, 100 MHz): δ =156.2 (d, *J*(C-P) = 10 Hz, C_q arom), 148.9 (C_q arom), 148.7 (C_q arom), 146.6 (C_q arom), 145.2 (C_q arom), 144.8 (2 C_q arom), 141.0 (C_q arom), 140.9 (C_q arom), 140.6 (C_q arom), 139.2 (C_q arom), 135.9 (C_q arom), 135.5 (C_q arom), 135.3 (d, *J*(C-P) = 11 Hz, CH arom), 134.8 (C_q arom), 134.1 (C_q arom), 133.7 (C_q arom), 132.8 (d, *J*(C-P) = 9 Hz, CH arom), 131.1 (CH arom), 129.9 (CH arom), 129.6 (CH arom), 128.7 (CH arom), 128.4 (2 CH arom), 128.2 (CH arom), 127.1 (d, *J*(C-P) = 5 Hz, CH arom), 126.9 (CH arom), 126.4 (CH arom), 125.0 (CH arom), 124.4 (CH arom), 122.8 (CH arom), 122.7 (CH arom), 122.5 (CH arom), 69.8 (NCH), 60.6 (NCH), 36.5 ($C(CH_3)_3$), 35.5 ($C(CH_3)_3$), 34.2 ($C(CH_3)_3$), 33.9 ($C(CH_3)_3$), 33.0 ($C(CH_3)_3$), 31.3 ($C(CH_3)_3$), 31.1 ($C(CH_3)_3$), 30.7 ($C(CH_3)_3$). Elem. Anal. (%): C 68.71 %, H 7.00 %, N 2.29 (calcd for $C_{60}H_{75}BN_2O_3P_2Ru$: C 68.82, H 7.32, N 2.68).

Representative catalytic hydrogenation of imines 5. In a glovebox, a 2 mL vial was charged with imine **5** (0.5 mmol), catalyst precursor (1.0 μmol), K^{t}BuO (10 μmol) and toluene (0.5 mL) placed in a parallel pressure HEL CAT18 reactor. The reactor was purged three times with H_2, pressurized at 4 bar of H_2 and reacted at room temperature for 24 h. After this time the reactor was slowly depressurized, the solution obtained evaporated and conversion determined by ^1H NMR of the resulting residue. This residue

was purified by passing through a short pad of silica using a EtOAc/*n*-hexane (1:9) mixture as eluent. The resulting solution was evaporated under reduced pressure and the residue obtained analyzed by chiral HPLC to determine enantiomeric excess as described below. Alternatively, to remove unreacted imine in uncompleted reactions, the residue obtained after the catalytic hydrogenation can be dissolved in CH_2Cl_2 (2 mL), treated with aqueous HCl (2 mL, 2 M) and the mixture stirred for 20 minutes. $NaHCO_3$ (satd, 3 mL) was added over the mixture, the organic layer extracted, dried over magnesium sulfate and concentrated. Racemic mixtures were prepared by a transfer hydrogenation reaction performed with the Shvo catalyst.[S3] All amines **6** are known compounds. ***N*-phenyl-1-phenylethylamine (6a):**[S4] Chiralcel OJ-H, 30° C, *n*-hexane/2-propanol (97:3), flow 1.0 mL/min, t_1 = 20.7 min (*R*), t_2 = 26.6 min (*S*). ***N*-(4-methoxyphenyl)-1-(4-bromophenyl)ethylamine (6b):**[S4] Chiralcel OD-H, 30° C, *n*-hexane/2-propanol (99:1), flow 1.0 mL/min, t_1 = 20.8 min (*R*), t_2 = 24.8 min (*S*). ***N*-(4-methoxyphenyl)-1-(4-trifluoromethylphenyl)ethylamine (6c):**[S4] Chiralcel OD-H, 30° C, *n*-hexane/2-propanol (97:3), flow 1.0 mL/min, t_1 = 12.9 min (*R*), t_2 = 16.5 min (*S*). ***N*-(4-methoxyphenyl)-1-(3,4-dimethoxyphenyl)ethylamine (6d):**[S4] Chiralcel OD-H, 30° C, *n*-hexane/2-propanol (90:10), flow 0.5 mL/min, t_1 = 27.7 min (*R*), t_2 = 31.9 min (*S*). ***N*-(4-fluorophenyl)-1-phenylethylamine (6e):**[S5] Chiralcel OD-H, 30° C, *n*-hexane/2-propanol (98:2), flow 0.5 mL/min, t_1 = 15.2 min (*R*), t_2 = 17.5 min (*S*). ***N*-(3,5-dimethoxyphenyl)-1-phenylethylamine (6f):**[S4] Chiralcel OB-H, 30° C, *n*-hexane/2-propanol (99:1), flow 1.0 mL/min, t_1 = 37.2 min (*S*), t_2 = 54.8 min (*R*). ***N*-(4-methoxyphenyl)-1-phenylethylamine (6g):**[S4] Chiralcel AD-H, 30° C, *n*-hexane/2-propanol (99:1), flow 1.0 mL/min, t_1 = 12.8 min (*R*), t_2 = 14.0 min (*S*). ***N*-(4-methoxyphenyl)-1-(3-methoxyphenyl)ethylamine (6h):**[S4] Chiralcel OD-H, 30° C, *n*-hexane/2-propanol (99:1), flow 1.0 mL/min, t_1 = 22.1 min (*R*), t_2 = 25.5 min (*S*). ***N*-(4-methoxyphenyl)-1-(2-methylphenyl)ethylamine (6i):**[S4]

Chiralcel OD-H, 30° C, *n*-hexane/2-propanol (99:1), flow 1.0 mL/min, t_1 = 8.3 min (*R*), t_2 = 9.5 min (*S*). ***N*-(4-methoxyphenyl)-1-(2-fluorophenyl)ethylamine (6j):**[S4] Chiralcel OD-H, 30° C, *n*-hexane/2-propanol (99:1), flow 1.0 mL/min, t_1 = 10.5 min (*R*), t_2 = 12.6 min (*S*). ***N*-(4-methoxyphenyl)-1-(4-methylphenyl)ethylamine (6k):**[S4] Chiralcel OD-H, 30° C, *n*-hexane/2-propanol (99:1), flow 1.0 mL/min, t_1 = 11.6 min (*R*), t_2 = 13.1 min (*S*). ***N*-phenyl-1-(4-chlorophenyl)ethylamine (6l):**[S4] Chiralcel OD-H, 30° C, *n*-hexane/2-propanol (99:1), flow 1.0 mL/min, t_1 = 16.5 min (*S*), t_2 = 20.6 min (*R*). ***N*-(4-methoxyphenyl)-1-(2-thienyl)ethylamine (6m):**[S6] Chiralcel OD-H, 30° C, *n*-hexane/2-propanol (99:1), flow 1.0 mL/min, t_1 = 17.2 min (*R*), t_2 = 19.1 min (*S*). ***N*-(4-methoxyphenyl)-1-(1-naphthyl)ethylamine (6n):**[S4] Chiralcel OD-H, 30° C, *n*-hexane/2-propanol (99:1), flow 1.0 mL/min, t_1 = 22.9 min (*R*), t_2 = 31.7 min (*S*). ***N*-(4-methoxyphenyl)-1-(2-naphthyl)ethylamine (6o):**[S4] Chiralcel OD-H, 30° C, *n*-hexane/2-propanol (99:1), flow 1.0 mL/min, t_1 = 23.6 min (*R*), t_2 = 28.7 min (*S*). ***N*-(4-methoxyphenyl)-1-phenylpropylamine (6p):**[S4] Chiralcel OD-H, 30° C, *n*-hexane/2-propanol (99:1), flow 1.0 mL/min, t_1 = 10.7 min (*R*), t_2 = 11.0 min (*S*).

X-ray crystallographic determinations

To ascertain the coordination mode of complexes **1** (i.e. *cis* or *trans*) several X-ray single crystal analysis were performed. Thus, in addition to **1d** included in our preliminary contribution,[S1a] complexes **1a**, **1c** and **1i** have been studied. Moreover, to authenticate a *cis* stereochemistry for the complex resulting from isomerization of **1a** a structural determination of major isomer resulting from this reaction was performed. This analysis showed a coincident structure with that of a *cis* isomer of $Ru(Cl)_2$(**2a**)(**3a**) detected previously from a mixture of isomers of this complex obtained by an alternative synthetic procedure.[S1b]

Suitable crystals for X-ray diffraction were obtained by recrystallization in Et_2O:*n*-hexane mixtures (**1a** and *cis*-**1a**) or CH_2Cl_2:*n*-hexane mixtures (**1c** and **1i**). Crystals were coated with perfluoropolyether and mounted on a glass fiber were placed in the goniometer head of a Bruker-Nonius X8 Apex-II CCD diffractometer and analyzed using graphite monochromatized Mo radiation (λ(Mo Kα) = 0.71073 Å) and fine-sliced ω and φ scans (scan widths 0.30° to 0.50°)[S7a] under a flow of cold nitrogen. Data obtained were reduced (SAINT) and corrected for absorption effects by the multiscan method (SADABS).[S7b] The structures were solved by direct methods (SIR2002, SHELXS) and refined against all F^2 data by full-matrix least squares techniques (SHELXL-2016/6) minimizing $w[F_o^2\text{-}F_c^2]^2$.[S8] All non-hydrogen atoms were refined with anisotropic displacement parameters. Hydrogen atoms were included in calculated positions and allowed to ride on their carrier atoms with the isotropic temperature factors U_{iso} fixed at 1.2 times (1.5 times for methyl groups) of the U_{eq} values of the respective carrier atoms. Complex **1a** (CCDC: 2045798) crystallizes in triclinic space group *P*1 with Z = 2, observing in the unit cell two identical pairs of diastereoisomers that differ from each other only in the configuration of the stereogenic biaryl axis, together with two molecules of diethyl ether as crystallization solvent. Some dynamic disorder was observed in some fragments of the molecules that it was not necessary to model but this required some geometric restraints (DFIX instruction), the ADP restraint SIMU and the rigid bond restraint DELU were used in order to obtain more reasonable geometric and ADP values of the disordered atoms. A search for solvent accessible voids for the crystal structure of **1a** using PLATON[S9] SQUEEZE[S10] method, showed some small volumes of potential solvents of 206 $Å^3$ (56 electron count) and 625 $Å^3$ (139 electron count), corresponding to tentative Et_2O occupancy of one and three molecules respectively of diffuse crystallization solvent. The compound **1c** (CCDC: 2045799) crystallizes in the

monoclinic space group *C*2 and Z = 8, with a pair of diastereoisomers that differ from each other only in the configuration of the stereogenic biaryl axis, together with two molecules of dichloromethane as crystallization solvent in the asymmetric unit. Some dynamic disorder was observed so it was required to use some geometric restraints (DFIX instruction), the ADP restraint SIMU and the rigid bond restraint DELU were used in order to obtain more reasonable geometric and ADP values of the disordered atoms. The compound **1i** (CCDC: 2045800) crystallizes in triclinic space group *P*1 with Z = 1, observing in the unit cell a pair of diastereoisomers that differ from each other only in the configuration of the stereogenic biaryl axis, together with three molecules of dichloromethane as crystallization solvent. Some methyl groups were observed disordered, as well as two of dichloromethane molecules, all of them modeled in two components and their occupation coefficients refined. Both positional and dynamic disorder required large geometric restraints (DFIX instruction), the ADP restraint SIMU and the rigid bond restraint DELU were used in order to obtain more reasonable geometric and ADP values of the disordered atoms. Moreover, a search for solvent accessible voids for the crystal structure of **1i** using PLATON SQUEEZE method, showed some small volumes of potential solvents of 94 $Å^3$ (24 electron count) and 235 $Å^3$ (80 electron count), were 42 electron count are expected for CH_2Cl_2 full occupancy. From this ratio, tentative CH_2Cl_2 occupancy of 0.57 of and two CH_2Cl_2 molecules can be calculated respectively of diffuse crystallization solvents.

As an unusual occurrence, compound *cis*-**1a** crystallizes in the Et_2O:*n*-hexane mixture in the form of two types of yellow prisms with slight differences between them, both morphologically and by colorimetric analysis under polarized light microscopy. A crystal from the predominant batch (*cis*-**1a**-M; CCDC: 2045801) crystallizes in the monoclinic system, Sohncke space group $P2_1$ with Z = 2, while a crystal from the minority

batch (*cis*-**1a-**min; CCDC: 2045802) crystallizes in the tetragonal system in the enantiomorphic space group $P4_12_12$ with Z = 8. Only a single identical stereoisomer of the Ru (II) complex with the same absolute configuration is observed in the asymmetric unit for both crystals. A search for solvent accessible voids for the crystal structure of *cis*-**1a**-M using PLATON SQUEEZE method, showed two small volumes of potential solvents of 207 $Å^3$ (42 electron count), were 42 electron count are expected for an Et_2O molecule with full occupancy. From this ratio, tentative occupancy of an Et_2O molecule can be calculated in both voids of diffuse crystallization. While a search for solvent accessible voids for the crystal structure of *cis*-**1a-**min using PLATON SQUEEZE method did not show voids with enough volume and electron counts to occupy solvent to mention. The corresponding CIF data represent SQUEEZE treated structures with the solvent molecules handling as a diffuse contribution to the overall scattering, without specific atom position and excluded from the structural model. The SQUEEZE results were automatically included by SHELXL (ABIN instruction) to the end of the CIF files.

As preliminary reported in the X-ray diffraction study of **1d**,[S1a] complexes **1a**, **1c** and **1i** show two diastereomers in the crystal with a *trans* stereochemistry, differing in the configuration of the biaryl stereogenic axis. Moreover, the structures of the two diastereomers are nearly enantiomeric each other thus conforming a *pseudoracemate*.[S11] In this regard, refinement in a centrosymmetric space group (shown in alerts in the checkCIF reports; *P*-1 for **1a**, *C*2/*c* for **1c** and *P*-1 for **1i**) would involve the presence of enantiomers of complexes **1**, which is not compatible with the enantiopurity of diamines used.[S12]

Among the new determinations of *trans* complexes **1**, that of **1i** led to a structure of satisfactory quality (as it was the case of **1d**). By the opposite, caused by the presence of disordered solvent and a relatively high number of weak reflections, the analysis of **1a**

and **1c** led to results of lower quality. Moreover, due to the high solubility of these compounds difficulties on obtaining crystalline samples were experienced. Best results were finally obtained using *n*-hexane along with tiny amounts of a cosolvent (CH_2Cl_2 or Et_2O). Upon the obtaining of suitable samples for X-ray diffraction, several crystals were examined until reaching an acceptable quality data. It seems that the difficulties posed by **1a** and **1c** are associated to the *trans* stereochemistry of these complexes and their easy atropisomerization of the biaryl fragment. This phenomenon is not that easy in the *cis* isomers (see main text) and the structural determination of *cis*-**1a** led to high quality results. As a result of the insufficient quality data for **1a** and **1c**, along with the additional difficulties due to the presence of diastereomers in the crystal,[S13] a deviation of the Flack parameter was observed for these complexes. By the opposite, the expected close to zero values were obtained for **1i** and *cis*-**1a** (as well as for **1d**). Notwithstanding that, a reliable configuration of the biaryl moiety can be done considering the known configuration of the diamine.

A summary of cell parameters, data collection, structures solution, and the refinement of crystal structures are provided below (Figures S1-S4 and Tables S1-S4). As well, cif files for **1a**, **1c**, **1i**, *cis*-**1a**-M and *cis*-**1a**-min have been uploaded as a part of the supplementary material.

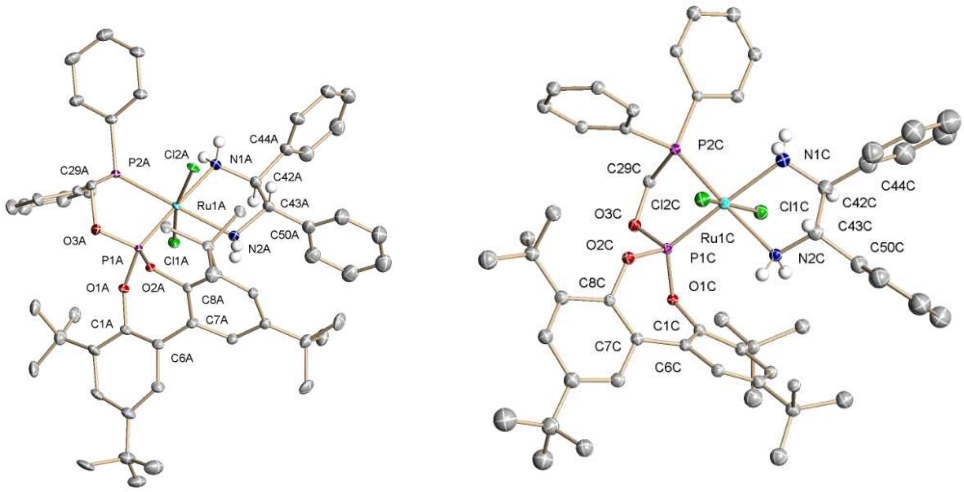

Figure S1. ORTEP view of diastereomers of complex **1a** observed in the crystal lattice: (S_{ax})-*trans*-**1a** (left) and (R_{ax})-*trans*-**1a** (right).

Table S1. Crystal data and structure refinement for **1a**.

Empirical formula	$C_{114}H_{146}Cl_4N_4O_7P_4Ru_2$	
	$[2(C_{55}H_{68}Cl_2N_2O_3P_2Ru), C_4H_{10}O]$	
Formula weight	2152.16	
Temperature	193(2) K	
Wavelength	0.71073 Å	
Crystal system	Triclinic	
Space group	P1	
Unit cell dimensions	a = 16.268(3) Å	α= 87.715(10)°.
	b = 17.763(3) Å	β= 81.350(10)°.
	c = 23.082(4) Å	γ = 66.621(9)°.
Volume	6051.5(18) $Å^3$	
Z	2	
Density (calculated)	1.181 Mg/m^3	
Absorption coefficient	0.441 mm^{-1}	
F(000)	2260	
Crystal size	0.400 x 0.150 x 0.100 mm^3	
Theta range for data collection	1.528 to 25.250°.	
Index ranges	-19<=h<=19, -21<=k<=21, -27<=l<=27	
Reflections collected	88132	
Independent reflections	43430 [R(int) = 0.0410]	
Completeness to theta = 25.242°	99.8 %	
Absorption correction	Semi-empirical from equivalents	
Max. and min. transmission	0.7461 and 0.6575	
Refinement method	Full-matrix-block least-squares on F^2	
Data / restraints / parameters	43430 / 4119 / 2387	
Goodness-of-fit on F^2	1.062	
Final R indices [I>2sigma(I)]	R1 = 0.0836, wR2 = 0.2425	
R indices (all data)	R1 = 0.1214, wR2 = 0.2708	
Absolute structure parameter	0.246(15)	
Extinction coefficient	n/a	
Largest diff. peak and hole	2.573 and -2.038 $e.Å^{-3}$	

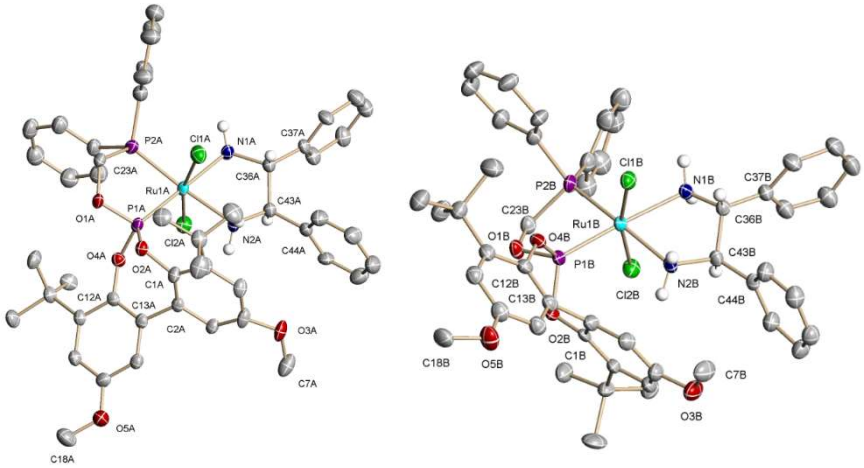

Figure S2. ORTEP view of diastereomers of complex **1c** observed in the crystal lattice: (S_{ax})-*trans*-**1c** (left) and (R_{ax})-*trans*-**1c** (right).

Table S2. Crystal data and structure refinement for **1c**.

Empirical formula	$C_{50}H_{58}Cl_4N_2O_5P_2Ru$	
	$[C_{49}H_{56}Cl_2N_2O_5P_2Ru, CH_2Cl_2]$	
Formula weight	1071.79	
Temperature	193(2) K	
Wavelength	0.71073 Å	
Crystal system	Monoclinic	
Space group	C2	
Unit cell dimensions	a = 29.604(14) Å	α= 90°.
	b = 12.869(4) Å	β= 114.68(2)°.
	c = 29.396(14) Å	γ = 90°.
Volume	10175(8) $Å^3$	
Z	8	
Density (calculated)	1.399 Mg/m^3	
Absorption coefficient	0.628 mm^{-1}	
F(000)	4432	
Crystal size	0.100 x 0.080 x 0.050 mm^3	
Theta range for data collection	1.382 to 25.247°.	
Index ranges	-32<=h<=35, -10<=k<=15, -27<=l<=35	
Reflections collected	48983	
Independent reflections	14744 [R(int) = 0.0951]	
Completeness to theta = 25.242°	98.6 %	
Absorption correction	Semi-empirical from equivalents	
Max. and min. transmission	1.0000 and 0.9121	
Refinement method	Full-matrix-block least-squares on F^2	

Data / restraints / parameters	14744 / 1925 / 1073
Goodness-of-fit on F^2	1.015
Final R indices [I>2sigma(I)]	R1 = 0.0617, wR2 = 0.1278
R indices (all data)	R1 = 0.1347, wR2 = 0.1524
Absolute structure parameter	0.32(7)
Extinction coefficient	n/a
Largest diff. peak and hole	0.963 and -0.658 e.$Å^{-3}$

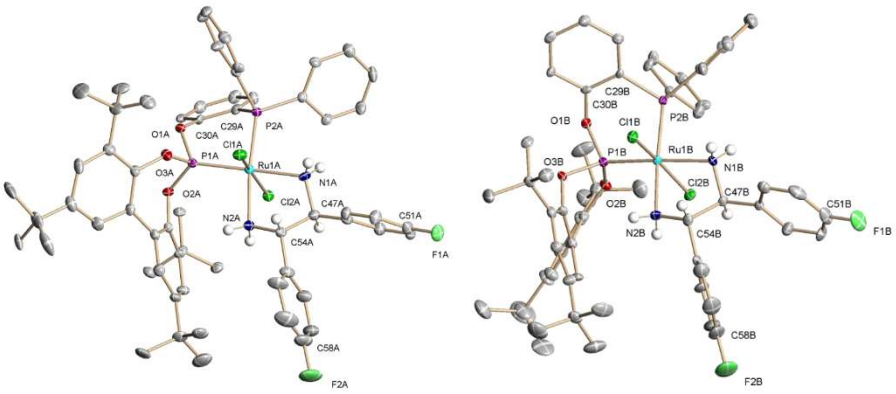

Figure S3. ORTEP view of diastereomers of complex **1i** observed in the crystal lattice: (S_{ax})-*trans*-**1i** (left) and (R_{ax})-*trans*-**1i** (right).

Table S3. Crystal data and structure refinement for **1i**.

Empirical formula	$C_{123}H_{142}Cl_{10}F_4N_4O_6P_4Ru_2$	
	$[2(C_{60}H_{68}Cl_2F_2N_2O_3P_2Ru), 3(CH_2Cl_2)]$	
Formula weight	2528.92	
Temperature	173(2) K	
Wavelength	0.71073 Å	
Crystal system	Triclinic	
Space group	P1	
Unit cell dimensions	a = 13.3642(3) Å	α= 89.2120(10)°.
	b = 15.0349(3) Å	β= 76.7380(10)°.
	c = 18.4697(4) Å	γ = 66.7710(10)°.
Volume	3307.09(13) $Å^3$	
Z	1	
Density (calculated)	1.270 Mg/m^3	
Absorption coefficient	0.535 mm^{-1}	
F(000)	1310	
Crystal size	0.450 x 0.250 x 0.200 mm^3	
Theta range for data collection	2.243 to 25.248°.	

Index ranges	-16<=h<=16, -18<=k<=18, -22<=l<=22
Reflections collected	102854
Independent reflections	23788 [R(int) = 0.0243]
Completeness to theta = 25.242°	99.9 %
Absorption correction	Semi-empirical from equivalents
Max. and min. transmission	1.0000 and 0.9315
Refinement method	Full-matrix least-squares on F^2
Data / restraints / parameters	23788 / 761 / 1540
Goodness-of-fit on F^2	1.052
Final R indices [I>2sigma(I)]	R1 = 0.0317, wR2 = 0.0901
R indices (all data)	R1 = 0.0361, wR2 = 0.0926
Absolute structure parameter	0.044(8)
Extinction coefficient	n/a
Largest diff. peak and hole	0.745 and -0.358 e.Å^{-3}

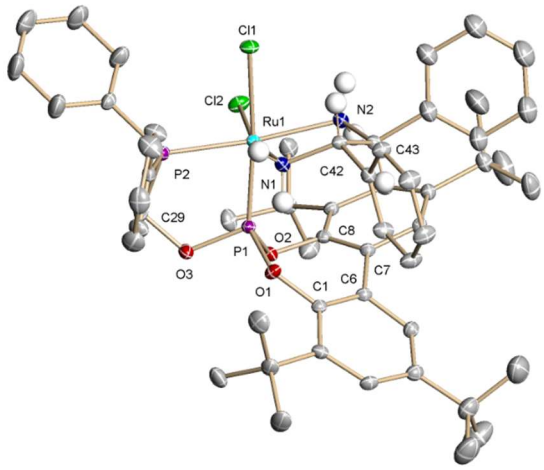

Figure S4. ORTEP view of complex diastereomers of complex ***cis*-1a**.

Table S4. Crystal data and structure refinement for ***cis*-1a** (*cis*-**1a**-M)

Empirical formula	$C_{55}H_{68}Cl_2N_2O_3P_2Ru$	
Formula weight	1039.02	
Temperature	193(2) K	
Wavelength	0.71073 Å	
Crystal system	Monoclinic	
Space group	$P2_1$	
Unit cell dimensions	a = 14.485(3) Å	α= 90°.
	b = 13.276(3) Å	β= 104.344(6)°.
	c = 16.008(4) Å	γ = 90°.

Volume	2982.4(12) $Å^3$
Z	2
Density (calculated)	1.157 Mg/m^3
Absorption coefficient	0.444 mm^{-1}
F(000)	1088
Crystal size	0.400 x 0.150 x 0.100 mm^3
Theta range for data collection	1.451 to 25.248°.
Index ranges	-17<=h<=17, -15<=k<=15, -19<=l<=19
Reflections collected	38350
Independent reflections	10789 [R(int) = 0.0237]
Completeness to theta = 25.242°	100.0 %
Absorption correction	Semi-empirical from equivalents
Max. and min. transmission	0.7461 and 0.6664
Refinement method	Full-matrix least-squares on F^2
Data / restraints / parameters	10789 / 151 / 598
Goodness-of-fit on F^2	1.219
Final R indices [I>2sigma(I)]	R1 = 0.0266, wR2 = 0.0702
R indices (all data)	R1 = 0.0284, wR2 = 0.0708
Absolute structure parameter	-0.022(6)
Extinction coefficient	n/a
Largest diff. peak and hole	0.701 and -0.408 $e.Å^{-3}$

Simulation of NMR spectra

Selected $^{31}P\{^1H\}$ NMR spectra of studies performed at different temperatures with **1a** and **1d** have been simulated with dnmr software included in Topspin program (version 4.0.9). For each compound the spectrum registered at -90 ºC has been simulated to validate the method and to obtain chemical shift, coupling constants and LB values to use as a starting point in the simulation of the spectrum at the temperature of coalescence. In both cases the phosphine region has been selected for the analysis as it shows a clearer coalescence point. Regarding the full collection of $^{31}P\{^1H\}$ NMR spectra registered at different temperatures it can be found in the main text in the case of **1a** or in the supplementary material of our preliminary communication in the case of **1d**.[S1a]

a) **1a** (Figure S5). *Spectrum at -90 ºC* (fitting region: 70.3-66.8 ppm). Ratio M/m = 0.70/0.30. δ_M = 69.47 ppm (J_{PP} = 45.9 Hz), δ_m = 67.59 ppm (J_{PP} = 45.5 Hz). LB = 12.0 Hz. k = 31.2 s^{-1} (93.5 % overlap). *Spectrum at -70 ºC* (coalescence, fitting region: 71.0-66.5 ppm). Ratio M/m = 0.72/0.28. δ_1 = 69.77 ppm (J_{PP} = 45.9 Hz), δ_2 = 68.01 ppm (J_{PP} = 45.5 Hz). LB = 12.0 Hz. k = 533 s^{-1} (93.4 % overlap). Upon the k value at -70 ºC a value of $\Delta G^{\neq}$ = 9.2 kcal mol^{-1} has been calculated.

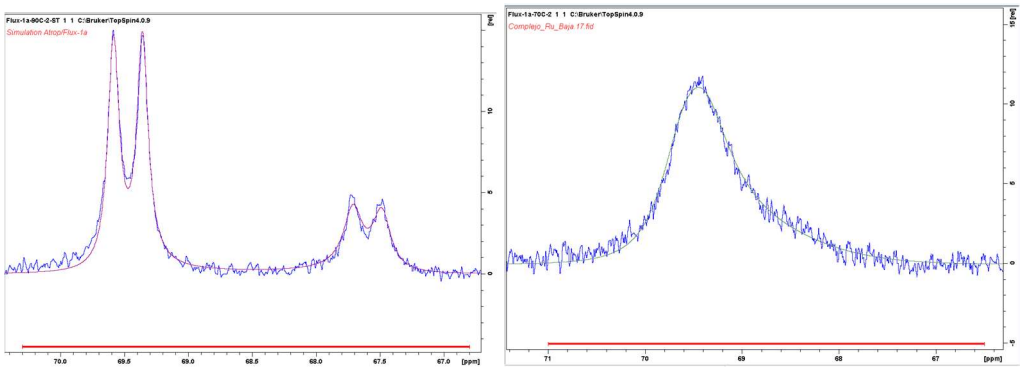

Figure S5. Overlapping of experimental and simulated of the phosphine región of the $^{31}P\{^1H\}$ NMR spectra of **1a** registered at -90 ºC (left) and at -70 ºC (coalescence, right).

b) **1d** (Figure S6). *Spectrum at -90 ºC* (fitting region: 39.0-35.0 ppm). Ratio M/m = 0.64/0.36. δ_M = 37.29 ppm (J_{PP} = 70.2 Hz), δ_m = 36.87 ppm (J_{PP} = 70.8 Hz). LB = 8.0 Hz. k = 0.394 s^{-1} (97.3 % overlap). *Spectrum at -65 ºC* (coalescence, fitting region: 39.0-35.0 ppm). Ratio M/m = 0.62/0.38. δ_M = 37.38 ppm (J_{PP} = 70.2 Hz), δ_m = 36.83 ppm (J_{PP} = 70.8 Hz). LB = 12.0 Hz. k = 80.5 s^{-1} (97.3 % overlap). Upon the k value at -65 ºC a value of $\Delta G^{\neq}$ = 10.2 kcal mol^{-1} has been calculated.

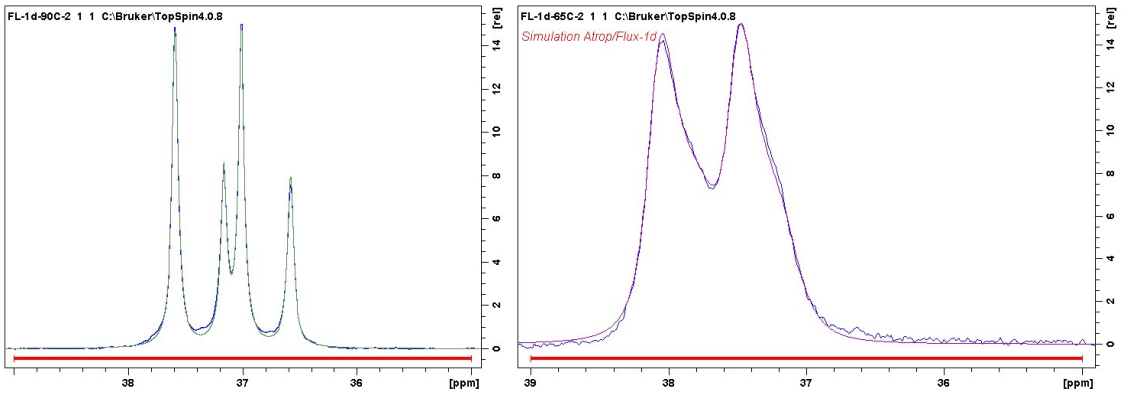

Figure S6. Overlapping of experimental and simulated of the phosphine región of the $^{31}P\{^{1}H\}$ NMR spectra of **1d** registered at -90 ºC (left) and at -65 ºC (coalescence, right).

Supplementary computational information

General considerations. Calculations were performed with Gaussian 09[S14] at the DFT level, using the Becke Three-Parameter functional[S15] with the non-local correlation by Perdew and Wang[S16] (B3PW91) and the D3 version of Grimme's dispersion with Becke-Johnson damping (GD3BJ).[S17] H, C, P, Cl and O atoms were represented with the 6-31G(d,p) basis set[S18] whereas Ru atoms were described by the Stuttgart/Dresden Effective Core Potential and the associated basis set as implemented in Gaussian 09 (BS1).[S19] Electronic energies of **TS1-d1R-RP-5a** and **TS1-d3S-SP-5a** were also calculated using 6-311++G(2d,p) basis set for the main group elements and def2-QZVP basis set for Ru (BS2).[S20] All molecular geometries were optimized within the SMD continuum solvent (toluene) model[S21] without any geometry constrains using BS1. Frequency calculations were performed at the same level of theory to characterize the stationary points as minima (no imaginary frequencies) or transition states (one imaginary frequency), as well as to calculate free energy (G) corrections. The two minima connected by a given transition state were confirmed from IRC analysis unless otherwise stated.[S22] Energies of calculated structures are given in the Table S5. Representation of non covalent interactions were performed with Multiwfn software.[S23] Molecular

representations were made either with the UCSF Chimera[S24] or VMD[S25] packages. A list of coordinates for computed structures is provided in a separate file, while the complete free energy profile for the preferred enantiomer is provided in Figure S7. Application of the energetic span model developep by Kozuch and Shaik[S26a] to this cycle using the AUTOF program[S26b] indicated that the intermediate (TDI) and transition state (TDTS) determining the rate of the reaction are **a1R-*R*-6a** and **TS4a**, respectively. Moreover, the energetic span of the reaction, which can be considered as the apparent activation energy of the cycle, corresponds to the Gibbs energy difference between these species, calculated as 17.5 kcal mol^{-1} in the present cycle.

Table S5. E and G values (a.u.) for computed complexes and TS[a]

Entry	Compound	E (RB3PW91)	G (298K)
1	**ctR**	-4169.732213	-4168.707794
2	**ctS**	-4169.731682	-4168.708002
3	**c1R**	-4169.745153	-4168.716225
4	**c1S**	-4169.732730	-4168.703367
5	**c2R**	-4169.722304	-4168.698571
6	**c2S**	-4169.726224	-4168.698703
7	**c3R**	-4169.734054	-4168.706410
8	**c3S**	-4169.744516	-4168.715751
9	**c4R**	-4169.724844	-4168.696948
10	**c4S**	-4169.720121	-4168.693014
11	**atrop-TS1** (*i*29 cm^{-1})	-4169.720310	-4168.692926
12	**conf-1**	-4169.724442	-4168.699461
13	**atrop-TS2** (*i*54 cm^{-1})	-4169.721834	-4168.696512
14	**conf-2**	-4169.724035	-4168.698654
15	**atrop-TS3** (*i*21 cm^{-1})	-4169.722829	-4168.696892
16	**conf-3**	-4169.728457	-4168.705202
17	**c1R'**	-4361.448721	-4360.368976
18	**c3S'**	-4361.446487	-4360.366396
19	**ctR'**	-4361.435625	-4360.360083
20	**ctS'**	-4361.435754	-4360.360707
21	**ctR"**	-4361.443257	-4360.367187
22	**ctS"**	-4361.441916	-4360.369616

23	**dtR**	-3250.496688	-3249.455896
24	**dtS**	-3250.496352	-3249.455902
25	**d1R**	-3250.512453	-3249.472431
26	**d1S**	-3250.503487	-3249.460593
27	**d2R**	-3250.497164	-3249.458786
28	**d2S**	-3250.499970	-3249.460392
29	**d3R**	-3250.503081	-3249.459795
30	**d3S**	-3250.514623	-3249.470825
31	**d4R**	-3250.498082	-3249.458072
32	**d4S**	-3250.496173	-3249.455923
33	**d1R'**	-3442.217508	-3441.124332
34	**d3S'**	-3442.217396	-3441.124214
35	**dtR'**	-3442.199896	-3441.113818
36	**dtS'**	-3442.198963	-3441.113040
37	**dtR"**	-3442.206191	-3441.118130
38	**dtS"**	-3442.205896	-3441.117635
39	**a1R**	-3249.296360	-3248.275155
40	**a1R'**	-3249.249679	-3248.228432
41	**a1S**	-3249.288634	-3248.268215
42	**a2R**	-3249.294975	-3248.276363
43	**a2S**	-3249.296883	-3248.278721
44	**a3R**	-3249.285561	-3248.264013
46	**a3S**	-3249.292569	-3248.269921
47	**a3S'**	-3249.259235	-3248.234971
48	**a4R**	-3249.293588	-3248.276090
49	**a4S**	-3249.290484	-3248.272247
50	**a5R**	-3249.282169	-3248.264431
51	**a5S**	-3249.287239	-3248.269607
52	**a6R**	-3249.289698	-3248.273388
53	**a6S**	-3249.282676	-3248.267068
54	**5a**	-595.921941	-595.730540
55	**d1R-RP-5a**	-3846.477645	-3845.214367
56	**d1R-SP-5a**	-3846.474475	-3845.214155
57	**d1R-RH-5a**	-3846.467395	-3845.204433
58	**d1R-SH-5a**	-3846.470325	-3845.210078
59	**d3S-RP-5a**	-3846.475862	-3845.214145
60	**d3S-SP-5a**	-3846.477883	-3845.214083
61	**d3S-RH-5a**	-3846.469400	-3845.207677
62	**d3S-SH-5a**	-3846.461527	-3845.202508
63	**dtR-RPC-5a**	-3846.463524	-3845.203392

64	**dtR-SPC-5a**	-3846.464457	-3845.205151
65	**dtR-RPO-5a**	-3846.463524	-3845.203410
66	**dtR-SPO-5a**	-3846.447390	-3845.189589
67	**dtS-RPC-5a**	-3846.467244	-3845.206520
68	**dtS-SPC-5a**	-3846.454271	-3845.192600
69	**dtS-RPO-5a**	-3846.455853	-3845.193584
70	**dtS-SPO-5a**	-3846.460973	-3845.200767
71a	**TS1-d1R-RP-5a** (*i*409 cm^{-1})	-3846.468490	-3845.204367
71b	**TS1-d1R-RP-5a**[a]	-3847.296958	
72	**TS1-d1R-SP-5a** (*i*348 cm^{-1})	-3846.461473	-3845.199050
73	**TS1-d1R-RH-5a** (*i*550 cm^{-1})	-3846.444480	-3845.183101
74	**TS1-d1R-SH-5a** (*i*444 cm^{-1})	-3846.455056	-3845.195441
75	**TS1-d3S-RP-5a** (*i*676 cm^{-1})	-3846.461438	-3845.196500
76a	**TS1-d3S-SP-5a** (*i*684 cm^{-1})	-3846.465501	-3845.201753
76b	**TS1-d3S-SP-5a**[a]	-3847.294123	
77	**TS1-d3S-RH-5a** (*i*540 cm^{-1})	-3846.458929	-3845.193864
78	**TS1-d3S-SH-5a** (*i*647 cm^{-1})	-3846.441976	-3845.177430
79	**TS1-dtR-RPC-5a** (*i*324 cm^{-1})	-3846.457750	-3845.195385
80	**TS1-dtR-SPC-5a** (*i*343 cm^{-1})	-3846.454256	-3845.190503
81	**TS1-dtR-RPO-5a** (*i*324 cm^{-1})*	-3846.457750	-3845.195386
82	**TS1-dtR-SPO-5a** (*i*439 cm^{-1})	-3846.432553	-3845.170796
83	**TS1-dtS-RPC-5a** (*i*336 cm^{-1})	-3846.458956	-3845.198117
84	**TS1-dtS-SPC-5a** (*i*840 cm^{-1})	-3846.436044	-3845.174616
85	**TS1-dtS-RPO-5a** (*i*820 cm^{-1})	-3846.435913	-3845.175414
86	**TS1-dtS-SPO-5a** (*i*330 cm^{-1})	-3846.452501	-3845.192108
87	**ag-*pro-R***	-3846.470731	-3845.204925
88	**ag-*pro-S***	-3846.467548	-3845.198686
89	**ip-*pro-R***	-3846.479450	-3845.210363
90	**ip-*pro-S***	-3846.476294	-3845.203654
91	**TS2-*pro-R*** (*i*1177 cm^{-1})	-3846.472579	-3845.208218
92	**TS2-*pro-S*** (*i*1114 cm^{-1})	-3846.469423	-3845.203004
93	**a1R-*R*-6a**	-3846.484946	-3845.219891
94	**a3S-*S*-6a**	-3846.483792	-3845.218032
95	**N1R**	-3846.491325	-3845.217047
96	H_2	-1.177160	-1.178522
97	(*R*)-**6a**	-597.137158	-596.921529
98	**TS3a** (*i*87 cm^{-1})	-3847.651445	-3846.375137
99	**h1R-*R*-6a-l**	-3847.654863	-3846.371134
100	**TS3b** (*i*331 cm^{-1})	-3847.650025	-3846.371572
101	**h1R-*R*-6a-t**	-3847.653710	-3846.373304

102	**TS4a** (*i*1195 cm^{-1})	-3847.646191	-3846.370443
103	**d1R-*R*-6a**	-3847.693728	-3846.409721
104	**TS3c** (*i*385 cm^{-1})	-3847.630072	-3846.349038
105	**d1R-*R*-6a** (2^{nd} conformer)	-3847.693008	-3846.404834
106	**TS3d** (*i*358 cm^{-1})	-3250.471995	-3249.437988
107	**h1R-l**	-3250.473256	-3249.435027
108	**TS3e** (*i*3048 cm^{-1})	-3250.466654	-3249.433148
109	**h1R-t**	-3250.471139	-3249.434298
110	**TS4b** (*i*886 cm^{-1})	-3250.462141	-3249.427076

[a]Calculated with BS1 unless otherwise stated. [b]Calculated with BS2 (only E).

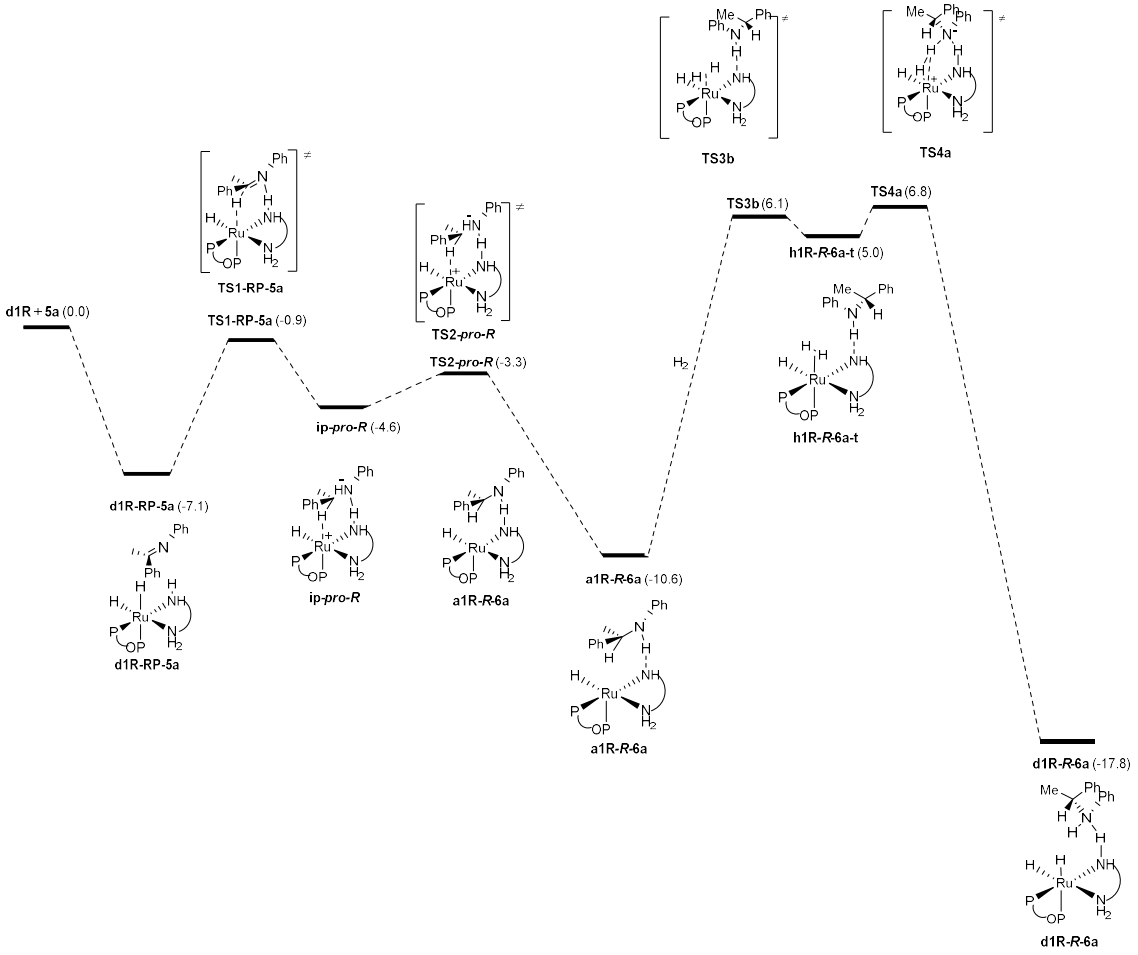

Figure S7. Complete free energy profile (ΔG in kcal mol^{-1} referred to **d1R** + **5a** + H_2) for the preferred enantiomer.

Interconversion between atropisomers of 1a. Atropisomerization of **1a** causes not only changes in the biaryl unit (Figure S8), but conformational changes in the backbone of the P-OP ligand as well. This dynamic process can be analyzed by examining

values of P-Ru-P'-O (P: phosphine phosphorus, P': phosphite phosphorus), P'-Ru-P-C and P-C-O-P' dihedral angles (Table S6). Thus, the dynamic process can be divided in several steps. Starting from **ctR**, a scan of the atropisomerization of the biaryl fragment led to **atrop-TS1** (Figure S9), with a $\Delta G^{\neq}$ of 9.3 kcal/mol above **ctR**. This TS is characterized by a biaryl dihedral angle of 1.9 degrees. In this case, IRC analysis failed and conformers around **atrop-TS1** were located by very small variations following the vector corresponding to the imaginary frequency around this TS followed by subsequent optimization to reach the two minima connected by **atrop-TS1**. Following this procedure, **Conf-1**, which already displays a S_{ax} configuration, was located. The remaining pathway towards **ctS** is composed by two additional conformers (**Conf-2** and **Conf-3**) as well as two transition states (**atrop-TS2** and **atrop-TS3**). Worth to note, a very small barrier was detected in the evolution of **Conf-3** to **ctS** and no transition state was located for this step.

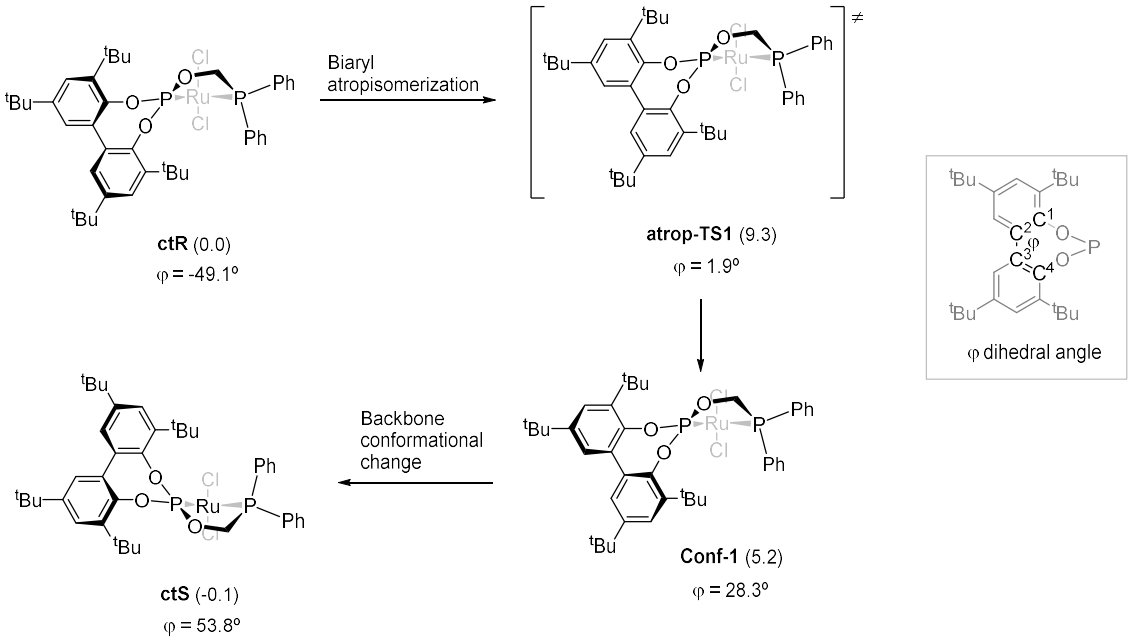

Figure S8. Schematic representation of the conformational changes of the Ru(P-OP) fragment of **1a** during the atropisomerization process.

Table S6. Selected dihedral angles and calculated energies of conformers generated along atropisomerization of **1a**[a]

Structure	φ[b]	P-Ru-P'-O	P'-Ru-P-C	P-C-O-P'	ΔE[c]	ΔG[c]
ctR	-49.1	24.3	-32.4	-23.5	8.1	0.0
atrop-TS1	1.9	15.3	-28.3	-32.9	7.5	9.3
Conf-1	28.3	6.6	-23.9	-40.4	5.2	5.3
atrop-TS2	29.2	15.1	-11.0	6.0	6.5	7.1

Conf-2	28.6	-5.8	22.3	37.8	5.1	5.7
atrop-TS3	32.7	-19.4	33.1	35.3	5.9	6.8
Conf-3[d]	40.2	-23.7	32.7	25.6	2.4	1.6
ctS	53.8	-23.3	32.1	25.0	0.3	-0.1

[a]Dihedral angles in degrees. P and P' denote phosphorus atoms of phosphine and phosphite ligands, respectively. [b]Dihedral angle determined by C^1-C^4 carbon atoms of the biaryl unit. [c]Relative energies in kcal/mol relative to **ctR**. [d]From Conf-3, barrierless evolution led to **ctS**.

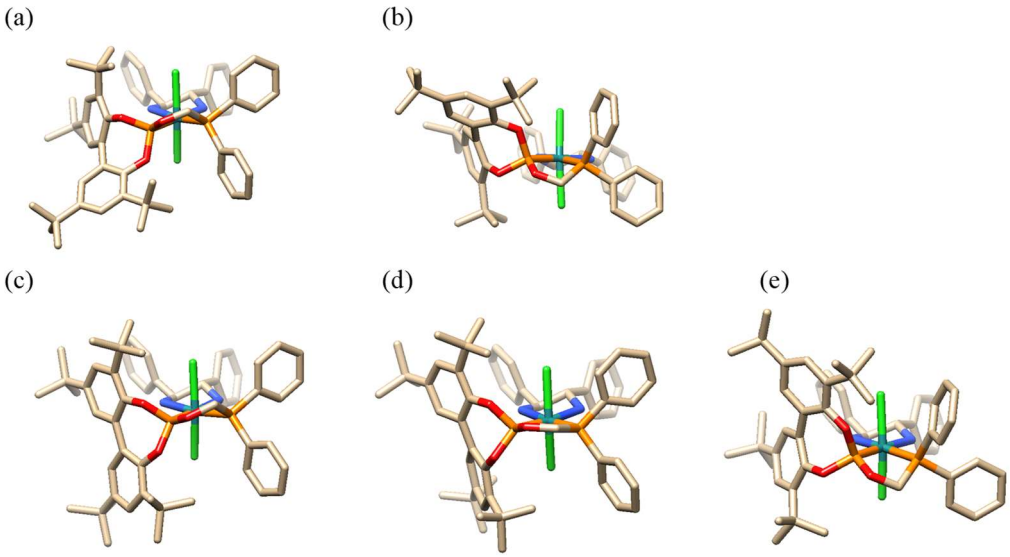

Figure S9. Structure of conformers of **1a** participating in the atropisomerization of the biaryl fragment: **ctR** (a), **ctS** (b), **atrop-TS1** (c), **atrop-TS2** (d), **atrop-TS3** (e).

Generation of amide complexes. For the study of structures of amido-hydride complexes of formulation Ru(H){(*S,S*)-NH-CHPh-CHPh-NH_2}(**2a**), it has been considered that hydrogen addition along the Ru-NH bond to these complexes produce corresponding dihydrides Ru$(H)_2$(**2a**)(**3a**) with a small structural rearrangement. Upon these considerations we have examined the formal abstraction of a hydride ligand and a NH_2 proton located in a near *synperiplanar* position to the hydride to give an amido-hydride complex which was then further optimized. Using this procedure compounds **a1R**, **a2R** and **a1R'** were generated from **d1R** (Figure S10a). These structures can be described as distorted trigonal bipyramidal (**a1R**, **a2R**) or square pyramid (**a1R'**) structures. Likewise, **a3S**, **a4S** and **a3S'** were obtained from **d1S**. Worth to note distorted square pyramid structures were less stable than trigonal bipyramidal ones. In the latter, the amino group occupies one apical position and the amido ligand an axial one, while it

seems that different combinations of the ancillary ligands provide structures with comparable energies. For the sake of completeness the whole set of trigonal bipyramidal structures were calculated including both atropisomers of each type (Figure S10b).

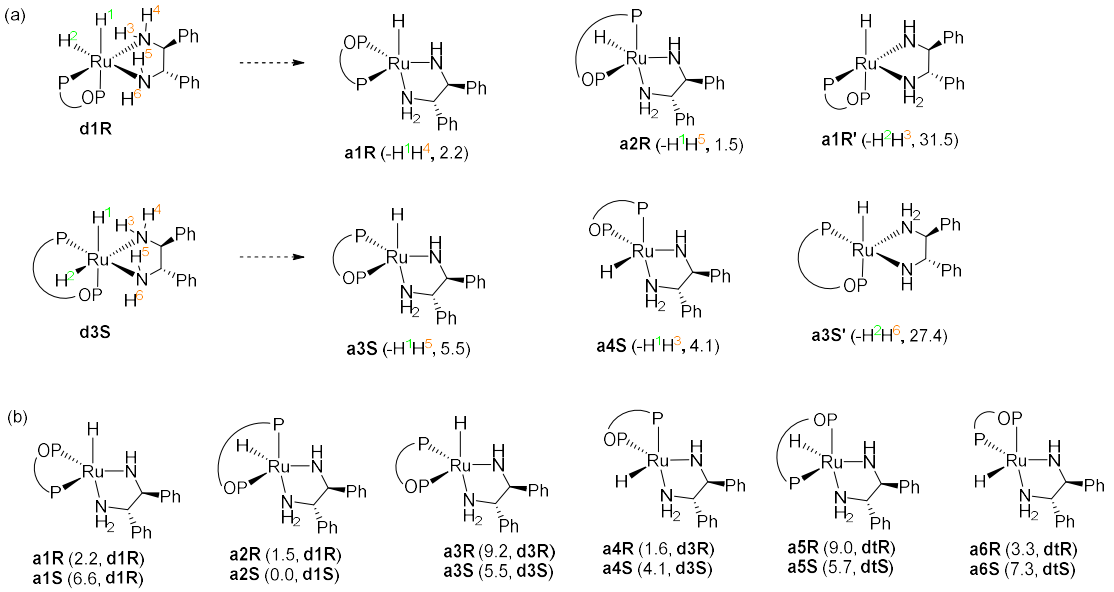

Figure S10. Generation of amido-hydride complexes by formal abstraction of a hydride and a NH_2 synperiplanar proton of **d1R** or **d3S** (a). Structures of amido-hydride complexes of types **a1**-**a6**, including both atropisomers for each type (b). Free energies in kcal mol^{-1} referred to **a2S**.

Intermediate agostic complexes in the hydride transfer step. IRC analysis from **TS1-d1R-RP-5a** and **TS1-d3S-SP-5a** lead in the product direction to ion pair species (**ag-*pro-R*** and **ag-*pro-S***, respectively) stabilized by a strong agostic interaction, in which the Ru···H-C fragment is characterized by a relatively short Ru-H distance (1.903 and 1.899 Å, Figure S11) and a long C-H one (1.228 and 1.223 Å). Thus, no complete hydride transfer is observed in these species. A scan of the lengthening of the Ru···H distance shows a very small grow in energy (Figure S12), being ΔE = 0.15 kcal mol^{-1} at 1.963 Å. After this point, energy abruptly decreases and a minimum is found at 2.038 Å. Minimization of this structure led to **ip-*pro-R*** structure, which is characterized by a weaker agostic interaction with Ru···H distance of 2.031 Å and C-H one of 1.201 Å. An analogous behavior was observed in the case of **ag-*pro-S***, leading to corresponding

ip-*pro-S* structure. All attempts to find a TS from the maximum of the scan were unsuccessful.

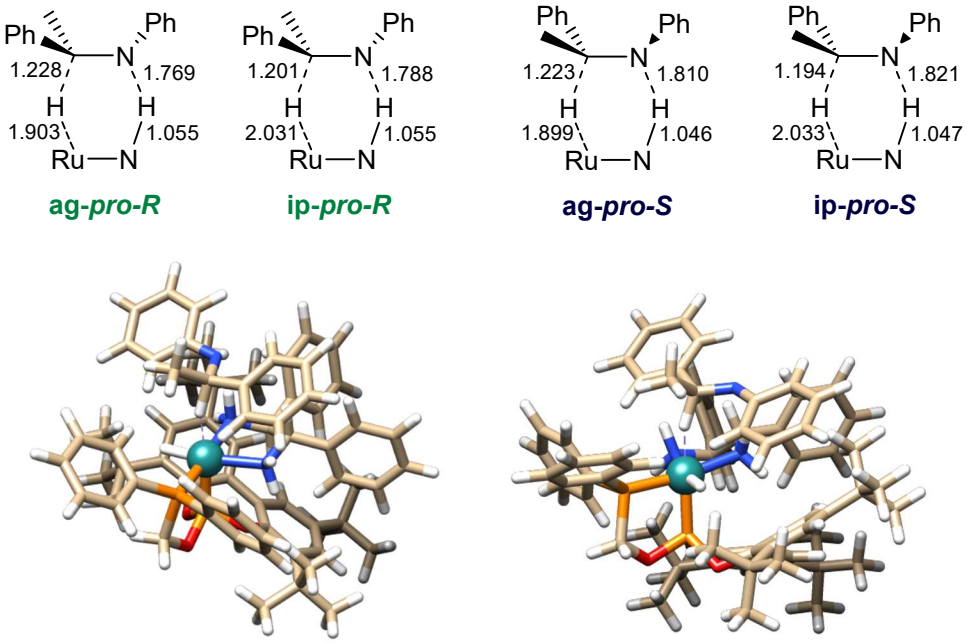

Figure S11. Selected distances of ion pair species (top). Structures of **ag-*pro-R*** (bottom left) and **ag-*pro-S*** (bottom right) complexes.

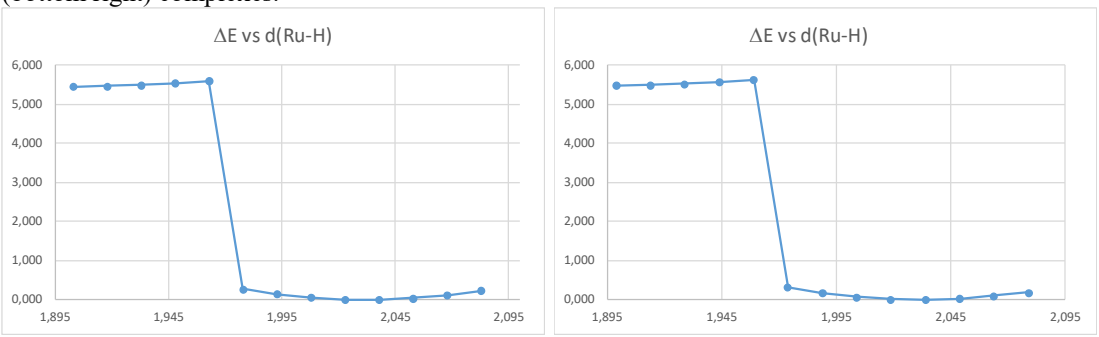

Figure S12. Energy profile scan of of the Ru-H distance from **ag-*pro-R*** (left) and **ag-*pro-S*** (right) structures to **ip-*pro-R*** and **ip-*pro-S***, respectively.

Conversion of ip-*pro-R* in N1R. Several attempts have been made to locate the transition state in the conversion of **ip-*pro-R*** into **N1R** by the scan of different structural parameters (e.g. release of the Ru-H distance, approach of N product to the metal). Among them, opening of the N-C-H angle (α, Figure S13) showed a clean scan starting at **ip-*pro-R*** and finishing at **N1R**. This shows an estimation of ΔE = 6.4 kcal mol^{-1} over **ip-*pro-R***. Use of the maximum of the scan to locate the corresponding TS was not successful. A frequency calculation of this maximum showed one imaginary frequency

(i74 cm^{-1}) and a free energy value of 4.0 kcal mol^{-1} over the starting ion-pair could be estimated.

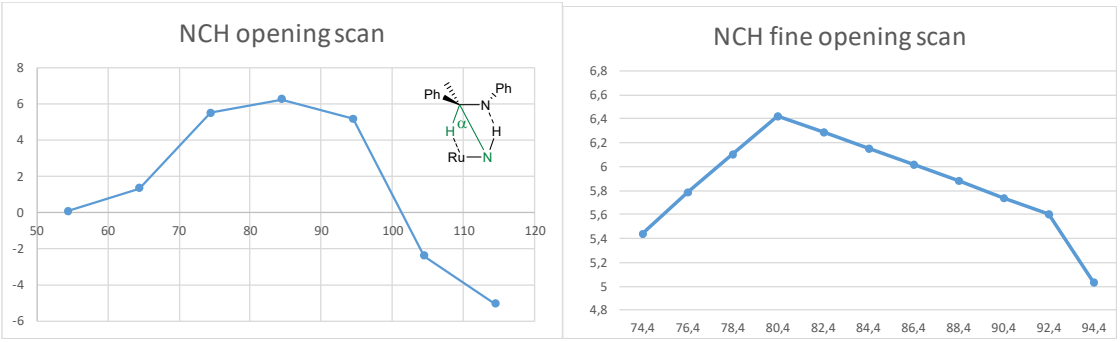

Figure S13. Energy profile of the scan of α angle from **ip-*pro-R***. (E values are referenced to **ip-pro-*R***).

Further comments on the hydrogen activation pathways from ip-*pro-R* and a1R. To complement the activation pathway from **a1R-R-6a** shown in the main text (Figure 14), below are provided more details in the hydrogenation pathways by **ip-*pro-R*** and **a1R**. Free energy and electronic energy values are referenced to **a1R** + ***R*-6a** + H_2.

As mentioned, **TS3c** shows a significantly free energy barrier, while corresponding IRC analysis in the product direction leads to an adduct between **d1R** and *R*-**6a** (Figure S14). From a scan of the approaching of H_2 to **ip-pro-*R*** complex it is possible to locate a hydrogen complex (**ip-pro-*R*-H$_2$**; ΔG = 1.4 kcal mol^{-1}, ΔE = -29.4 kcal mol^{-1}, Figure S15), being 14.9 kcal mol^{-1} in free energy below **TS3c**. Moreover, an inspection of the H_2 activation in this compound shows a barrier lower than 1 kcal/mol leading to the dihydride amine complex. Therefore, most of the cost in accessing **TS3c** seems associated to the separation of the components of the ion pair by a slightly coordinating H_2. Worth to note, comparison between structures of **ip-pro-*R*** and **ip-pro-*R*-H$_2$** indicates a shorter C-H (1.110 vs 1.201 Å) and a longer C-N (1.448 vs 1.394 Å) distances of the product amido fragment in the second case, indicative of completion of hydride transfer in **ip-*pro*-*R*-H$_2$**.

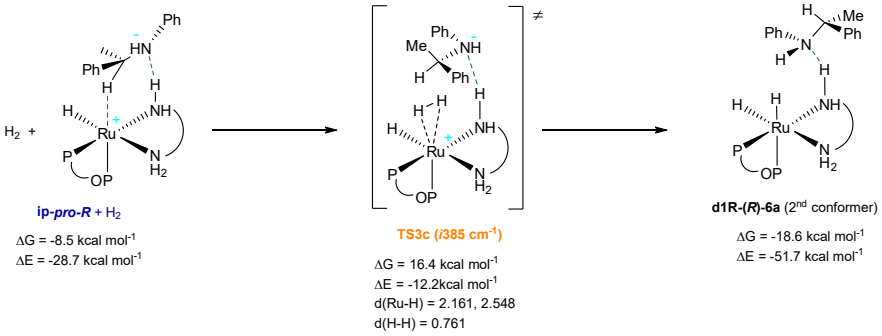

Figure S14. Hydrogen activation by **ip-pro-*R***.

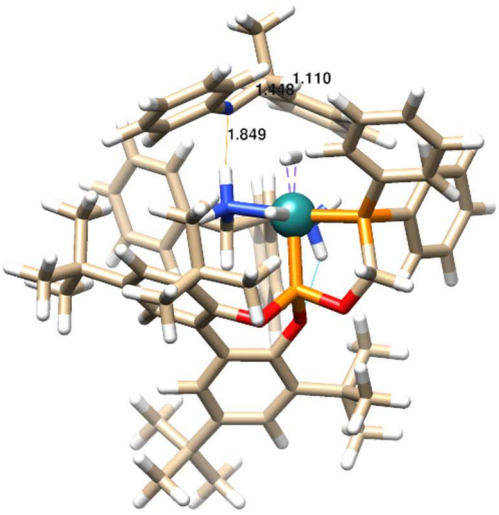

Figure S15. Structure of **ip-*pro*-*R*-H$_2$**.

On the other hand, hydrogen coordination and activation by **a1R** (Figure S16) shows a similar pathway to that described for **a1R-*R*-6a** in the main text. Thus, hydrogen interaction with **a1R** starts with **TS3d**, with a $\Delta G^{\neq}$ = 9.8 kcal mol^{-1}. The latter leads to a loose hydrogen complex **H1R-l** characterized by d(Ru-H) distances of 2.131 and 2.206 Å, which shows little interaction between the metal atom and dihydrogen (d(H-H) = 0.769 Å). Coordination pathway is followed by **TS3e** and then by a tight hydrogen complex, characterized **H1R-t** by d(Ru-H) distances of 1.777 and 1.814 Å, while d(H-H) = 0.824 Å. This complex has a ΔG = 12.1 kcal mol^{-1} with respect to **a1R** and H_2, in line with literature precedents.[S27]

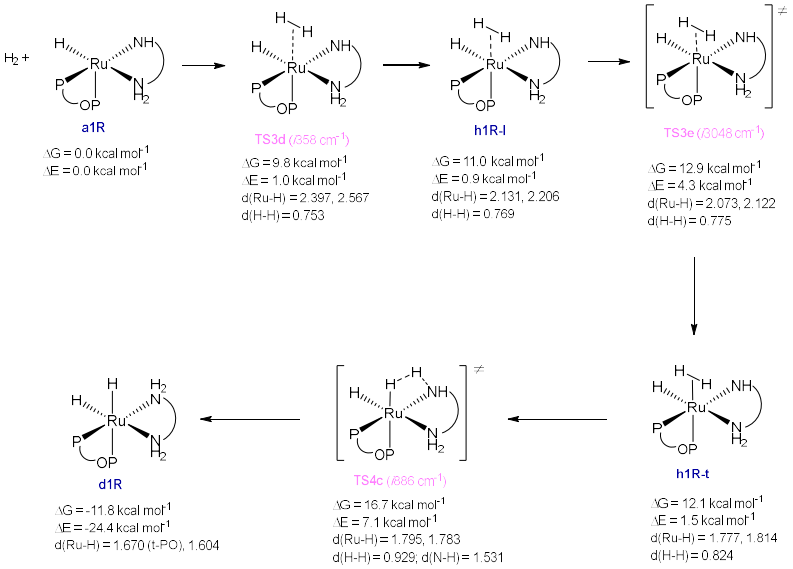

Figure S16. Hydrogen coordination/activation pathway by **a1R**.

References

S1. (a) M. Vaquero, A. Suárez, S. Vargas, G. Bottari, E. Álvarez and A. Pizzano, *Chem. Eur. J.*, 2012, **18**, 15586; (b) P. Kleman, M. Vaquero, I. Arribas, A. Suárez, E. Álvarez and A. Pizzano, *Tetrahedron Asymmetry*, 2014, **25**, 744.

S2. In our original report of complex Ru(Cl)$_2$(**2a**)(**3a**)[S1b] data in solution corresponded to *trans* isomer (**1a** in the present paper), while X-ray diffraction study corresponded to a *cis* isomer (*cis*-**1a** in the present paper). This uncorrect correlation was probably due to some isomerization in solution of **1a**, studied in the present contribution, along with a much better crystallinity of *cis*-**1a**.

S3. J. S. M. Samec and J.-E. Bäckvall, *Chem. Eur. J.*, 2002, **8**, 2955.

S4. E. de Julián, E. Menéndez-Pedregal, M. Claros, M. Vaquero, J. Díez, E. Lastra, P. Gamasa and A. Pizzano, *Org. Chem. Front.*, 2018, **5**, 841.

S5. W. Li, G. Hou, M. Chang and X. Zhang, *Adv. Synth. Catal.*, 2009, **351**, 3123.

S6. S. Zhou, S. Fleischer, K. Junge and M. Beller, *Angew. Chem. Int. Ed.*, 2011, **50**, 5120.

S7. (a) Bruker *APEX2*; Bruker AXS, Inc.; Madison, WI, 2007. (b) Bruker Advanced X-ray solutions. *SAINT* and *SADABS* programs. Bruker AXS Inc. Madison, WI, 2004.

S8. M. C. Burla, M. Camalli, B. Carrozzini, G. L. Cascarano, C. Giacovazzo, G. Polidori, and R. Spagna, *J. Appl. Crystallogr.* 2003, **36**, 1103.

S9. A. L. Spek, *J. Appl. Crystallogr.*, 2003, **36**, 7.

S10. P. v. d. Sluis and A. L. Spek, *Acta Crystallogr., Sect. A*. 1990, **46**, 194.

S11. J. W. Faller and P. P. Fontaine, *J. Organomet. Chem.*, 2007, **692**, 1110.

S12. (a) H. D. Flack, G. Bernardinelli, *Chirality* 2008, **690**, 681; (b) A. Linden, *Tetrahedron: Asymmetry*, 2017, **28**, 1314.

S13. H. D. Flack, *Physical and Spectrometric Analysis : Absolute Configuration Determination by X-Ray Crystallography*; in Comprehensive Chirality, Volume 8, Chapter 8.33. Elsevier Ltd., 2012.

S14. Gaussian 09, Revision E.01, M. J. Frisch, G. W. Trucks, H. B. Schlegel, G. E. Scuseria, M. A. Robb, J. R. Cheeseman, G. Scalmani, V. Barone, B. Mennucci, G. A. Petersson, H. Nakatsuji, M. Caricato, X. Li, H. P. Hratchian, A. F. Izmaylov, J. Bloino, G. Zheng, J. L. Sonnenberg, M. Hada, M. Ehara, K. Toyota, R. Fukuda, J. Hasegawa, M. Ishida, T. Nakajima, Y. Honda, O. Kitao, H. Nakai, T. Vreven, J. A. Montgomery, Jr., J. E. Peralta, F. Ogliaro, M. Bearpark, J. J. Heyd, E. Brothers, K. N. Kudin, V. N. Staroverov, T. Keith, R. Kobayashi, J. Normand, K. Raghavachari, A. Rendell, J. C. Burant, S. S. Iyengar, J. Tomasi, M. Cossi, N. Rega, J. M. Millam, M. Klene, J. E. Knox, J. B. Cross, V. Bakken, C. Adamo, J. Jaramillo, R. Gomperts, R. E. Stratmann, O. Yazyev, A. J. Austin, R. Cammi, C. Pomelli, J. W. Ochterski, R. L. Martin, K. Morokuma, V. G. Zakrzewski, G. A. Voth, P. Salvador, J. J. Dannenberg, S. Dapprich, A. D. Daniels, O. Farkas, J. B. Foresman, J. V. Ortiz, J. Cioslowski, and D. J. Fox, Gaussian, Inc., Wallingford CT, 2013.

S15. A. D. Becke, *J. Chem. Phys.*, 1993, **98**, 5648.

S16. (a) J. P. Perdew, K. Burke, Y. Wang, *Phys. Rev. B.*, 1996, **54**, 16533; (b) K. Burke, J. P. Perdew, Y. Wang, in *Electronic Density Functional Theory: Recent Progress and New Directions*, Ed. J. F. Dobson, G. Vignale, and M. P. Das (Plenum, 1998).

S17. S. Grimme, S. Ehrlich and L. Goerigk, *J. Comp. Chem.*, 2011, **32**, 1456.

S18. (a) W. J. Hehre, K. Ditchfield, and J. A. Pople, *J. Chem. Phys.* **1972**, *56*, 2257; (b) P. C. Hariharan and J. A. Pople, *Theor. Chim. Acta*, **1973**, *28*, 213; (c) M. M. Francl, W. J. Pietro, W. J. Hehre, J. S. Binkley, M. S. Gordon, D. J. DeFrees and J. A. Pople, *J. Chem. Phys.*, **1982**, *77*, 3654.

S19. H. T. Andrae, D.; Häußermann, U.; Dolg, M.; Stoll, H.; Preuß, *Theor. Chim. Acta*, 1990, **77**, 123.

S20. F. Weigend, F. Furche and R. Ahlrichs, *J. Chem. Phys.* 2003, **119**, 12753.

S21. A. V Marenich, C. J. Cramer and D. G. Truhlar, *J. Phys. Chem. B.*, 2009, **113**, 6378.

S22. C. Gonzalez and B. Schlegel, *J. Chem. Phys.* 1989, **90**, 2154.

S23. T. Lu and F. Chen, *J. Comput. Chem.*, 2012, **33**, 580. http://sobereva.com/multiwfn/

S24. E. F. Pettersen, T. D. Goddard, C. C. Huang, G. S. Couch, D. M. Greenblatt, E. C. Meng and T. E. Ferrin, *J. Comput. Chem.* 2004, **25**, 1605. http://www.rbvi.ucsf.edu/chimera/

S25. W. Humphrey, A. Dalke and K. Schulten, *J. Molec. Graphics*, 1996, **14**, 33. http://www.ks.uiuc.edu/Research/vmd/

S26. (a) S. Kozuch and S. Shaik, *Acc. Chem. Res.*, 2011, **44**, 101; (b) A. Uhe, S. Kozuch and S. Shaik, *J. Comput. Chem.*, 2011, **32**, 978.

S27. P. A. Dub, N. J. Henson, R. L. Martin and J. C. Gordon, *J. Am. Chem. Soc.*, 2014, **136**, 3505.

$Ru(Cl)_2$(**2a**)(**3b**) (**1b**).

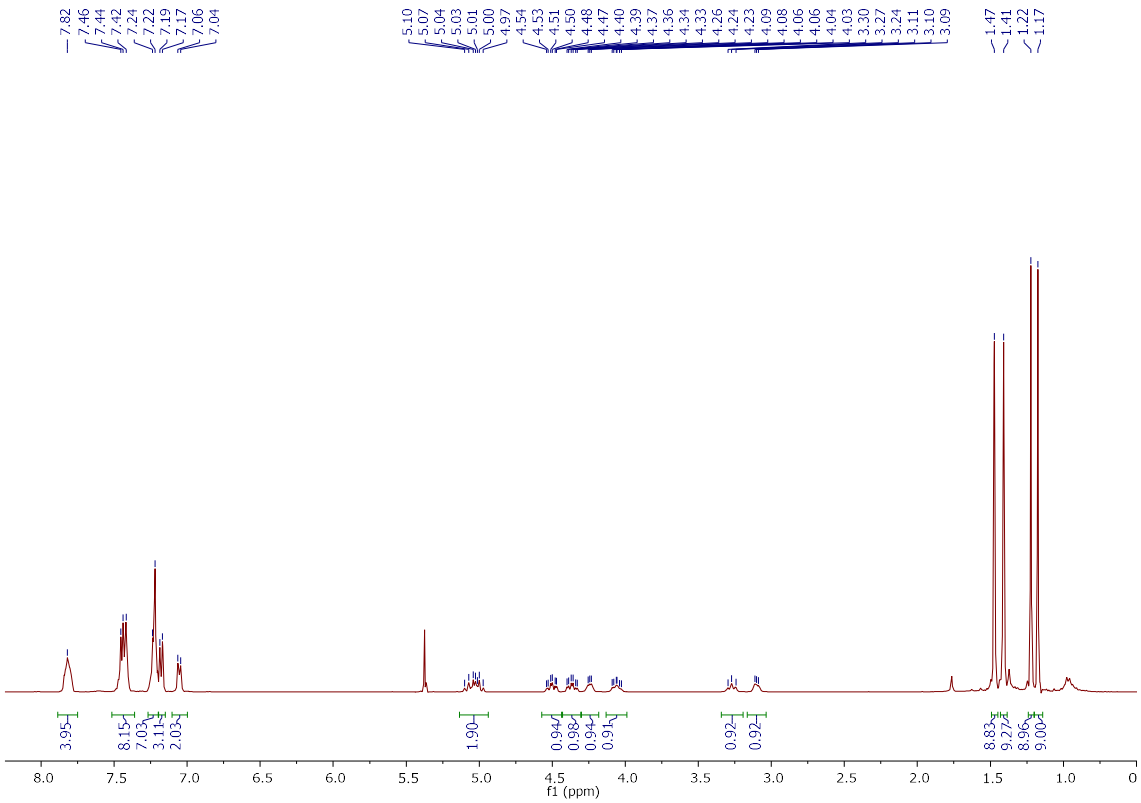

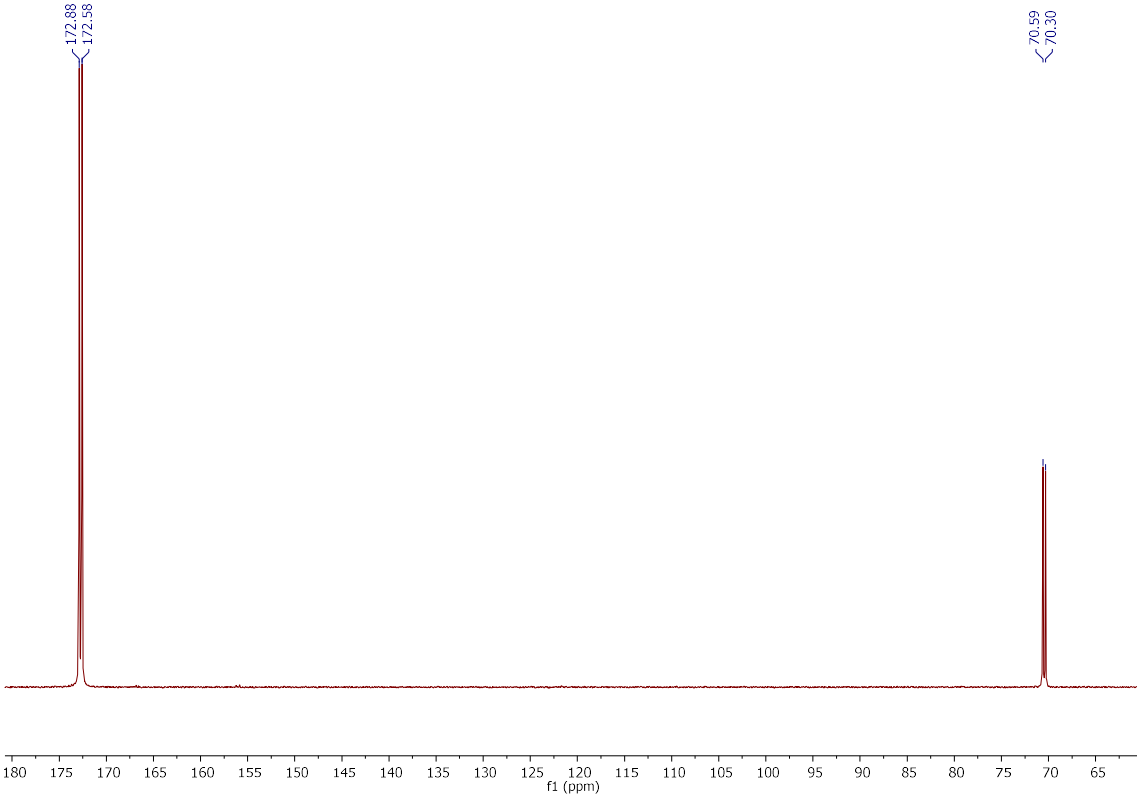

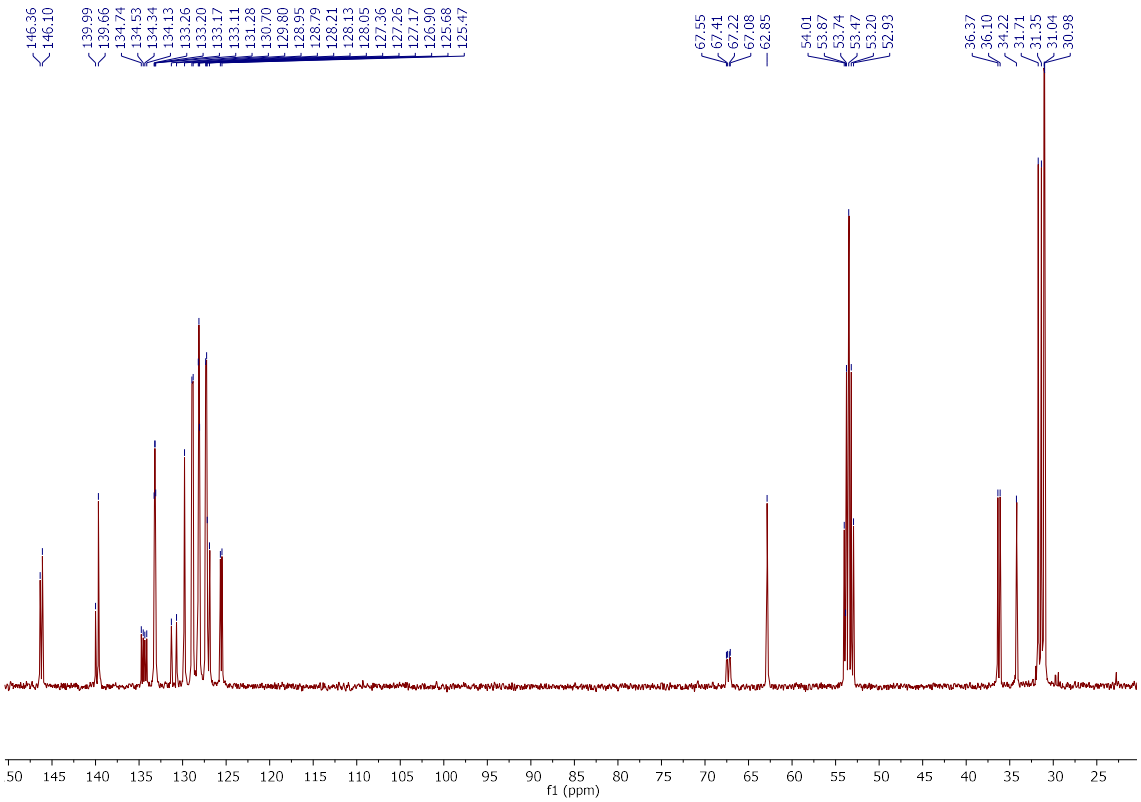

Ru(Cl)$_2$(**2b**)(**3b**) (**1c**)

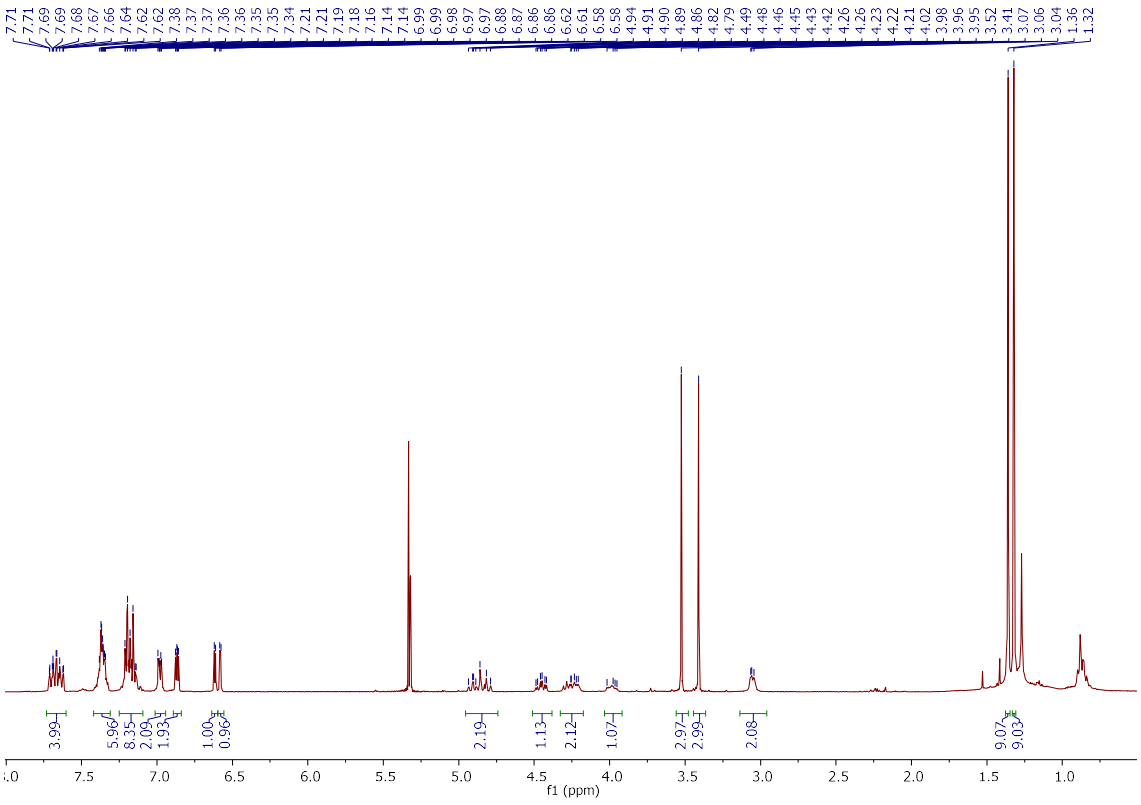

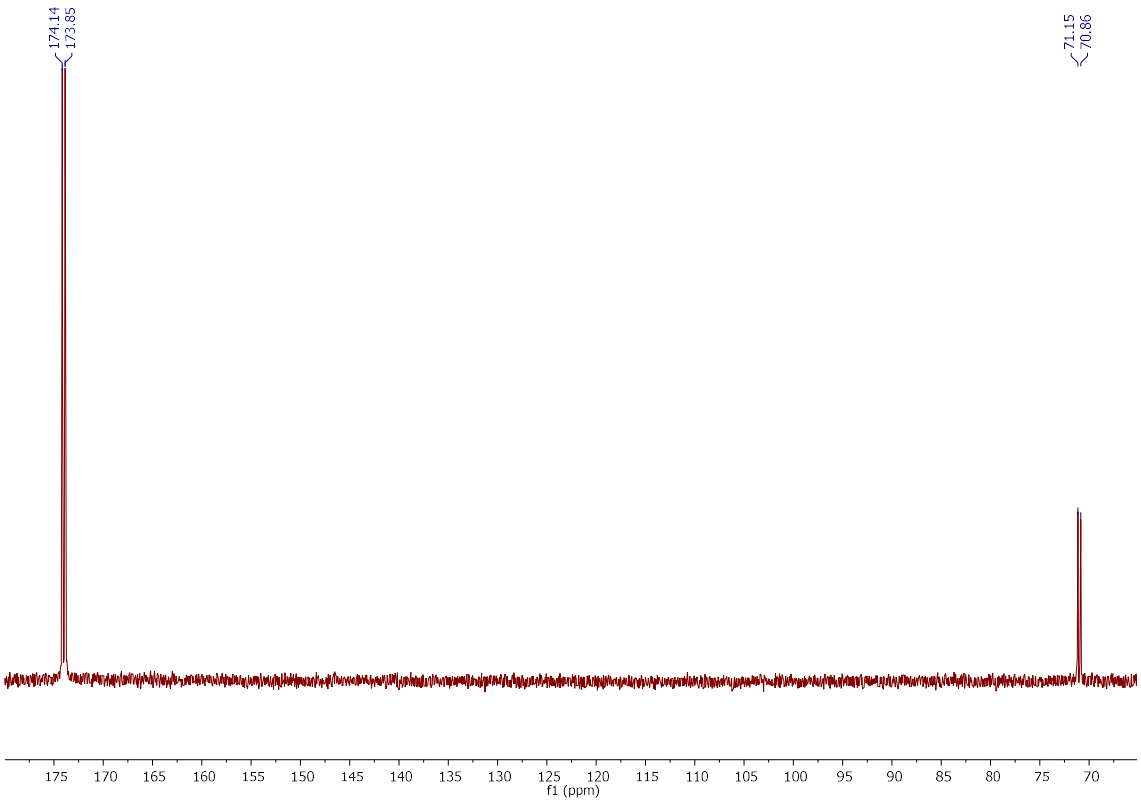
174.14
173.85
71.15
70.86
175 170 165 160 155 150 145 140 135 130 125 120 115 110 105 100 95 90 85 80 75 70
f1 (ppm)

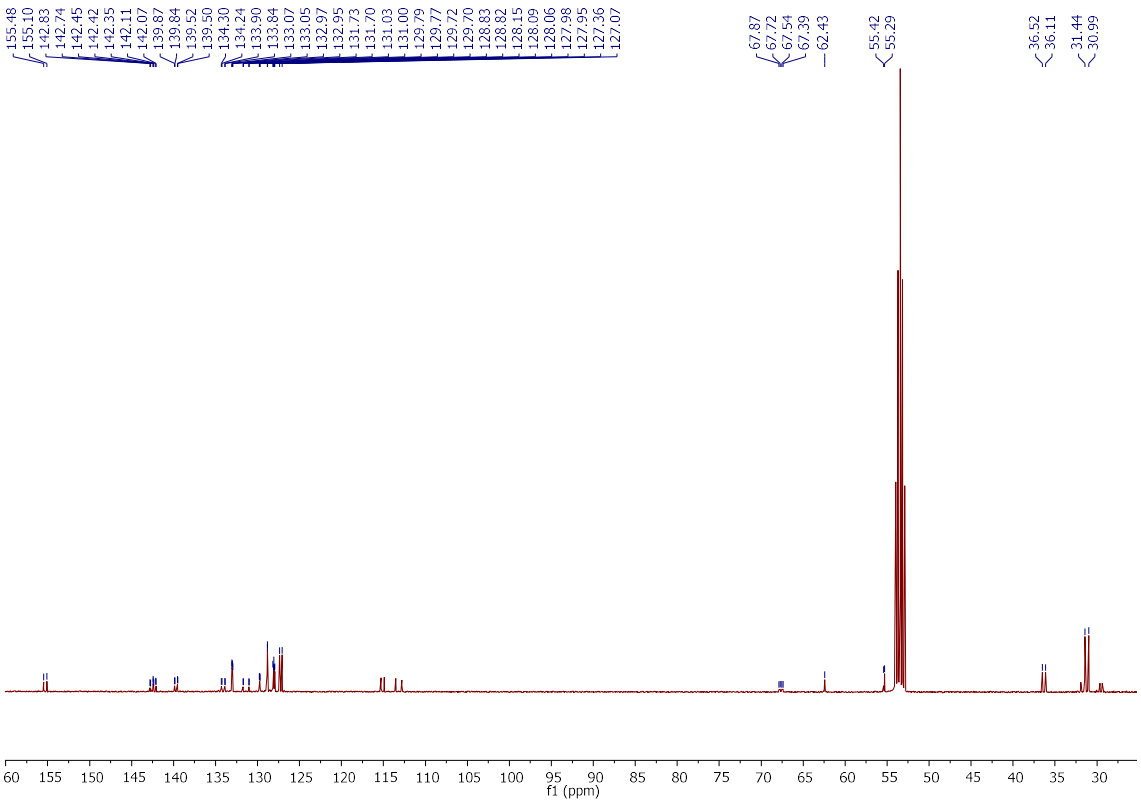
155.48
155.10
142.83
142.74
142.45
142.42
142.35
142.11
142.07
139.87
139.84
139.52
139.50
134.30
134.24
133.90
133.84
133.07
133.05
132.97
132.95
131.73
131.70
131.03
131.00
129.79
129.77
129.72
129.70
128.83
128.82
128.15
128.09
128.06
127.98
127.95
127.36
127.07
67.87
67.72
67.54
67.39
62.43
55.42
55.29
36.52
36.11
31.44
30.99
60 155 150 145 140 135 130 125 120 115 110 105 100 95 90 85 80 75 70 65 60 55 50 45 40 35 30
f1 (ppm)

$Ru(Cl)_2$(**2d**)(**3b**) (**1f**).

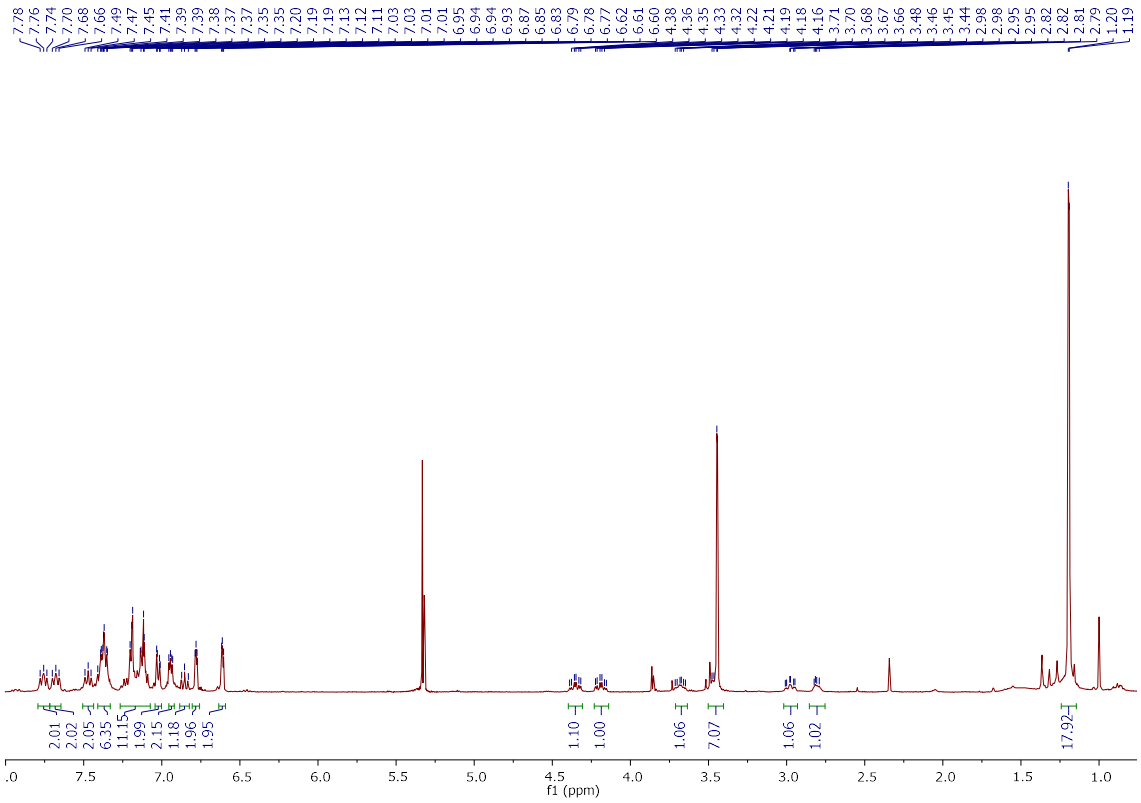

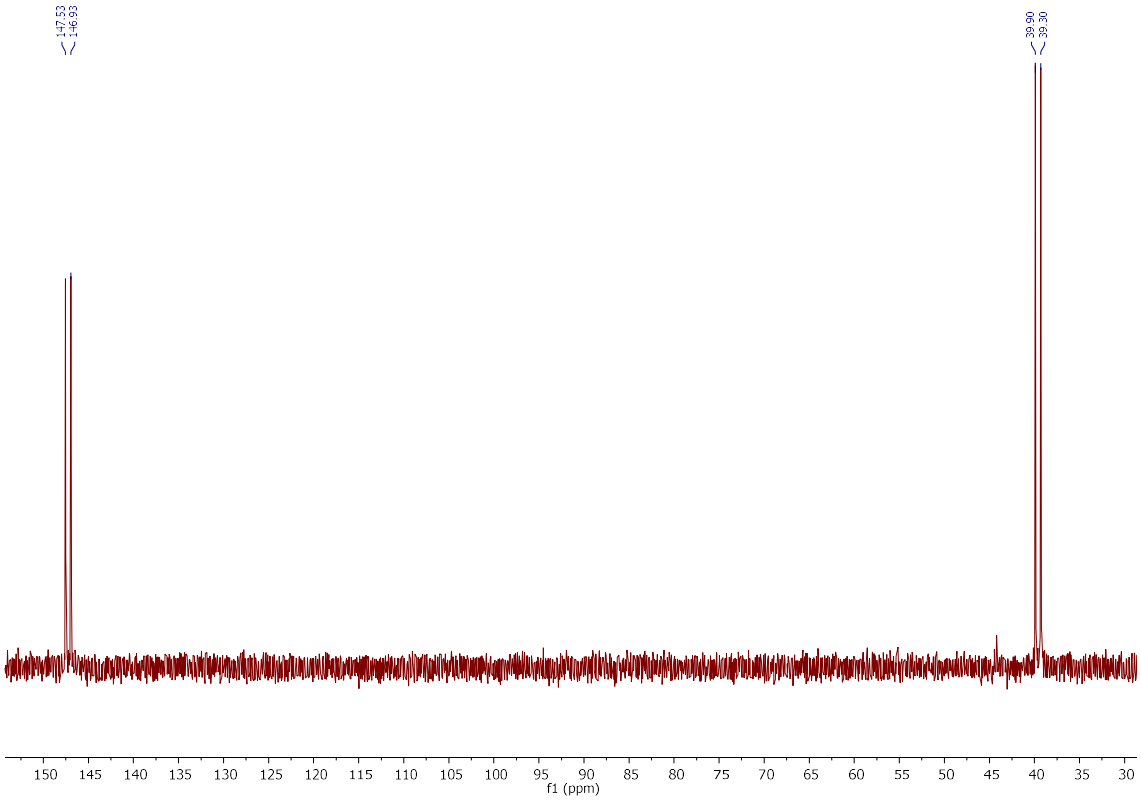

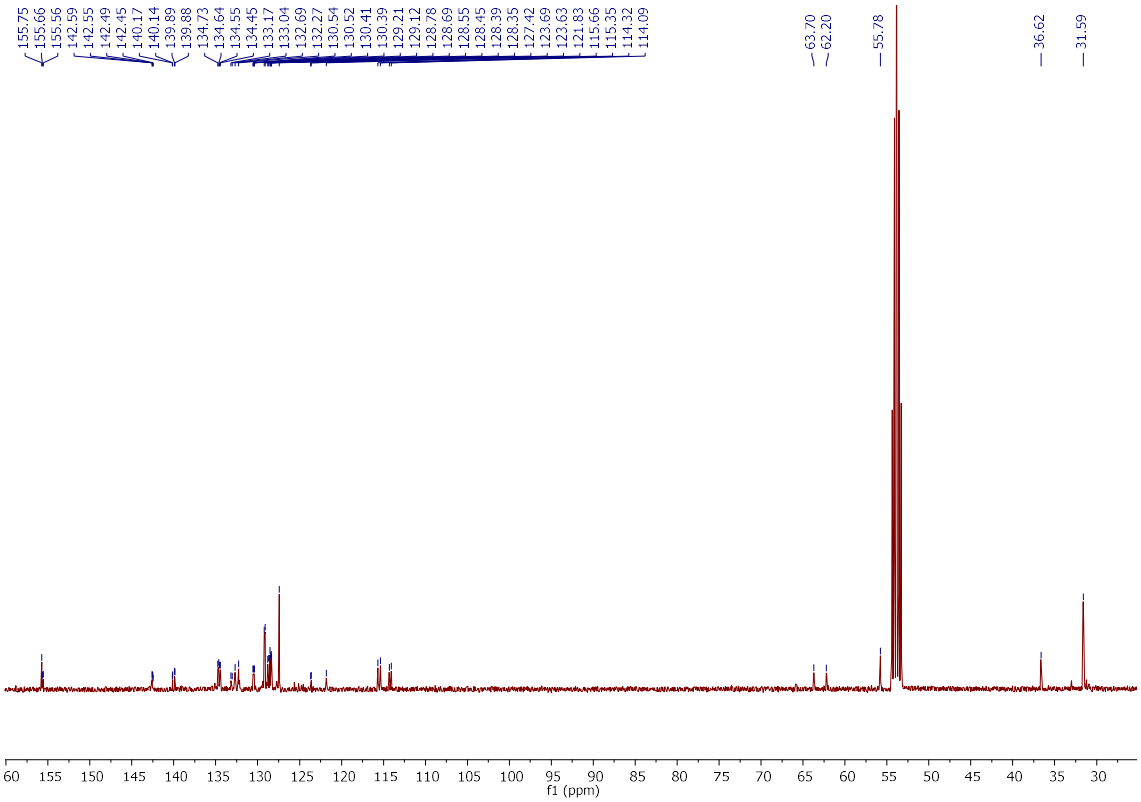

Ru(Cl)$_2$(**2e**)(**3a**) (**1g**).

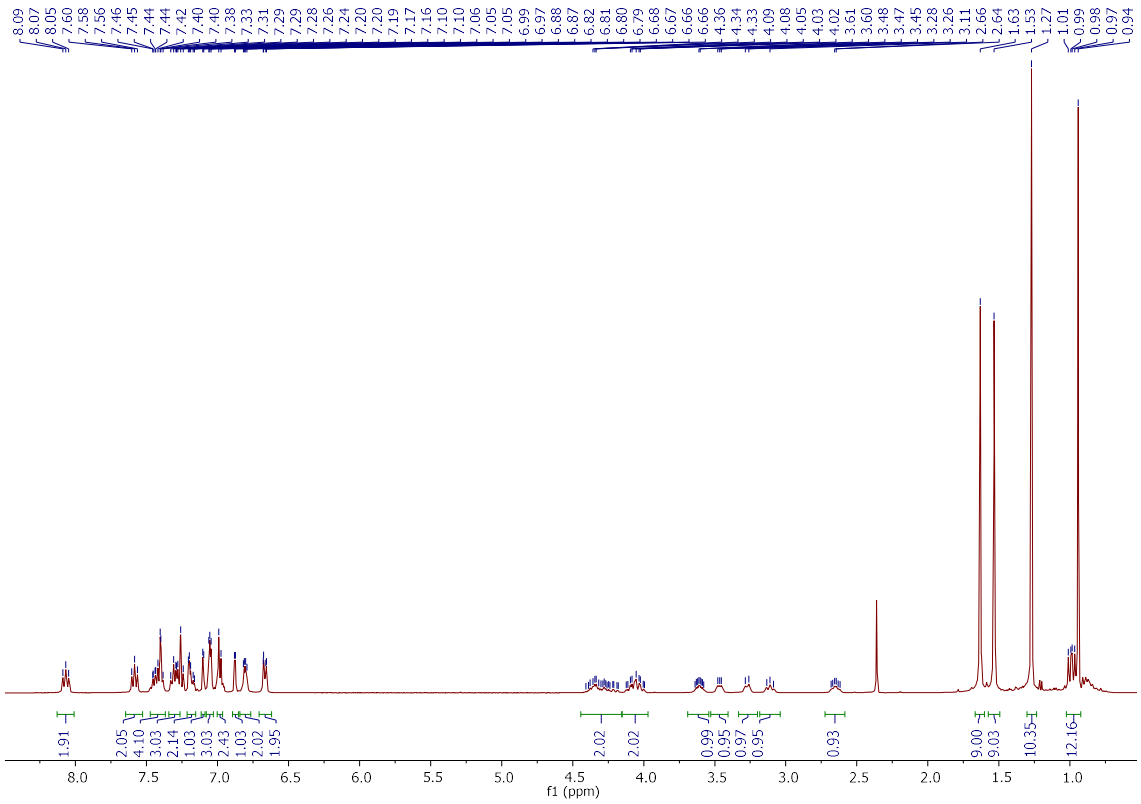

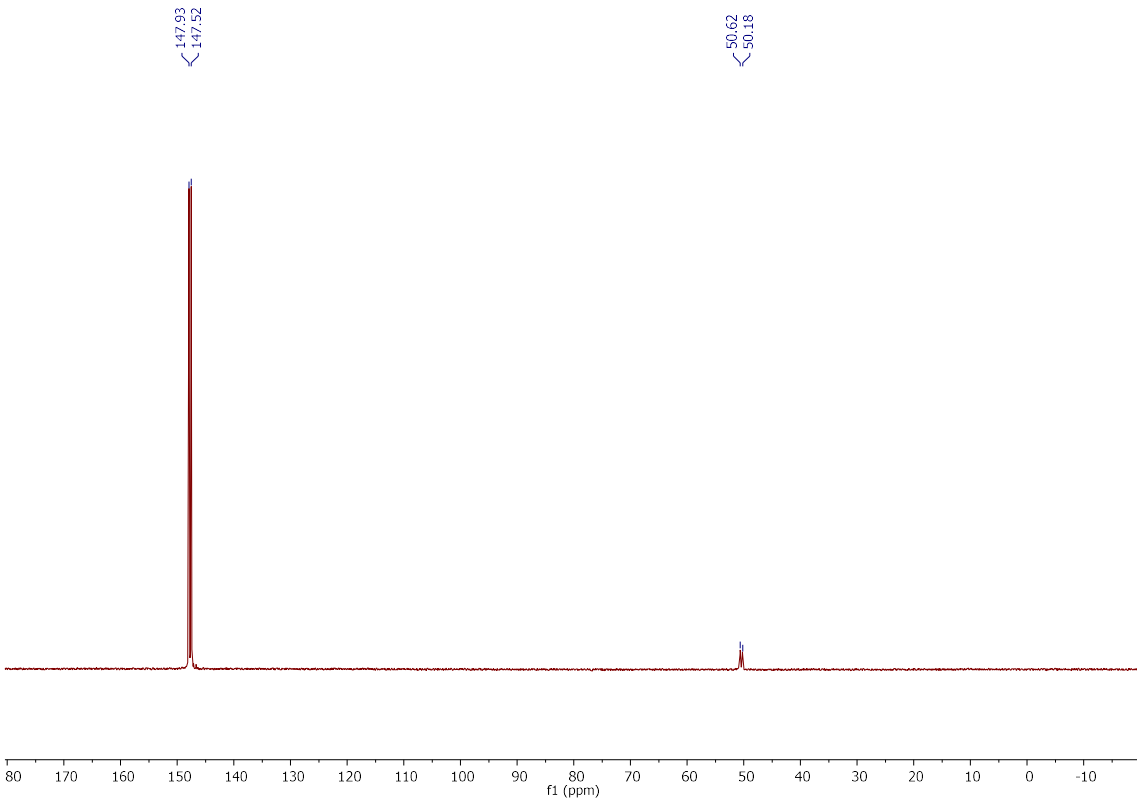
147.93
147.52
50.62
50.18
f1 (ppm)

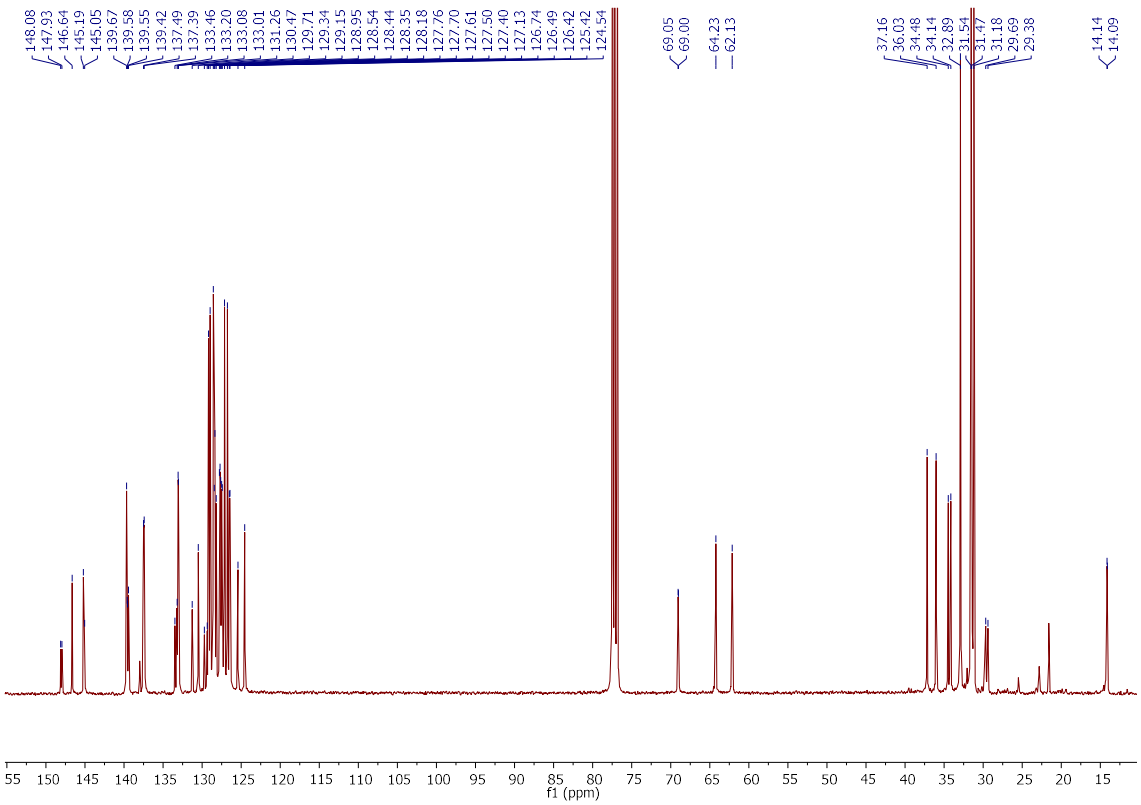
148.08
147.93
146.64
145.19
145.05
139.67
139.58
139.55
139.42
137.49
137.39
133.46
133.20
133.08
133.01
131.26
130.47
129.71
129.34
129.15
128.95
128.54
128.44
128.35
128.18
127.76
127.70
127.61
127.50
127.40
127.13
126.74
126.49
126.42
125.42
124.54
69.05
69.00
64.23
62.13
37.16
36.03
34.48
34.14
32.89
31.54
31.47
31.18
29.69
29.38
14.14
14.09
f1 (ppm)

$Ru(Cl)_2$(**2e**)(**3b**) (**1h**).

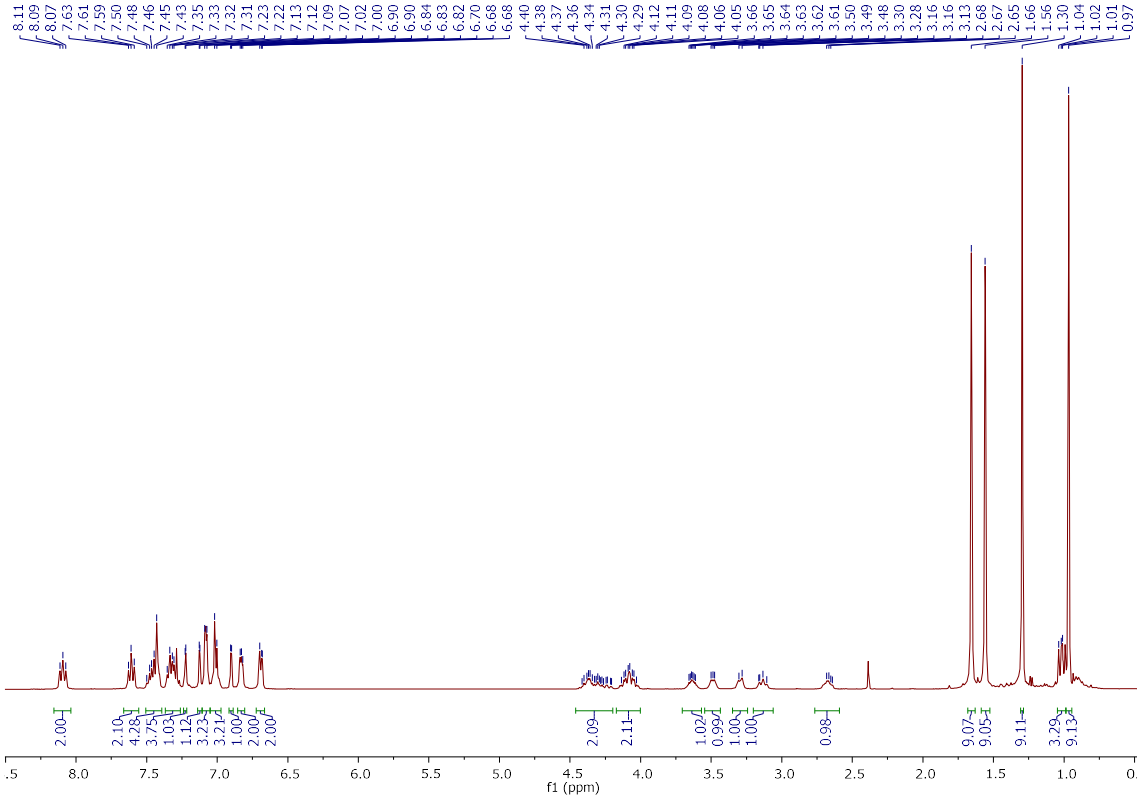

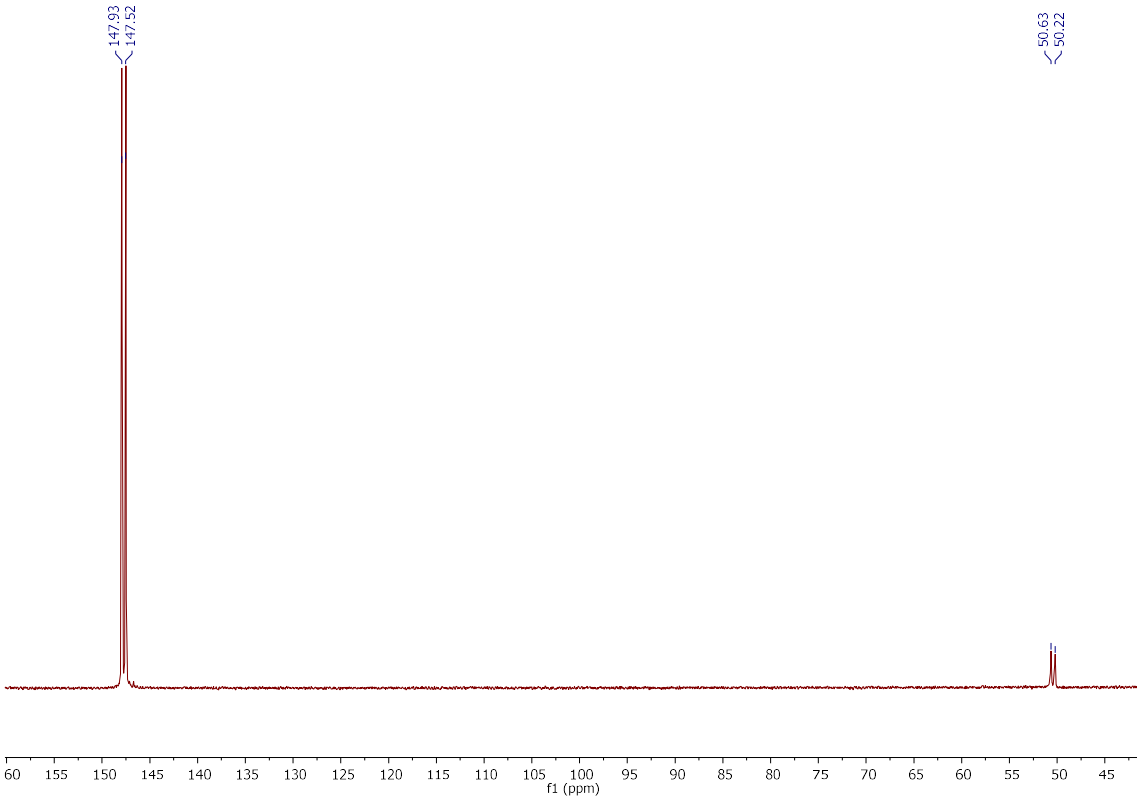

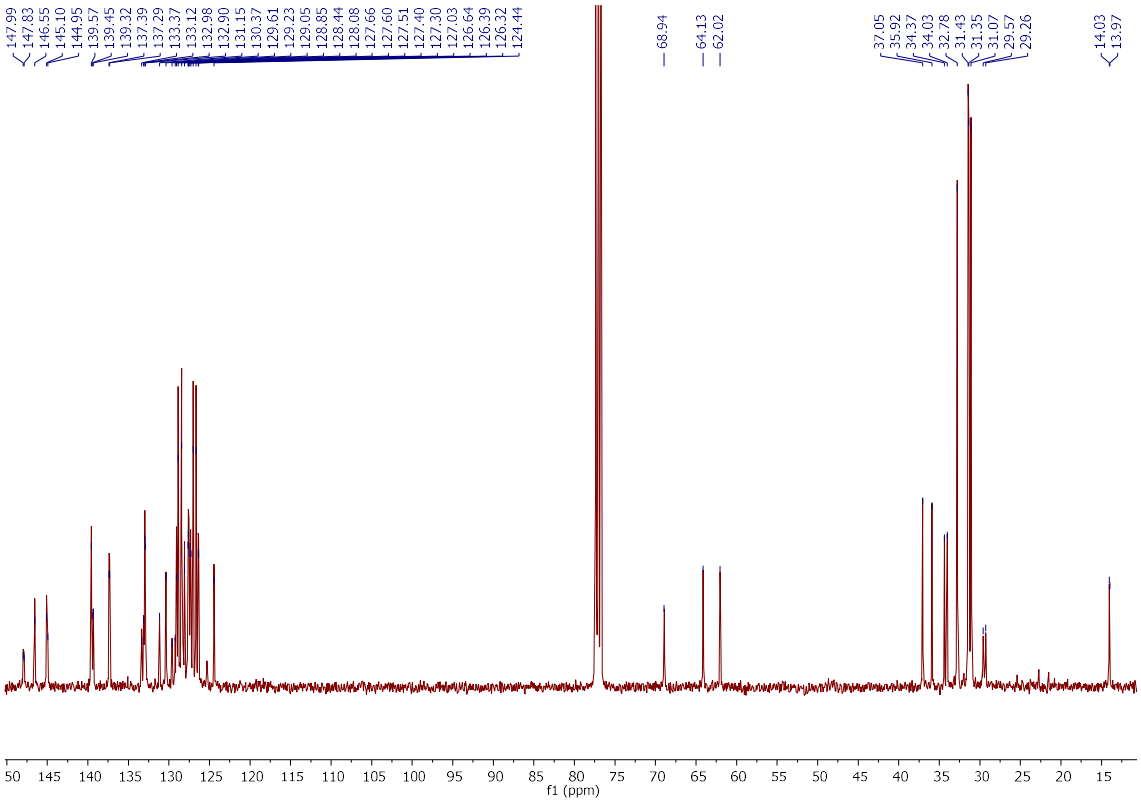

Ru(Cl)$_2$(**2c**)(**3c**) (**1i**)

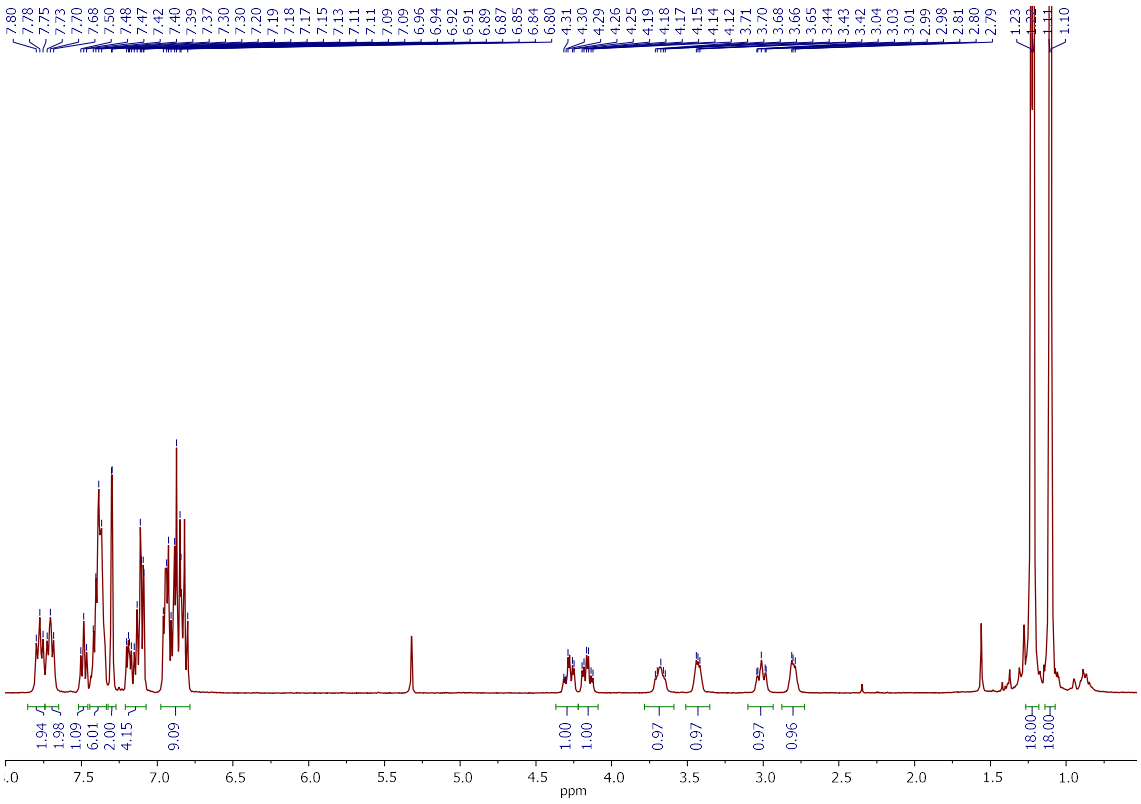

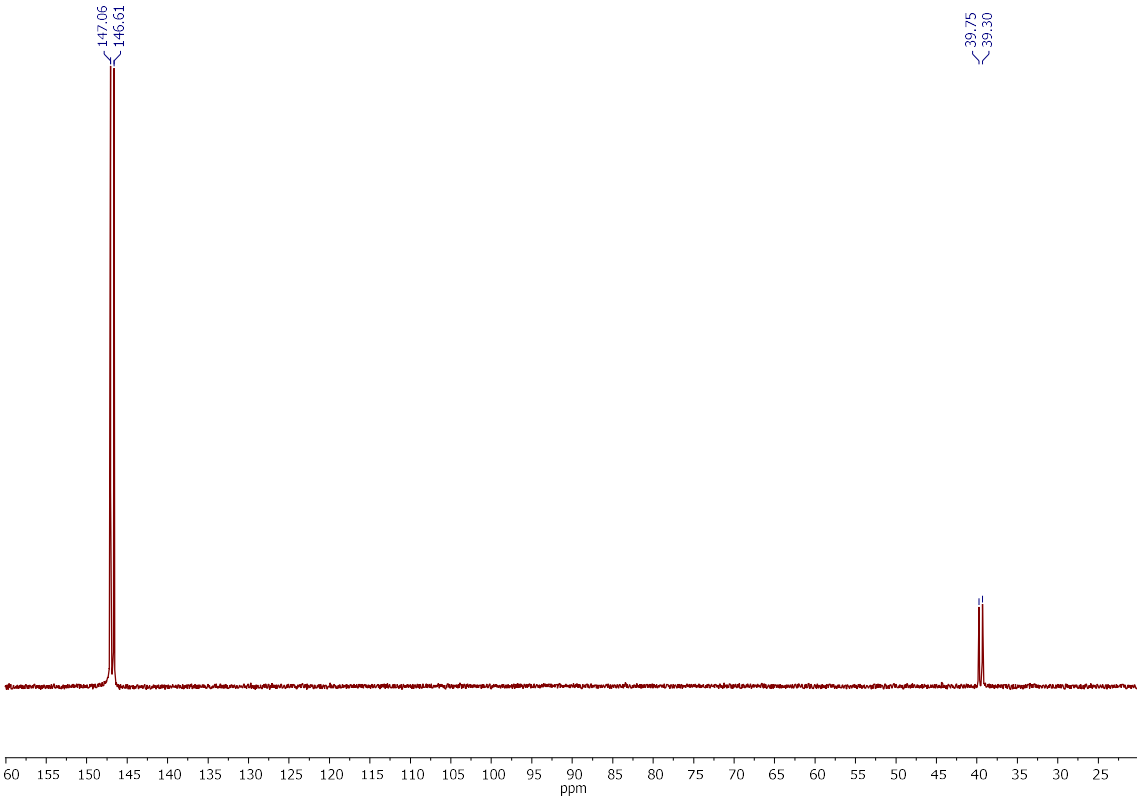
147.06
146.61
39.75
39.30
ppm

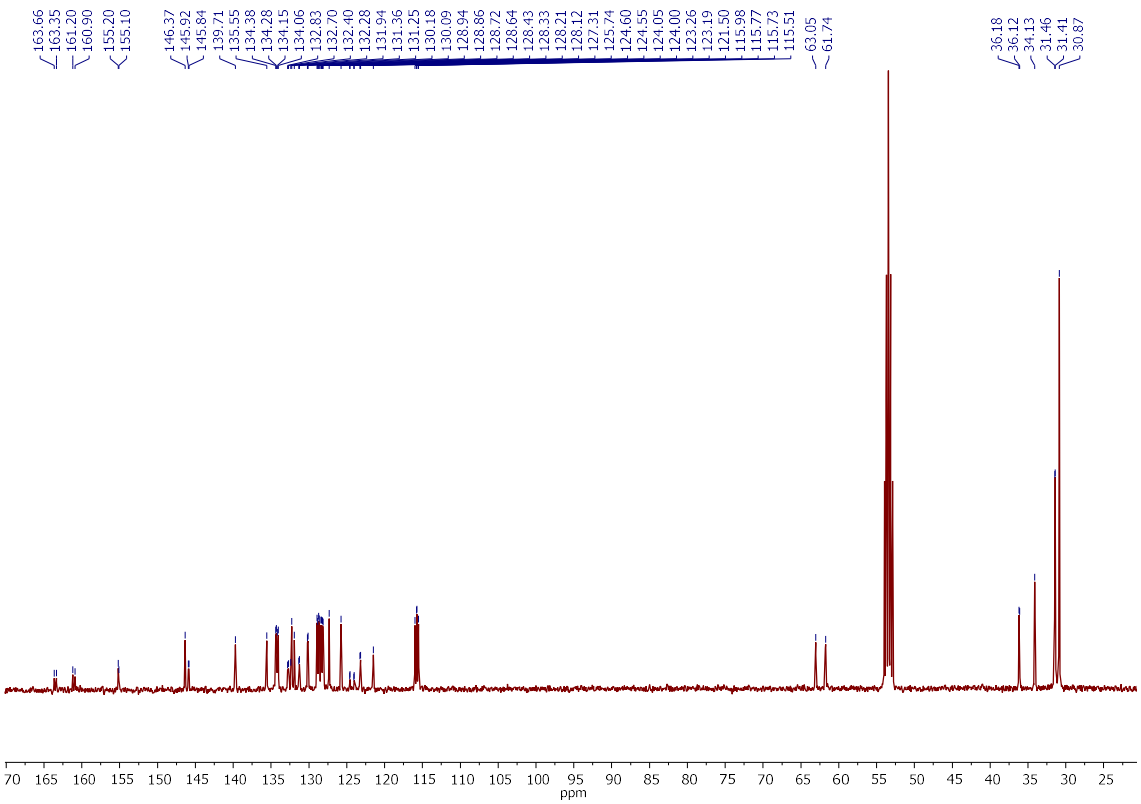
163.66
163.35
161.20
160.90
155.20
155.10
146.37
145.92
145.84
139.71
135.55
134.38
134.28
134.15
134.06
132.83
132.70
132.40
132.28
131.94
131.36
131.25
130.18
130.09
128.94
128.86
128.72
128.64
128.43
128.33
128.21
128.12
127.31
125.74
124.60
124.55
124.05
124.00
123.26
123.19
121.50
115.98
115.77
115.73
115.51
63.05
61.74
36.18
36.12
34.13
31.46
31.41
30.87
ppm

Ru(Cl)$_2$(**2c**)(**3d**) (**1j**)

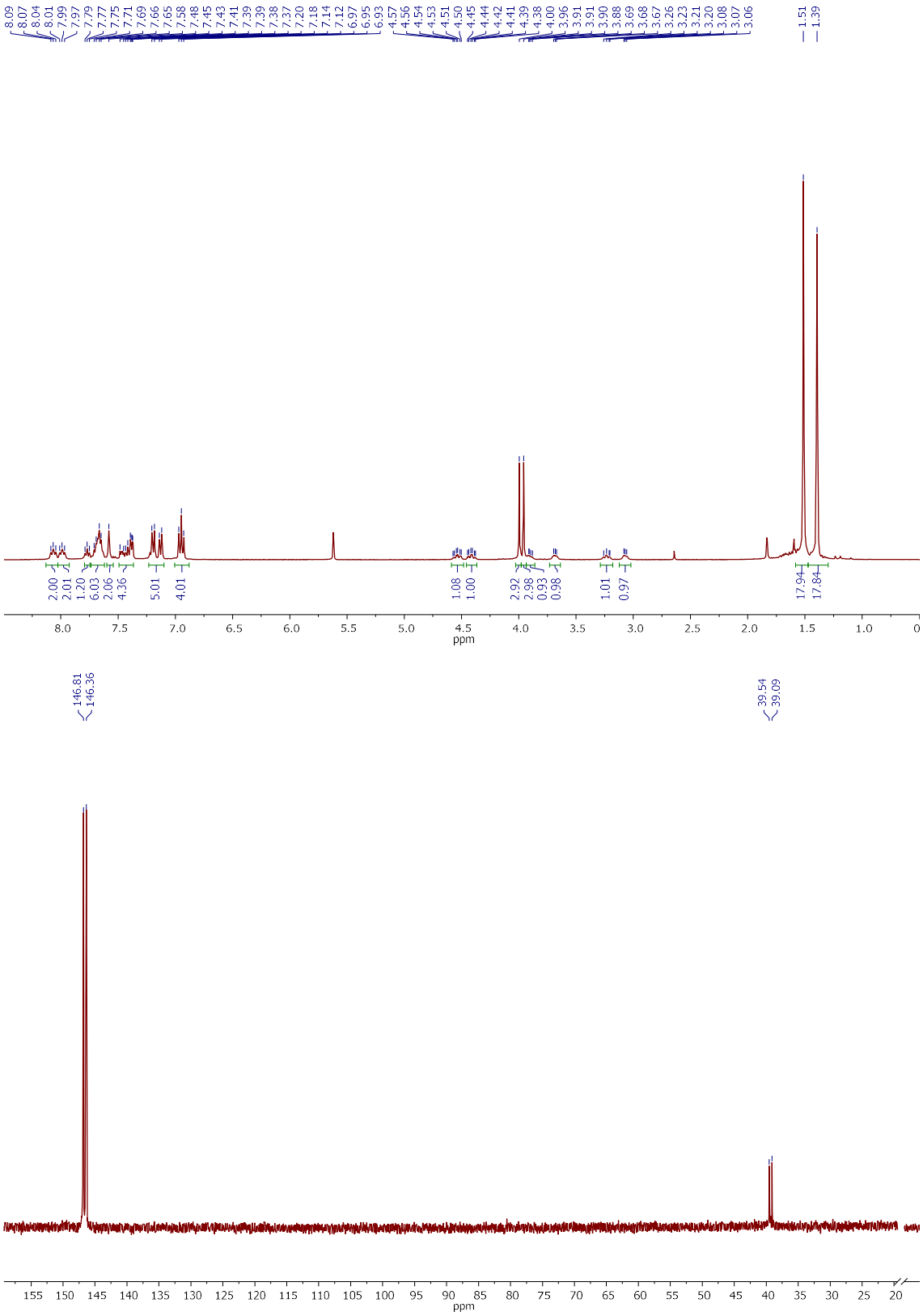

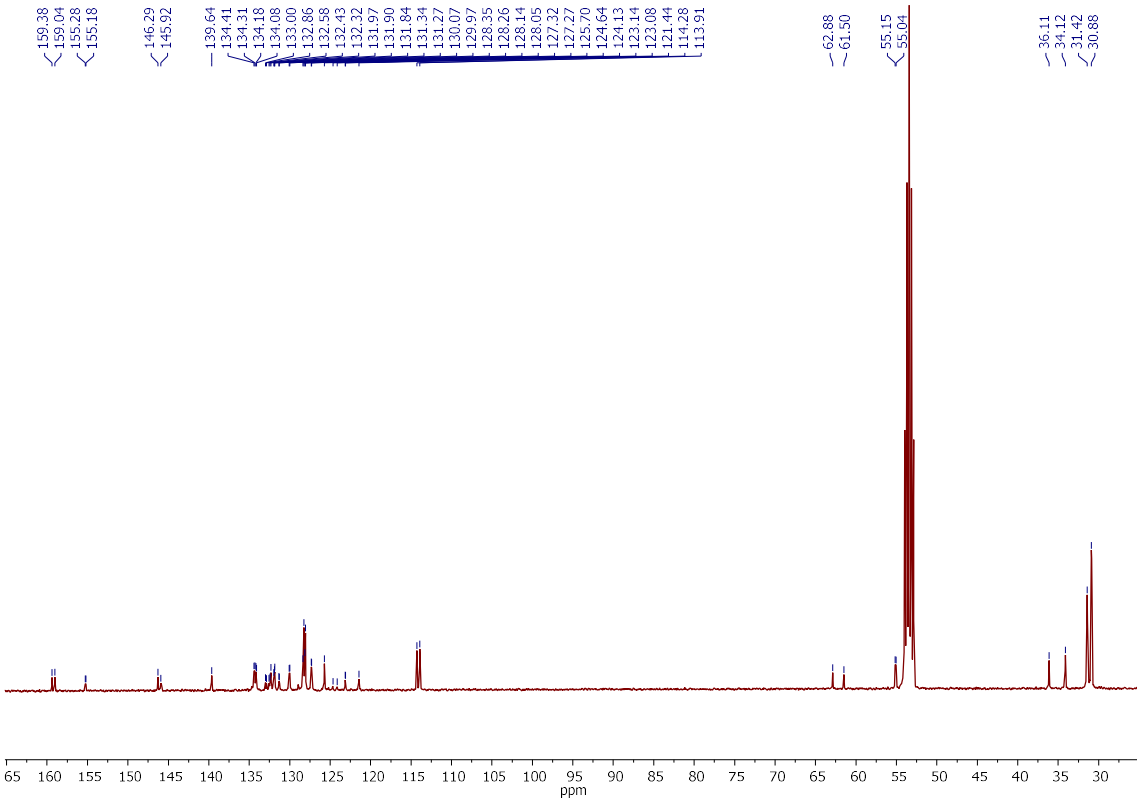
159.38
159.04
155.28
155.18
146.29
145.92
139.64
134.41
134.31
134.18
134.08
133.00
132.86
132.58
132.43
132.32
131.97
131.90
131.84
131.34
131.27
130.07
129.97
128.35
128.26
128.14
128.05
127.32
127.27
125.70
124.64
124.13
123.14
123.08
121.44
114.28
113.91
62.88
61.50
55.15
55.04
36.11
34.12
31.42
30.88
65 160 155 150 145 140 135 130 125 120 115 110 105 100 95 90 85 80 75 70 65 60 55 50 45 40 35 30
ppm

Ru(Cl)$_2$(**2c**)(**4**) (**1k**)

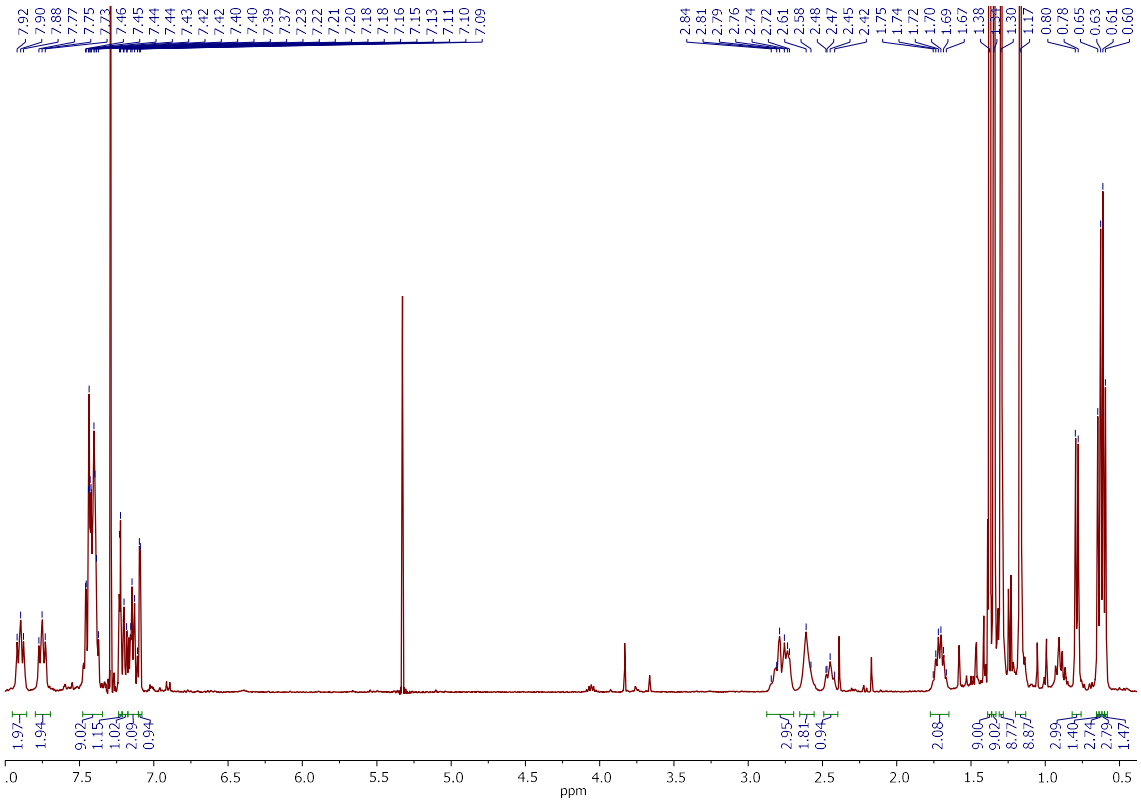
7.92
7.90
7.88
7.77
7.75
7.73
7.46
7.45
7.44
7.44
7.43
7.42
7.42
7.40
7.40
7.39
7.37
7.23
7.22
7.21
7.20
7.18
7.18
7.16
7.15
7.13
7.11
7.10
7.09
2.84
2.81
2.79
2.76
2.74
2.72
2.61
2.58
2.48
2.47
2.45
2.42
1.75
1.74
1.72
1.70
1.69
1.67
1.38
1.30
1.17
0.80
0.78
0.65
0.63
0.61
0.60
1.97
1.94
9.02
1.15
1.02
2.09
0.94
2.95
1.81
0.94
2.08
9.00
9.02
8.77
8.87
2.99
1.40
2.74
2.79
1.47
.0 7.5 7.0 6.5 6.0 5.5 5.0 4.5 4.0 3.5 3.0 2.5 2.0 1.5 1.0 0.5
ppm

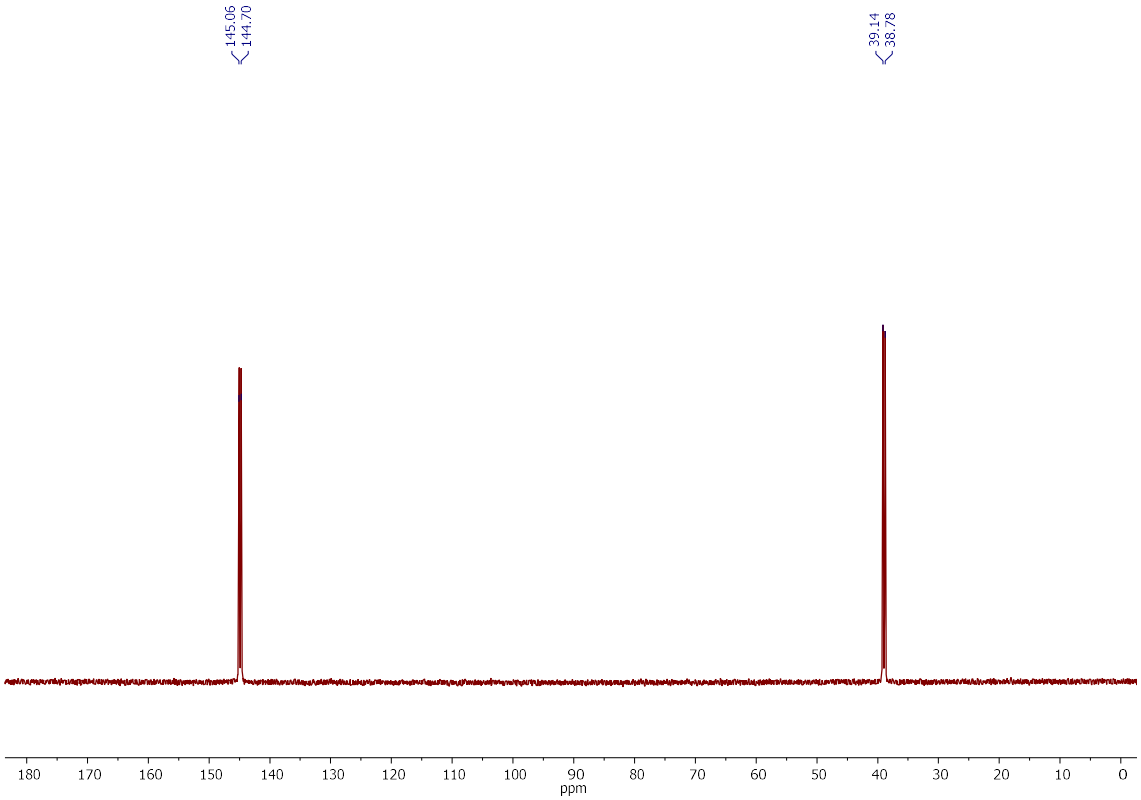
145.06
144.70
39.14
38.78
180 170 160 150 140 130 120 110 100 90 80 70 60 50 40 30 20 10 0
ppm

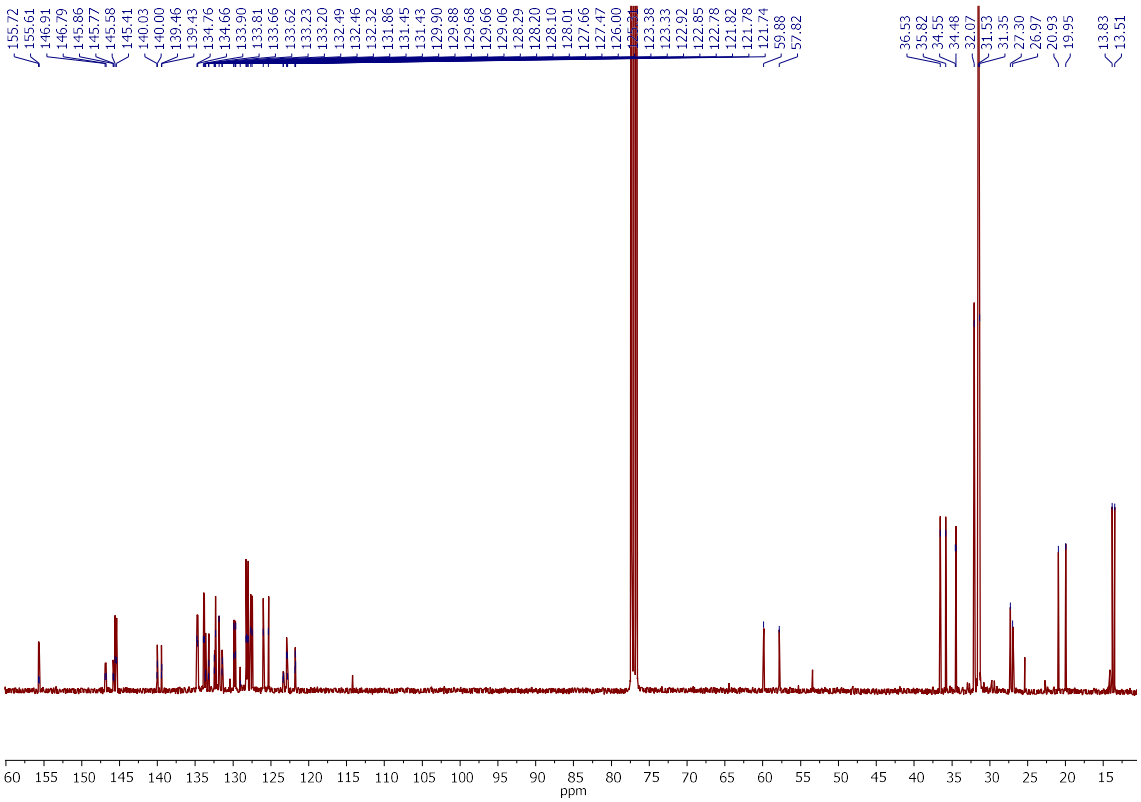
155.72
155.61
146.91
146.79
145.86
145.77
145.58
145.41
140.03
140.00
139.46
139.43
134.76
134.66
133.90
133.81
133.66
133.62
133.23
133.20
132.49
132.46
132.32
131.86
131.45
131.43
129.90
129.88
129.68
129.66
129.06
128.29
128.20
128.10
128.01
127.66
127.47
126.00
123.38
123.33
122.92
122.85
122.78
121.82
121.78
121.74
59.88
57.82
36.53
35.82
34.55
34.48
32.07
31.53
31.35
27.30
26.97
20.93
19.95
13.83
13.51
60 155 150 145 140 135 130 125 120 115 110 105 100 95 90 85 80 75 70 65 60 55 50 45 40 35 30 25 20 15
ppm

Isomerization of 1a

a) Mixture of diastereomers

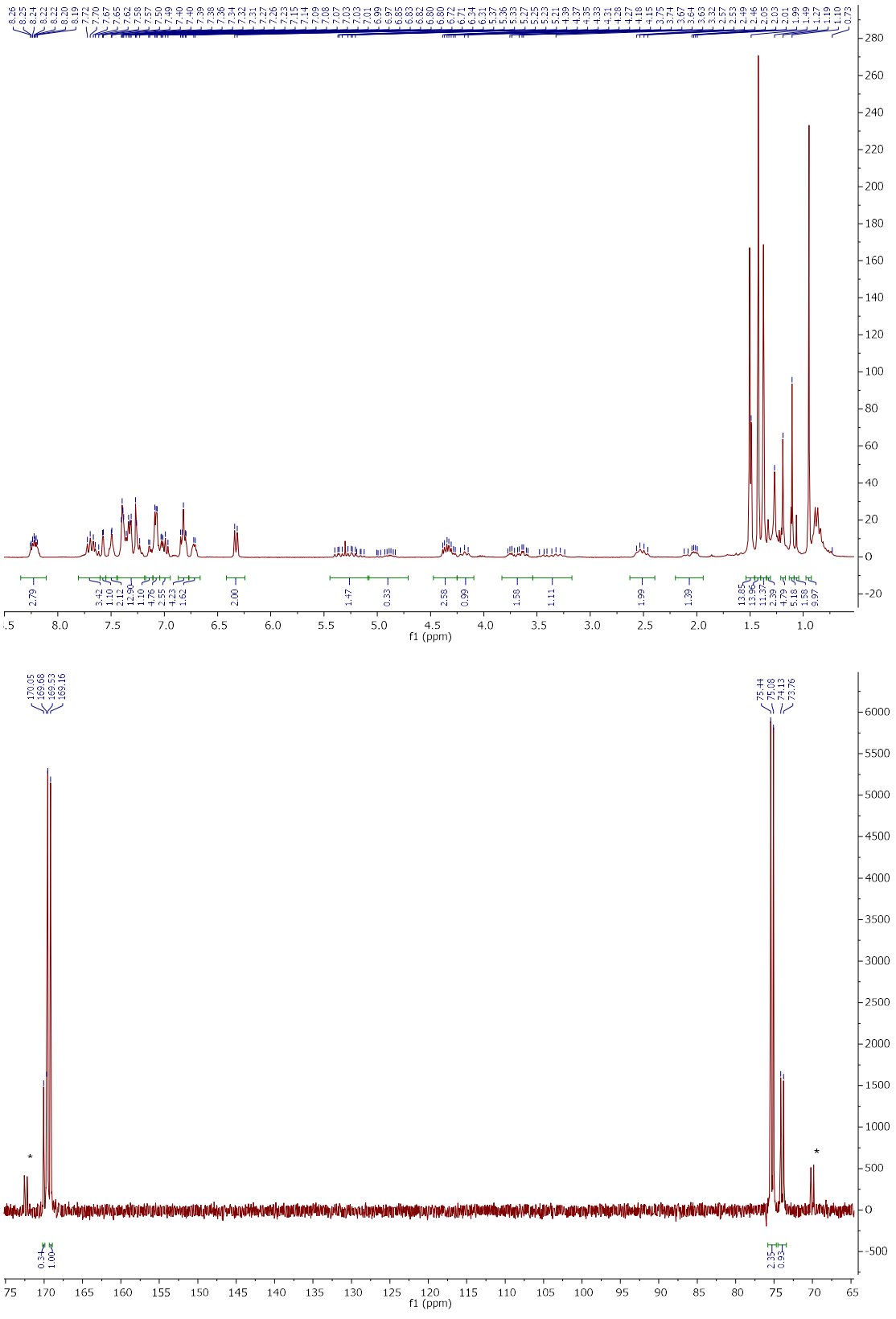

Signals marked with an asterisk (*) correspond to remaining *trans*-**1a**.

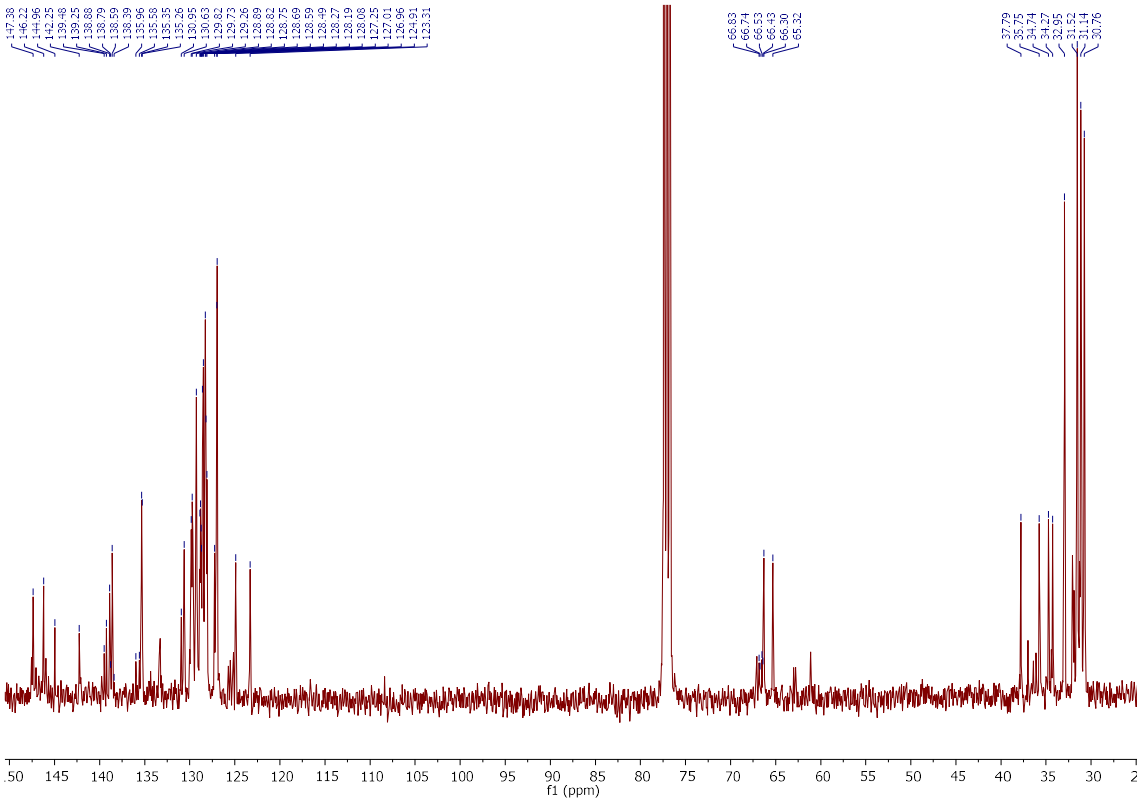

b) Major isomer

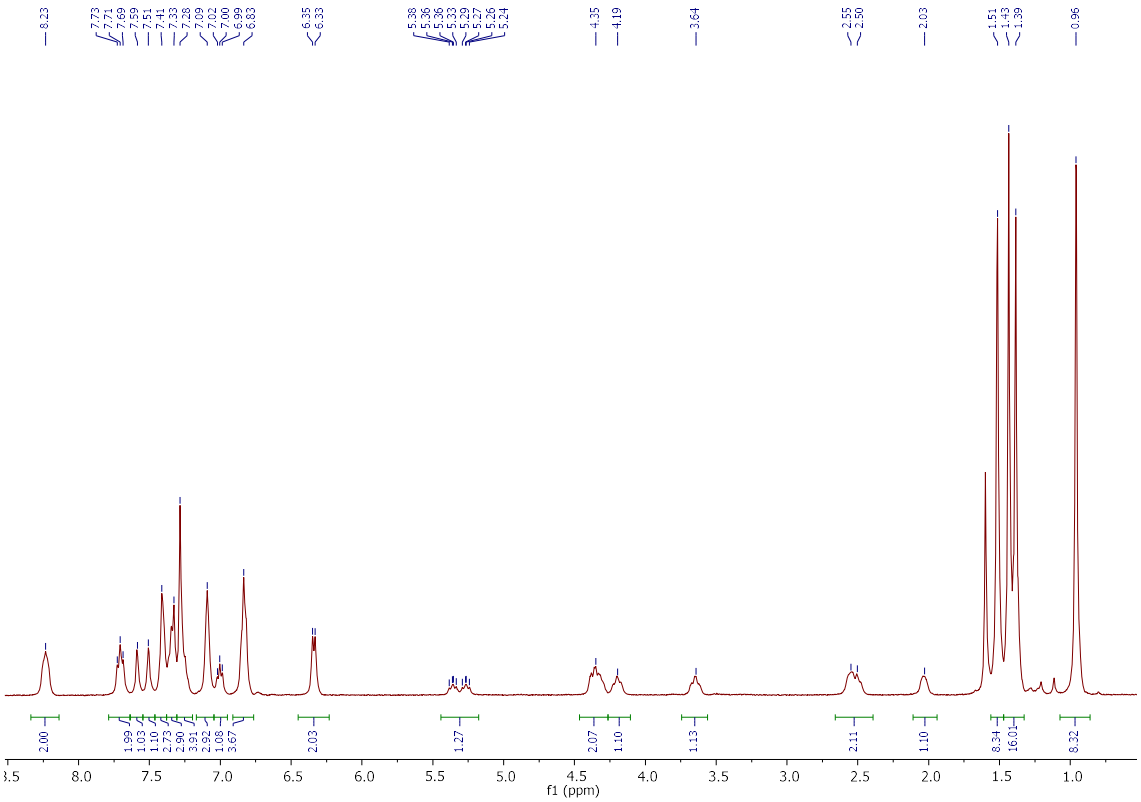

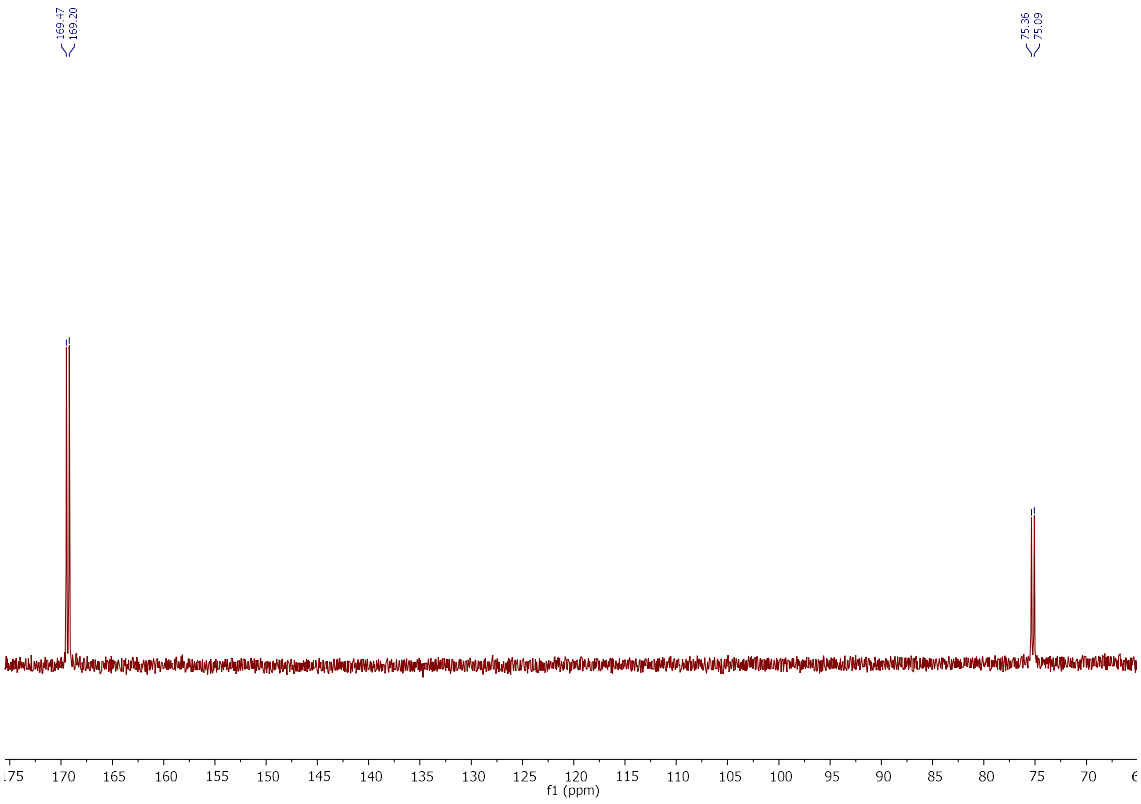
169.47
169.20
75.36
75.09
.75
170
165
160
155
150
145
140
135
130
125
120
115
110
105
100
95
90
85
80
75
70
f1 (ppm)

Ru(H)(BH_4)(**2c**)(**3b**) (**7**)

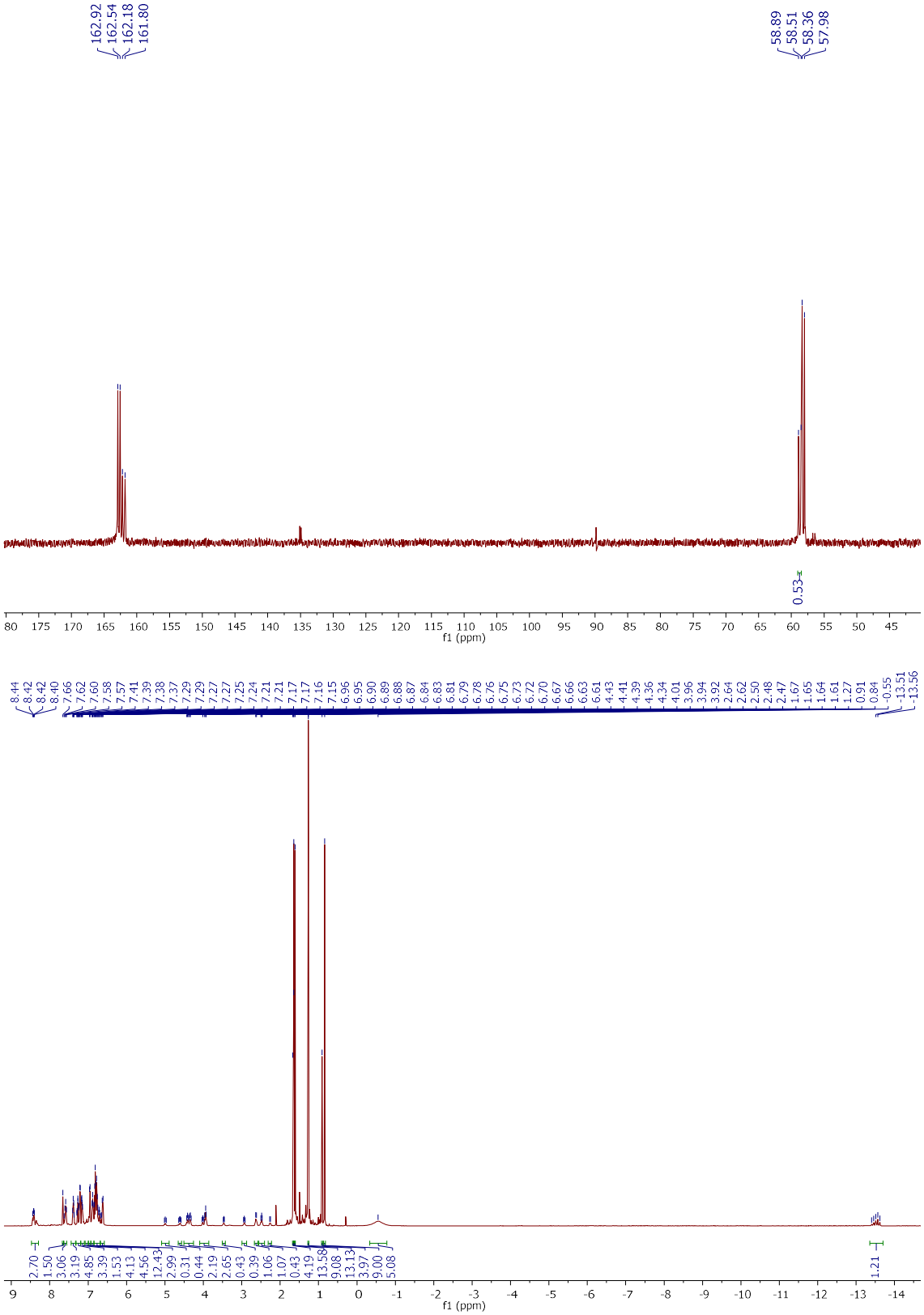

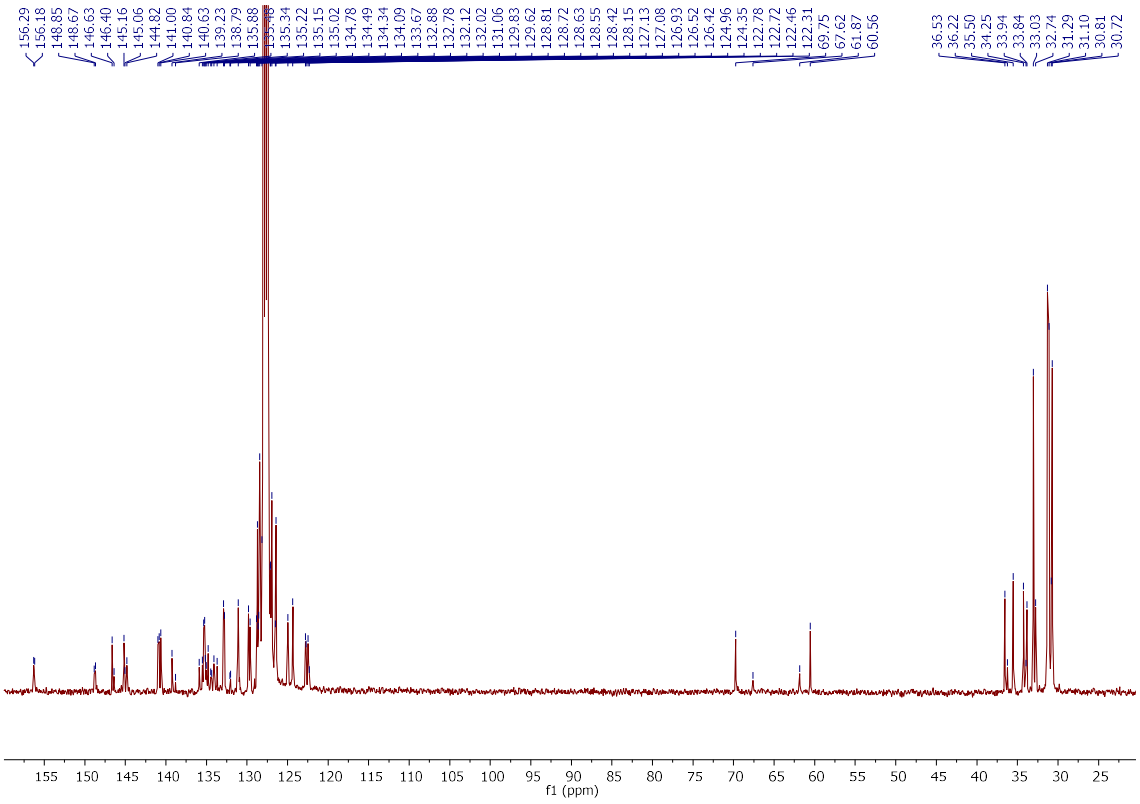
156.29
156.18
148.85
148.67
146.63
146.40
145.16
145.06
144.82
141.00
140.84
140.63
139.23
138.79
135.88
135.48
135.34
135.22
135.15
135.02
134.78
134.49
134.34
134.09
133.67
132.88
132.78
132.12
132.02
131.06
129.83
129.62
128.81
128.72
128.63
128.55
128.42
128.15
127.13
127.08
126.93
126.52
126.42
124.96
124.35
122.78
122.72
122.46
122.31
69.75
67.62
61.87
60.56
36.53
36.22
35.50
34.25
33.94
33.84
33.03
32.74
31.29
31.10
30.81
30.72
155 150 145 140 135 130 125 120 115 110 105 100 95 90 85 80 75 70 65 60 55 50 45 40 35 30 25
f1 (ppm)

6a

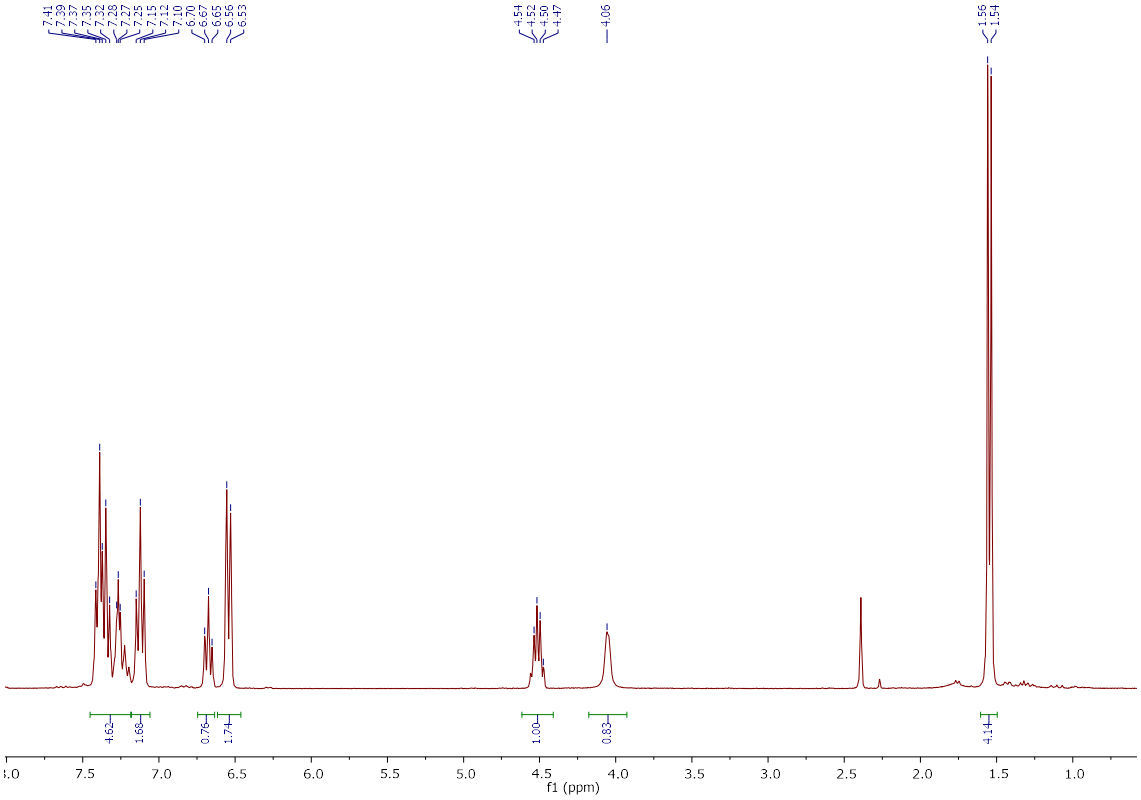
7.41
7.39
7.37
7.35
7.32
7.28
7.27
7.25
7.15
7.12
7.10
6.70
6.67
6.65
6.56
6.53
4.54
4.52
4.50
4.47
4.06
1.56
1.54
4.62
1.68
0.76
1.74
1.00
0.83
4.14
7.5
7.0
6.5
6.0
5.5
5.0
4.5
4.0
3.5
3.0
2.5
2.0
1.5
1.0
f1 (ppm)

6b

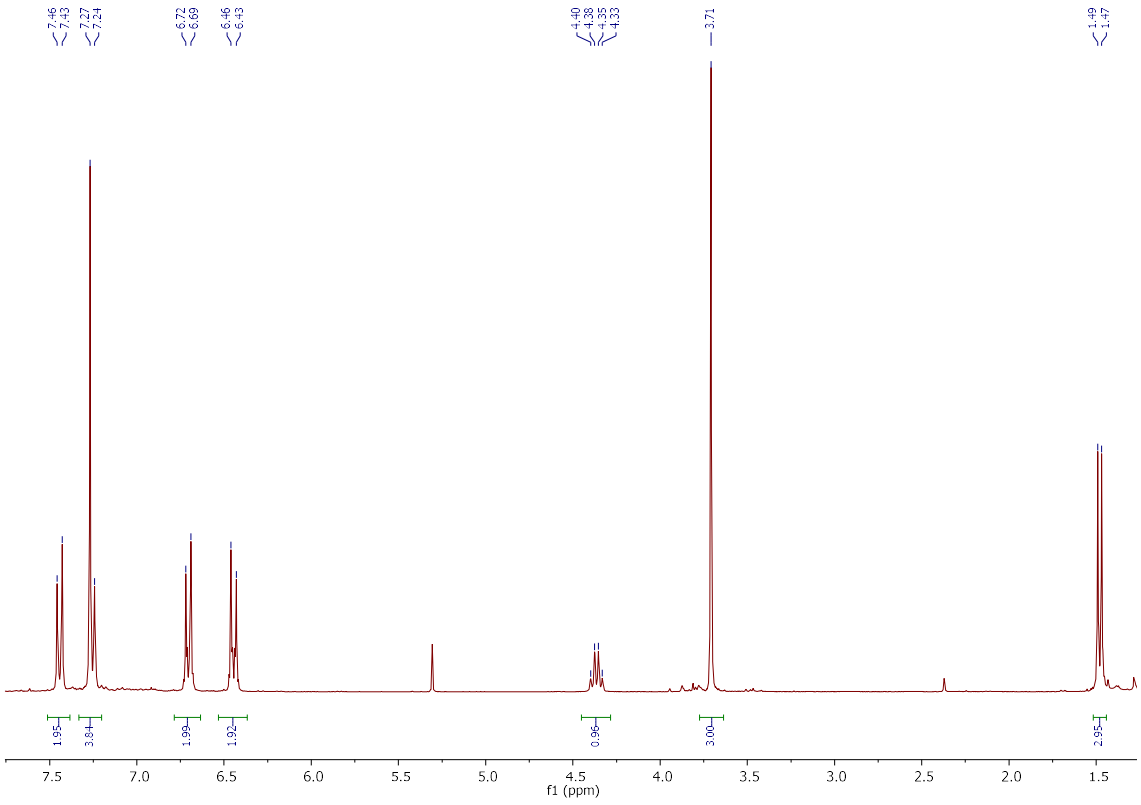
7.46
7.43
7.27
7.24
6.72
6.69
6.46
6.43
4.40
4.38
4.35
4.33
3.71
1.49
1.47
1.95
3.84
1.99
1.92
0.96
3.00
2.95
7.5
7.0
6.5
6.0
5.5
5.0
4.5
4.0
3.5
3.0
2.5
2.0
1.5
f1 (ppm)

6c

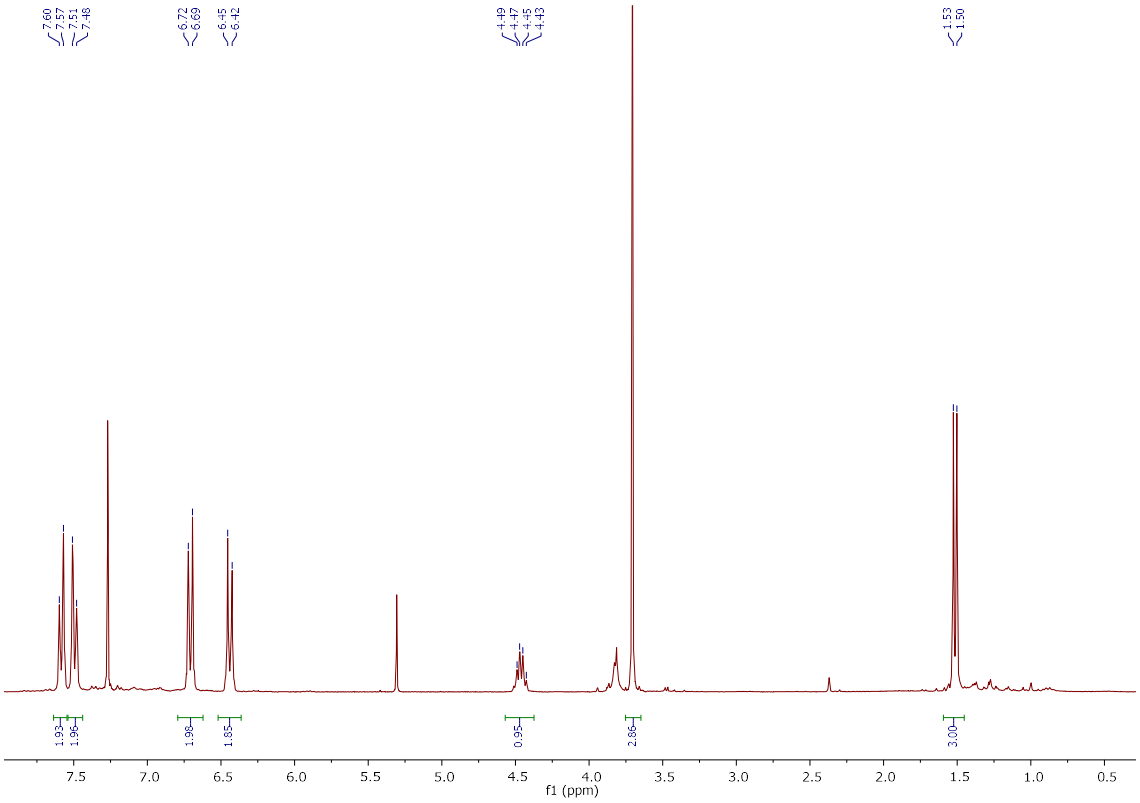

6d

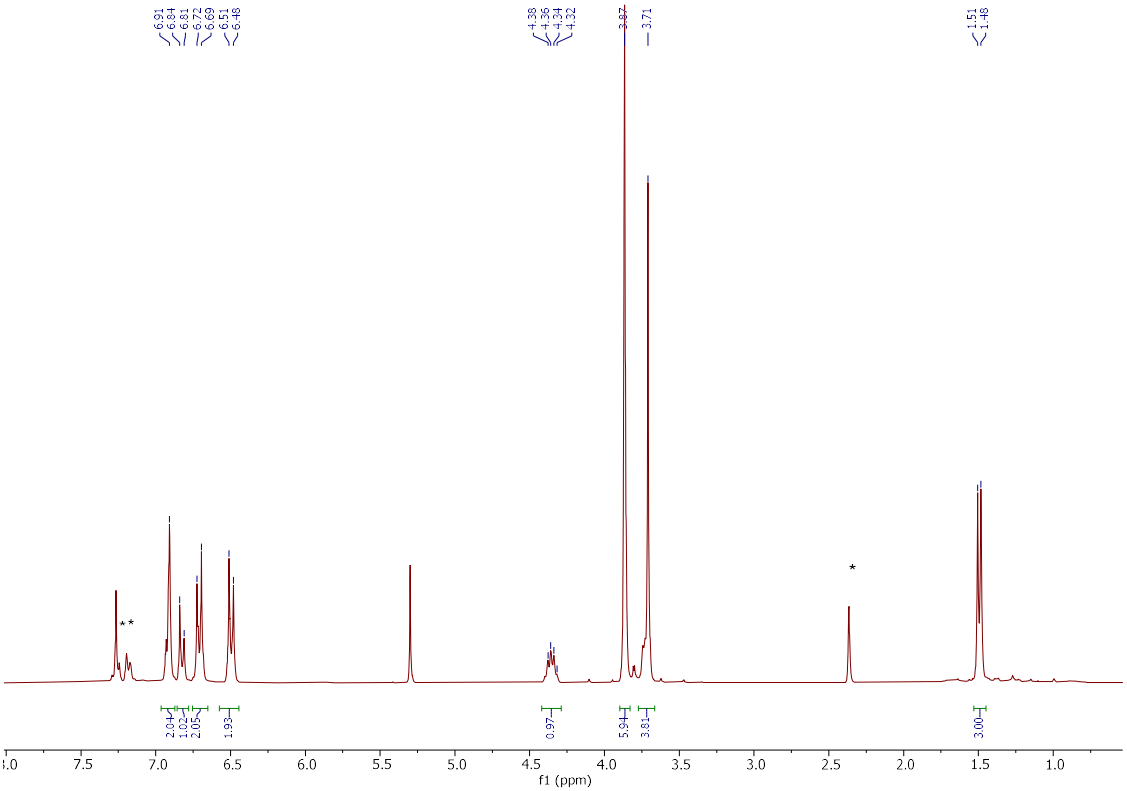

Toluene impurities marked with an asterisk (*)

6e

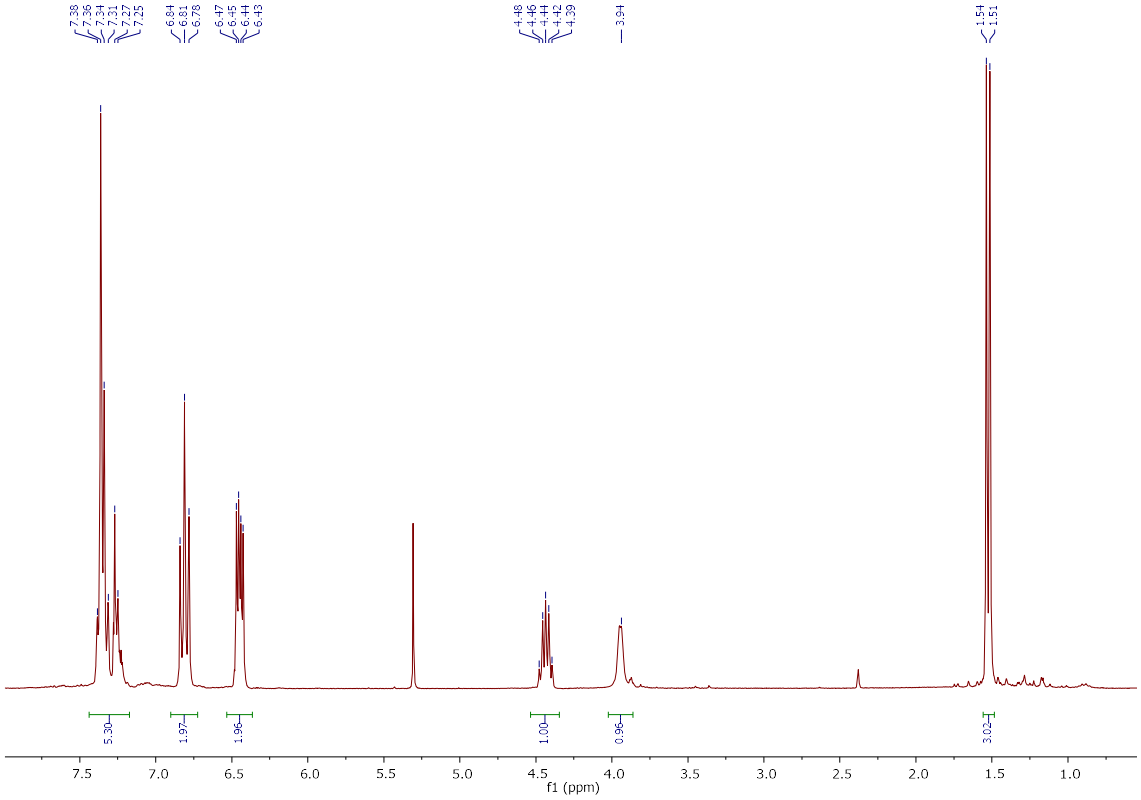
7.38
7.36
7.34
7.31
7.27
7.25
6.84
6.81
6.78
6.47
6.45
6.44
6.43
4.46
4.46
4.44
4.42
4.39
3.94
1.54
1.51
5.30
1.97
1.96
1.00
0.96
3.02
7.5
7.0
6.5
6.0
5.5
5.0
4.5
4.0
3.5
3.0
2.5
2.0
1.5
1.0
f1 (ppm)

6f

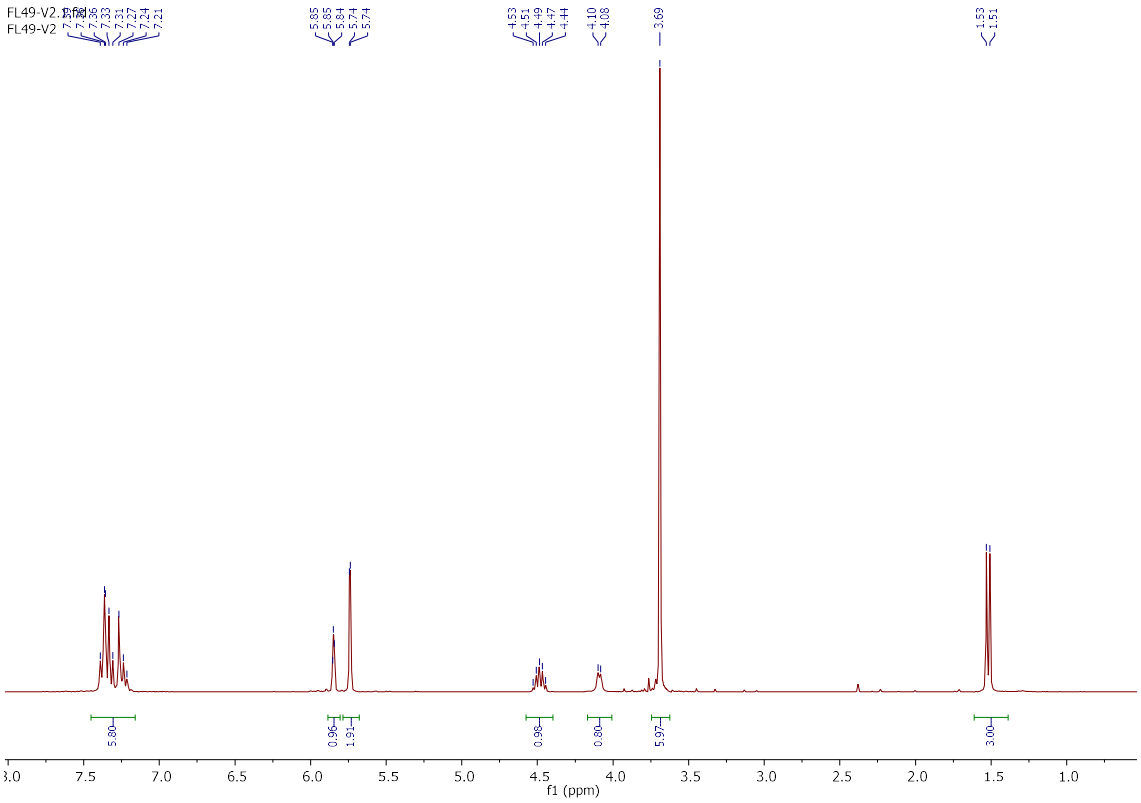
FL49-V2
5.85
5.85
5.84
5.74
5.74
4.53
4.51
4.49
4.47
4.44
4.10
4.08
3.69
1.53
1.51
5.80
0.96
1.91
0.98
0.80
5.97
3.00
7.5
7.0
6.5
6.0
5.5
5.0
4.5
4.0
3.5
3.0
2.5
2.0
1.5
1.0
f1 (ppm)

6g

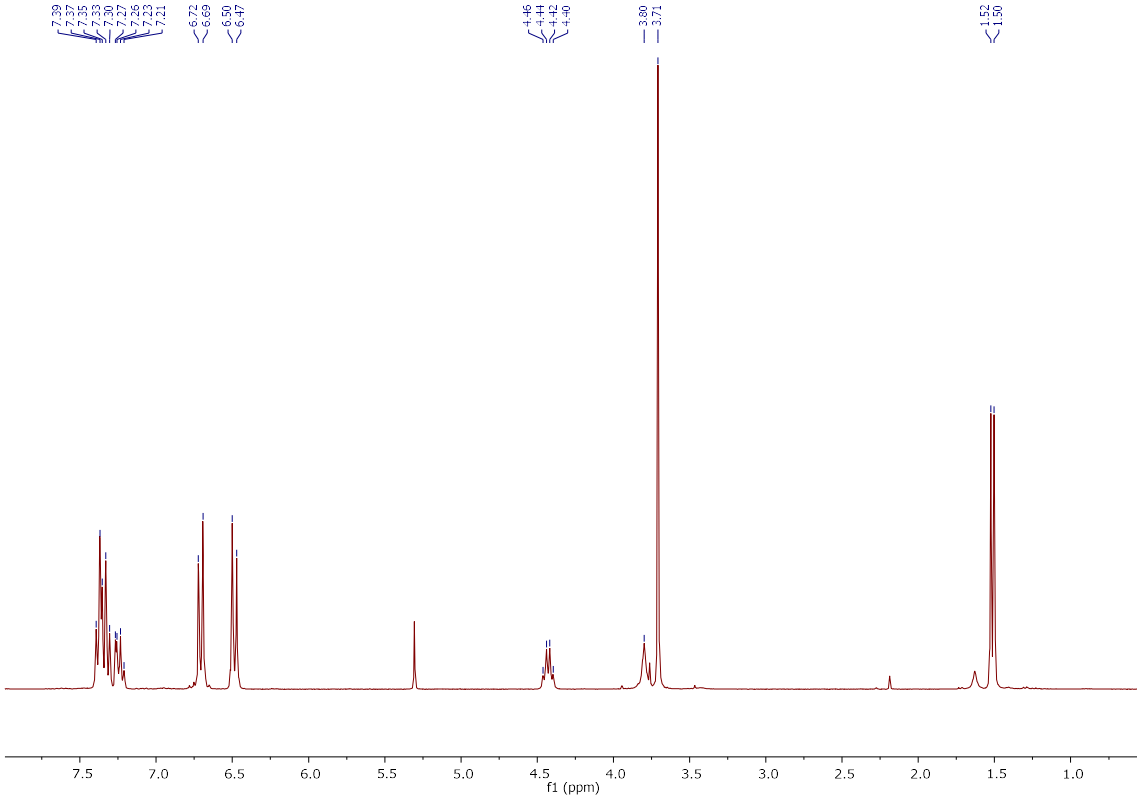
7.39
7.37
7.35
7.33
7.30
7.27
7.26
7.23
7.21
6.72
6.69
6.50
6.47
4.46
4.44
4.42
4.40
3.80
3.71
1.52
1.50
f1 (ppm)

6h

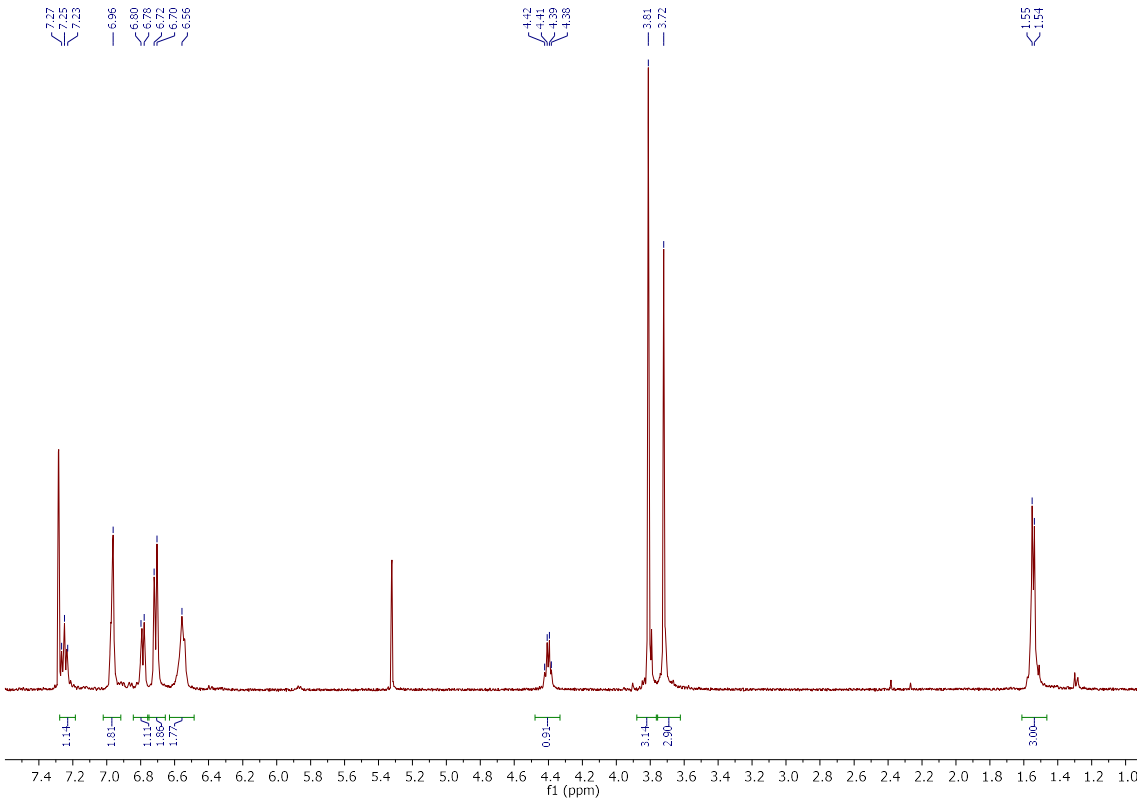
7.27
7.25
7.23
6.96
6.80
6.78
6.72
6.70
6.56
4.42
4.41
4.39
4.38
3.81
3.72
1.55
1.54
1.14
1.81
1.11
1.86
1.77
0.91
3.14
2.90
3.00
f1 (ppm)

6i

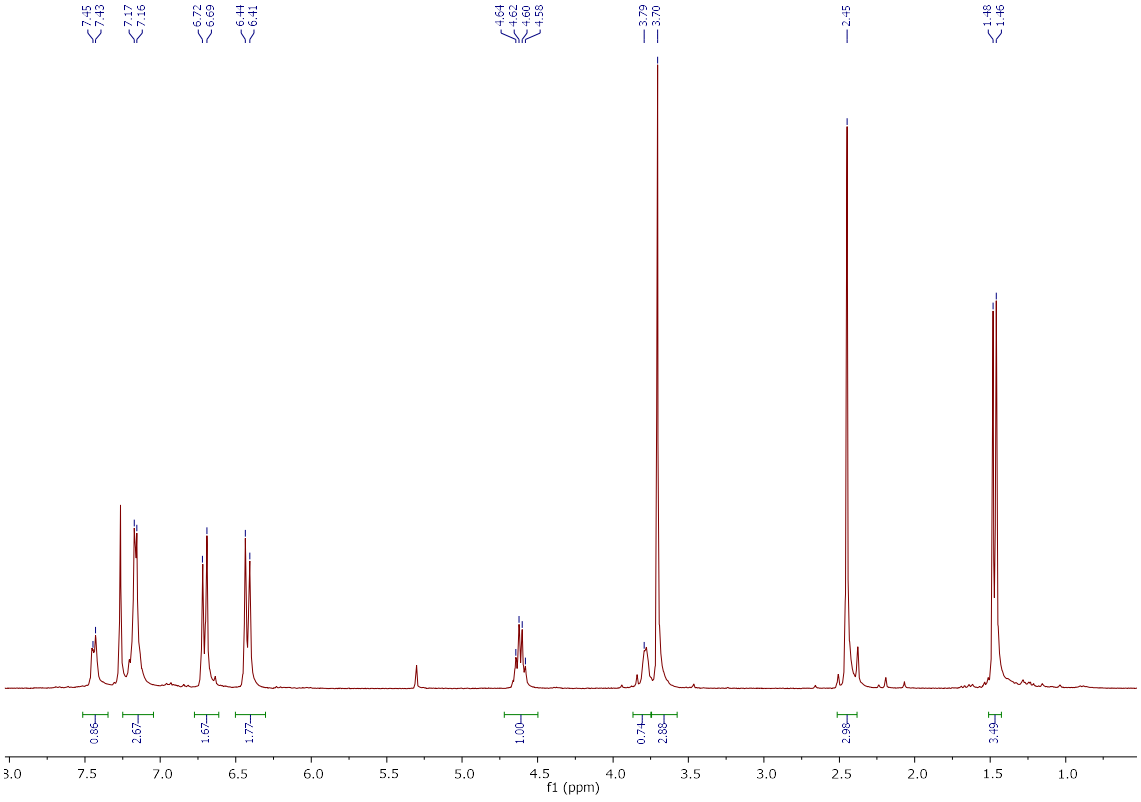
7.45
7.43
7.17
7.16
6.72
6.69
6.44
6.41
4.64
4.62
4.60
4.58
3.79
3.70
2.45
1.48
1.46
0.86
2.67
1.67
1.77
1.00
0.74
2.88
2.96
3.49
f1 (ppm)

6j

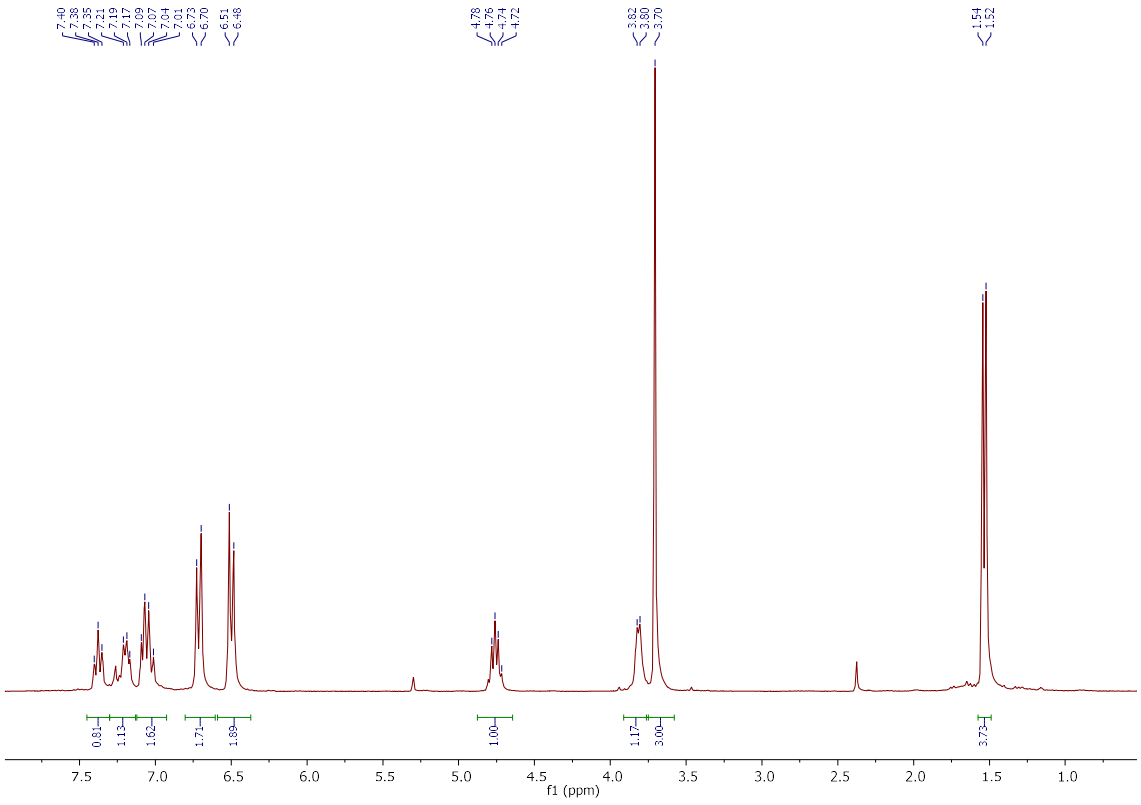
7.40
7.38
7.35
7.21
7.19
7.17
7.09
7.07
7.04
7.01
6.73
6.70
6.51
6.48
4.78
4.76
4.74
4.72
3.82
3.80
3.70
1.54
1.52
0.81
1.13
1.62
1.71
1.89
1.00
1.17
3.00
3.73
f1 (ppm)

6k

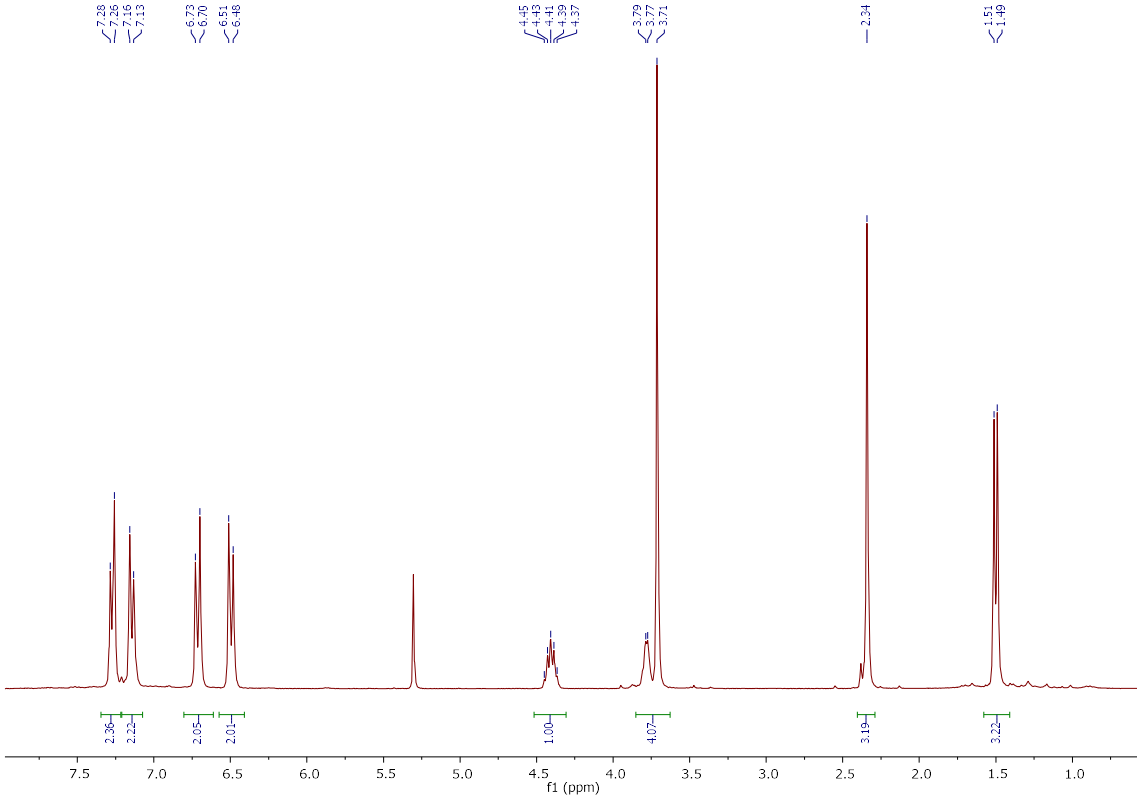
7.28
7.26
7.15
7.13
6.73
6.70
6.51
6.48
4.45
4.43
4.41
4.39
4.37
3.79
3.77
3.71
2.34
1.51
1.49
2.36
2.25
2.05
2.01
1.00
4.07
3.19
3.22
f1 (ppm)

6l

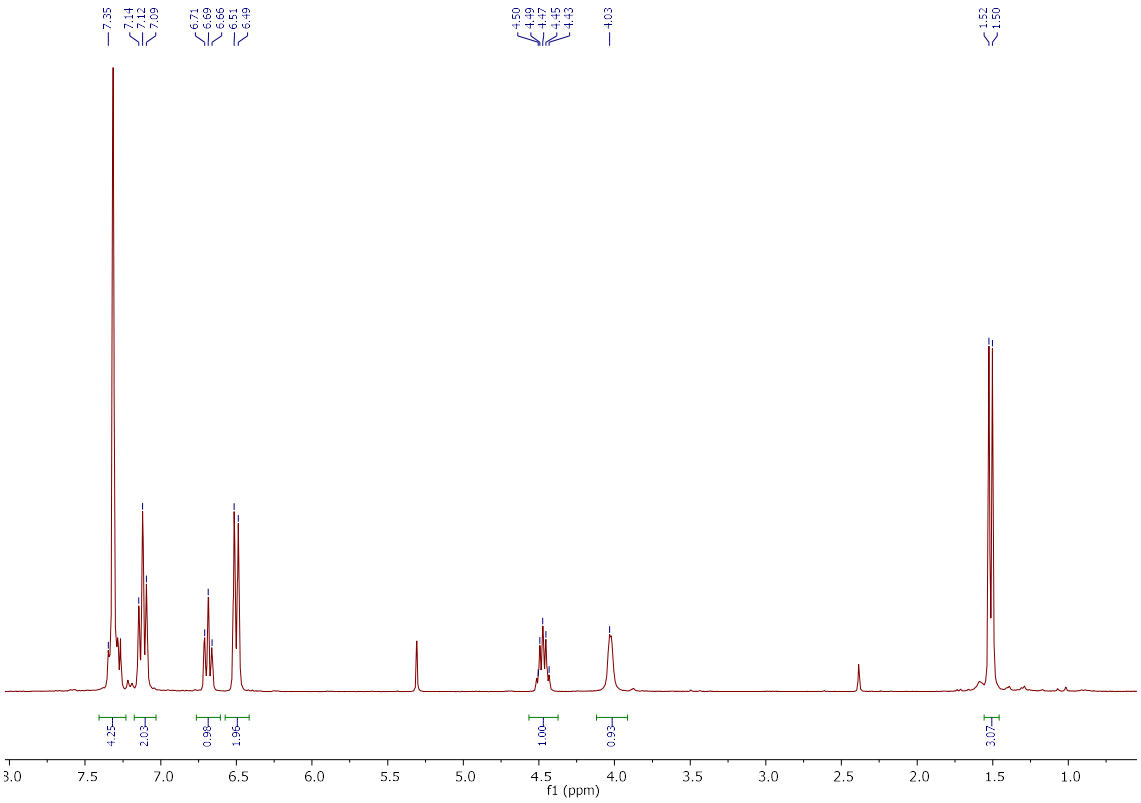
7.35
7.14
7.12
7.09
6.71
6.69
6.66
6.51
6.49
4.50
4.49
4.47
4.45
4.43
4.03
1.52
1.50
4.25
2.03
0.98
1.96
1.00
0.93
3.07
f1 (ppm)

6m

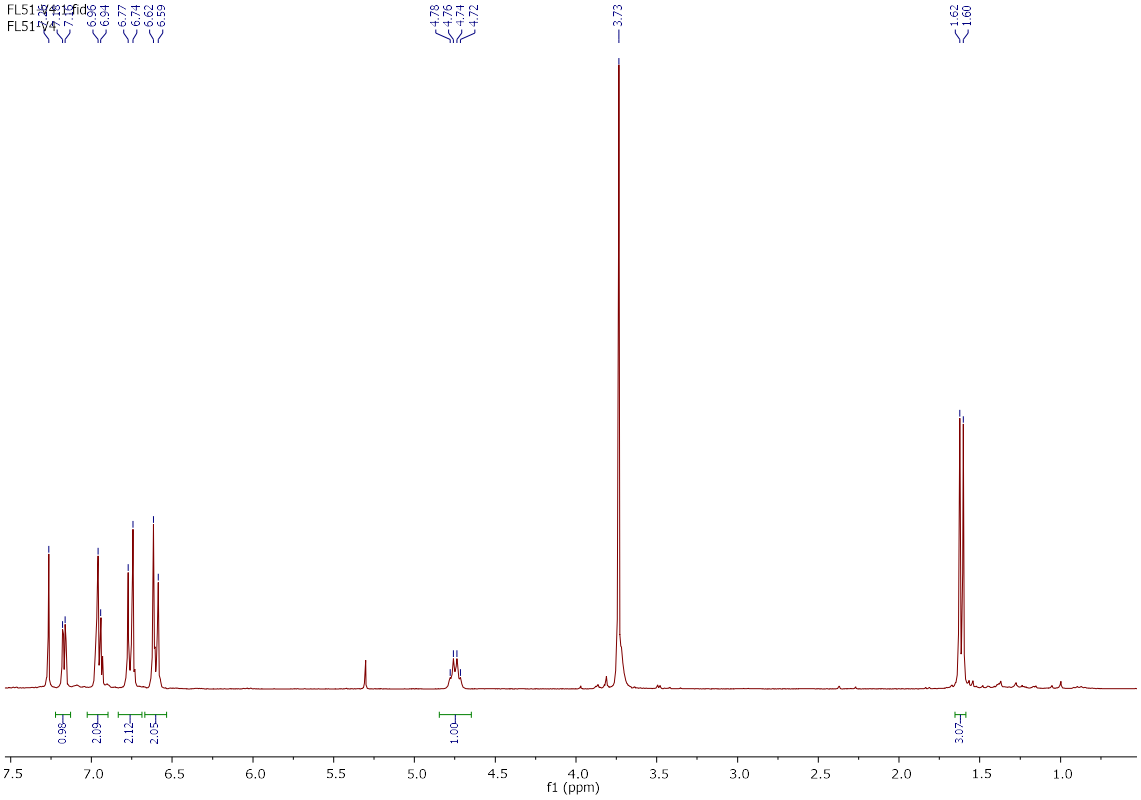
FL51fy4-1.fid
FL51fy4
7.15
6.96
6.94
6.77
6.74
6.62
6.59
4.78
4.76
4.74
4.72
3.73
1.62
1.60
0.96
2.09
2.12
2.05
1.00
3.07
f1 (ppm)

6n

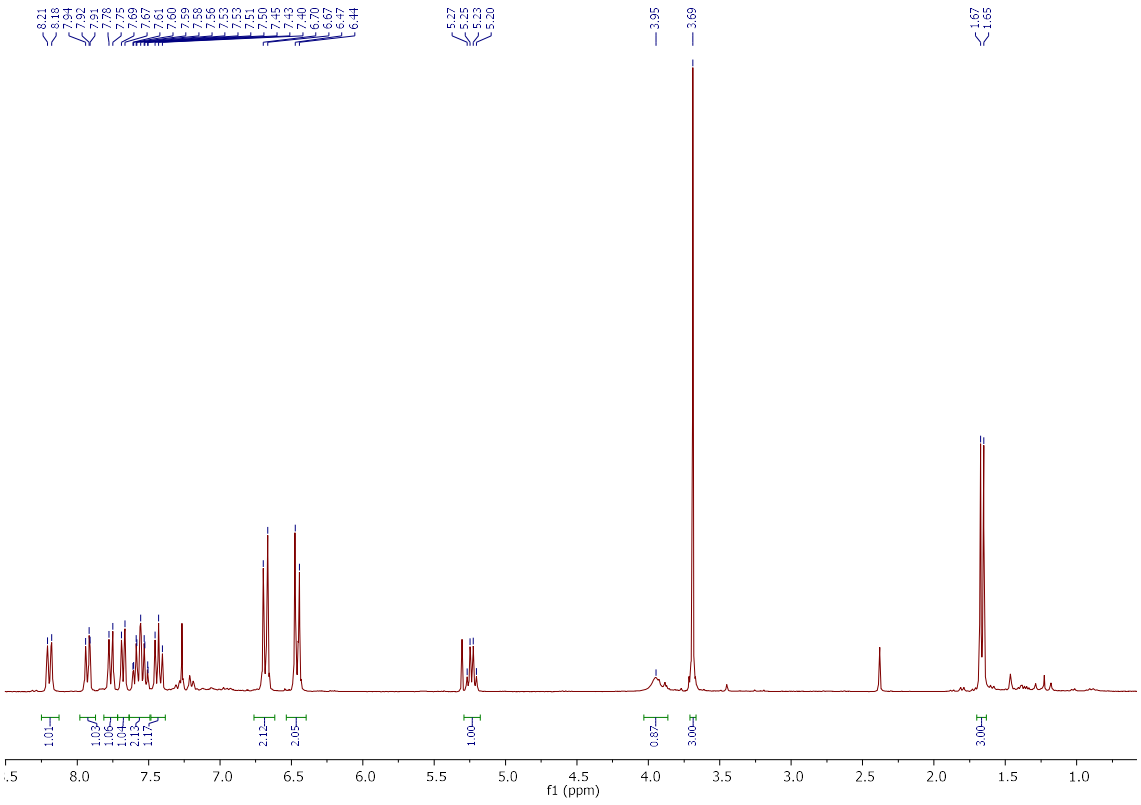
8.21
8.18
7.94
7.92
7.91
7.78
7.75
7.69
7.67
7.61
7.60
7.59
7.58
7.56
7.53
7.53
7.51
7.50
7.45
7.43
7.40
6.70
6.67
6.47
6.44
5.27
5.25
5.23
5.20
3.95
3.69
1.67
1.65
1.01
1.03
1.06
1.04
2.13
1.17
2.12
2.05
1.00
0.87
3.00
3.00
f1 (ppm)

6o

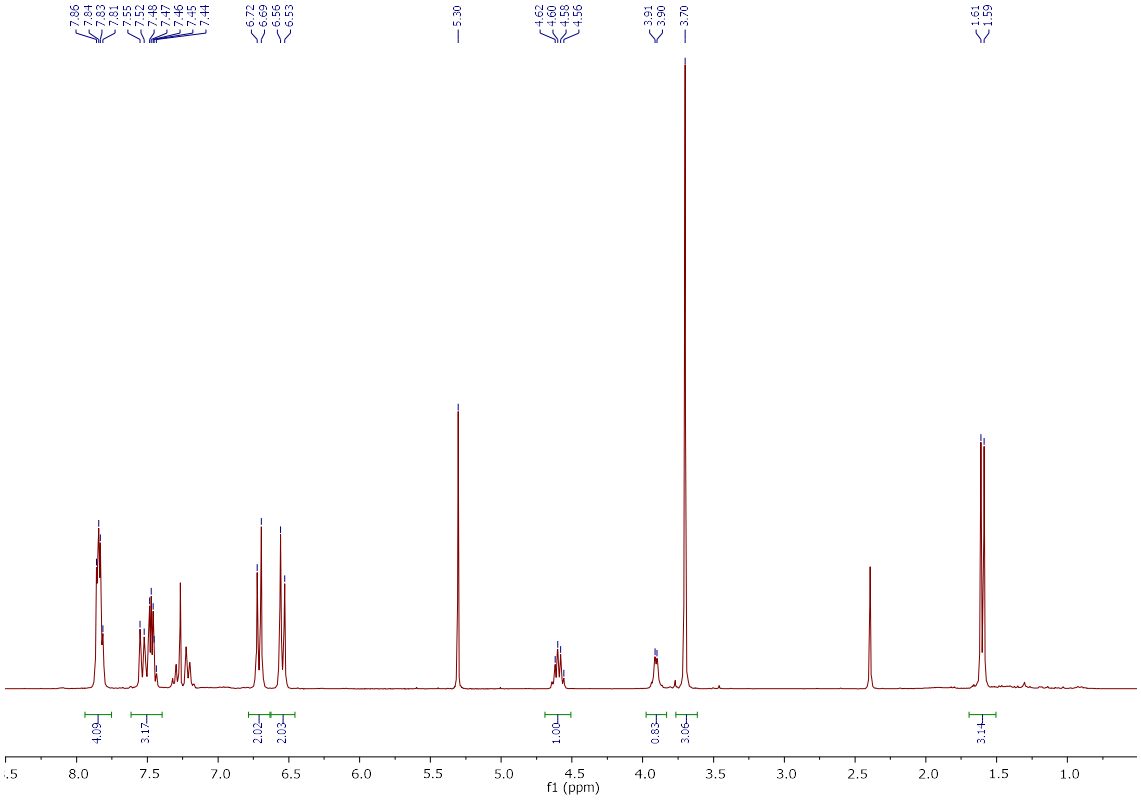
7.86
7.84
7.83
7.81
7.55
7.52
7.48
7.47
7.46
7.45
7.44
6.72
6.69
6.56
6.53
5.30
4.62
4.60
4.58
4.56
3.91
3.90
3.70
1.61
1.59
4.09
3.17
2.02
2.03
1.00
0.83
3.06
3.14
f1 (ppm)

6p

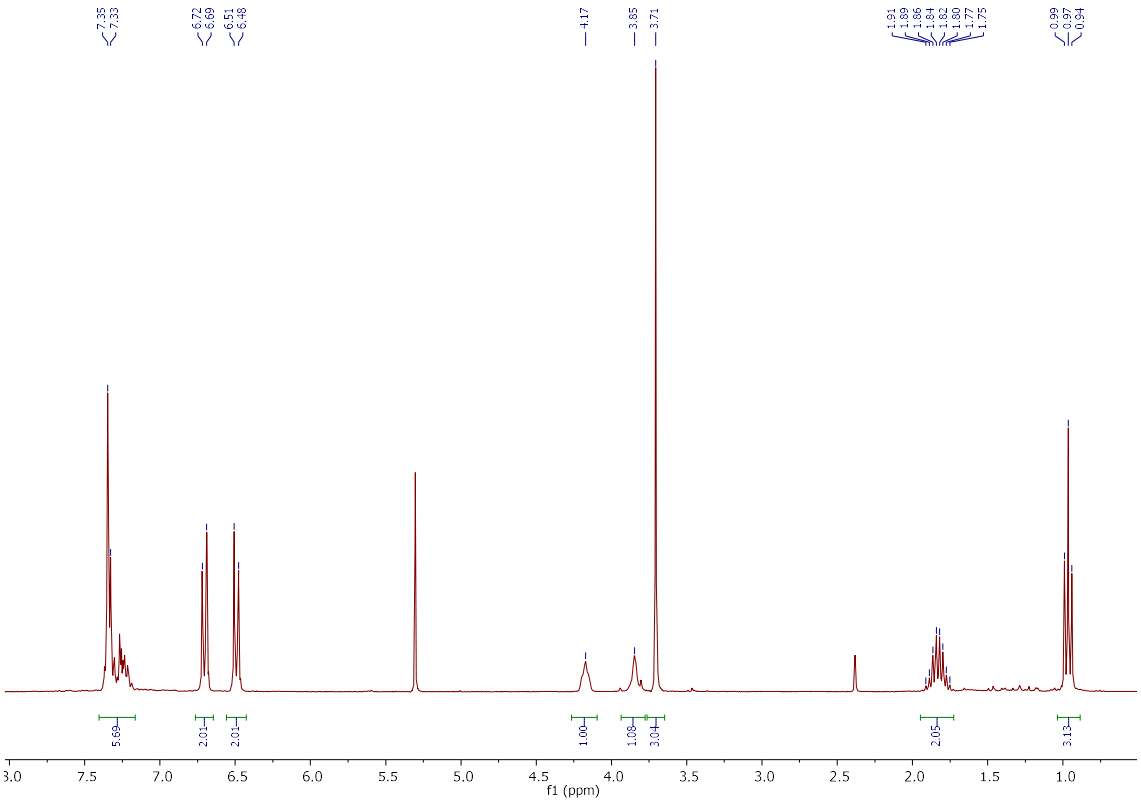
7.35
7.33
6.72
6.69
6.51
6.48
4.17
3.85
3.71
1.91
1.89
1.86
1.84
1.82
1.80
1.77
1.75
0.99
0.97
0.94
5.69
2.01
2.01
1.00
1.08
3.04
2.05
3.13
f1 (ppm)

***N*-phenyl-1-phenylethylamine (6a):** Chiralcel OJ-H, 30° C, *n*-hexane/2-propanol (97:3), flow 1.0 mL/min, t_1 = 20.7 min (*R*), t_2 = 26.6 min (*S*).

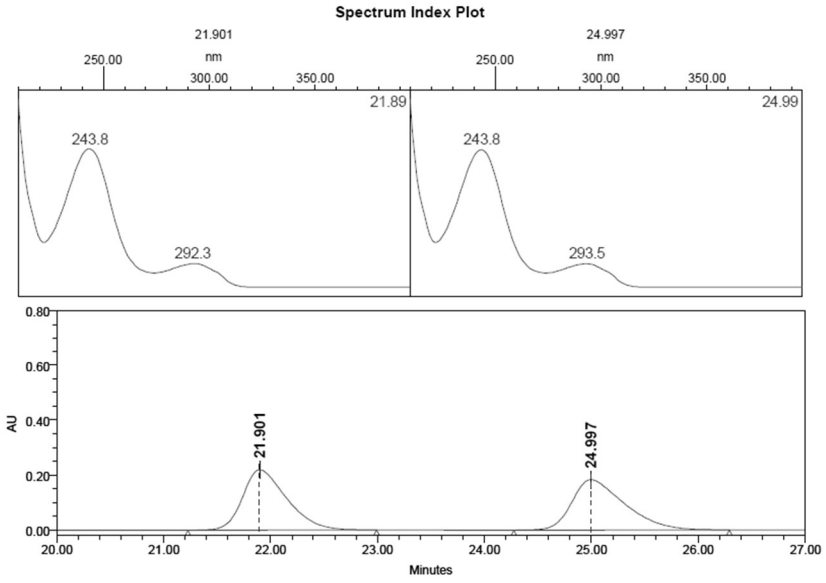

Peak Results

	RT	Area	% Area
1	21.901	6253450	50.00
2	24.997	6253704	50.00

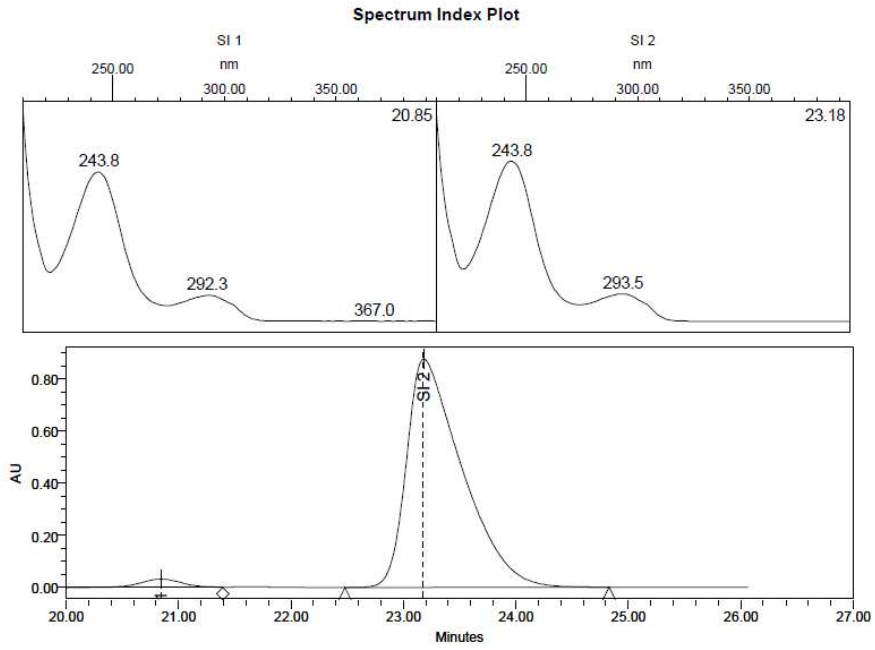

Peak Results

	Name	RT	% Area	Area	Height
1		20.844	2.63	812324	31689
2		23.182	97.37	30065868	877311

***N*-(4-methoxyphenyl)-1-(4-bromophenyl)ethylamine (6b):** Chiralcel OD-H, 30° C, *n*-hexane/2-propanol (99:1), flow 1.0 mL/min, t_1 = 20.8 min (*R*), t_2 = 24.8 min (*S*).

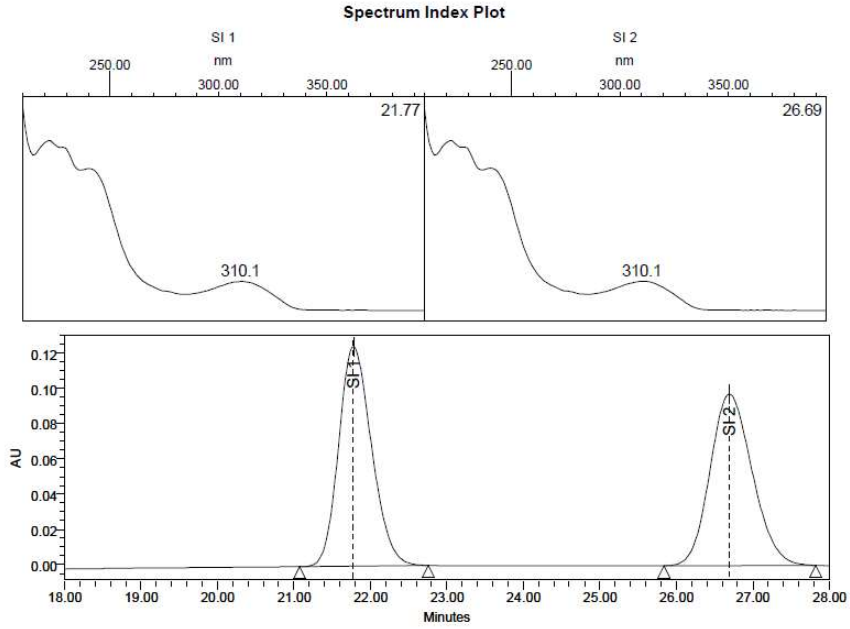

Peak Results

	Name	RT	% Area	Area	Height
1		21.777	50.06	3737156	124652
2		26.692	49.94	3727525	97401

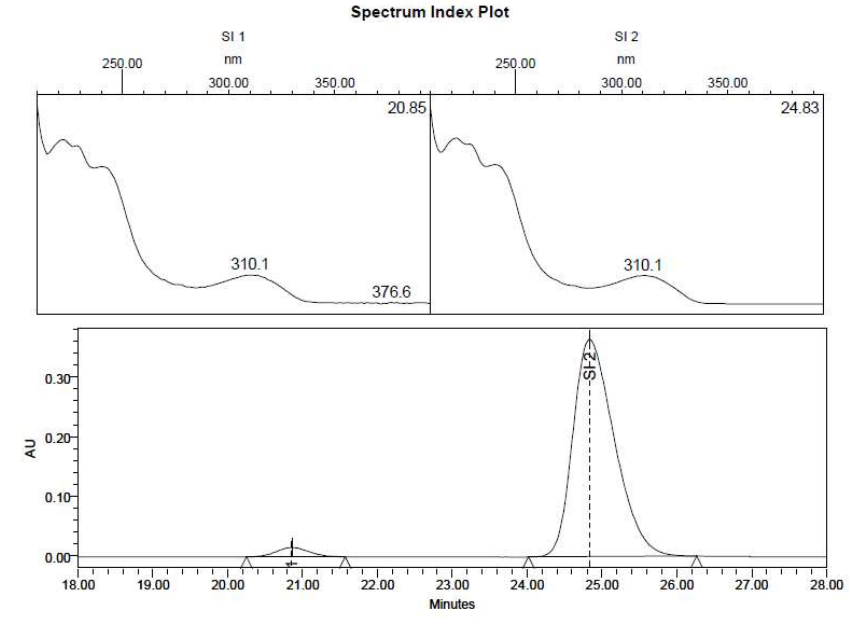

Peak Results

	Name	RT	% Area	Area	Height
1		20.858	3.20	462981	15266
2		24.834	96.80	13988495	363599

***N*-(4-methoxyphenyl)-1-(4-trifluoromethylphenyl)ethylamine (6c):** Chiralcel OD-H, 30° C, *n*-hexane/2-propanol (97:3), flow 1.0 mL/min, t_1 = 12.9 min (*R*), t_2 = 16.5 min (*S*).

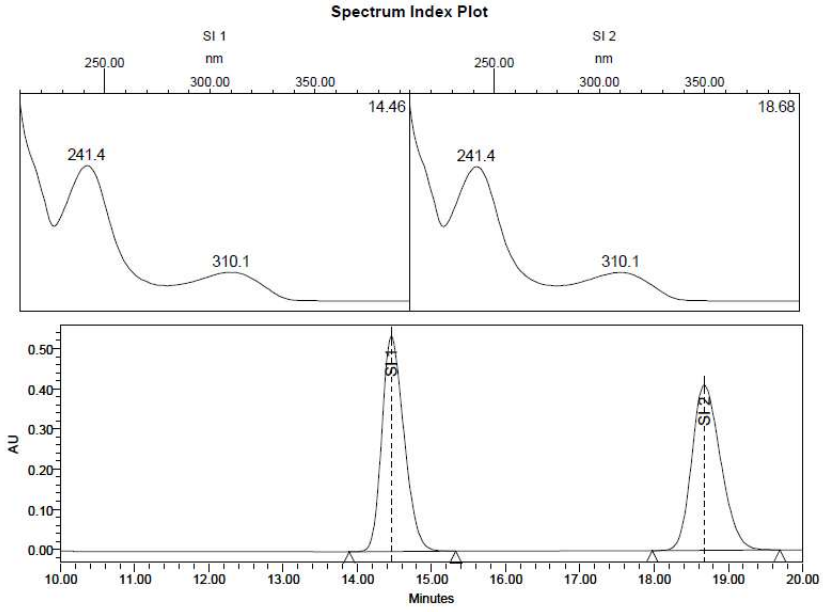

Peak Results

	Name	RT	% Area	Area	Height
1		14.458	49.98	11144450	535942
2		18.676	50.02	11151715	411357

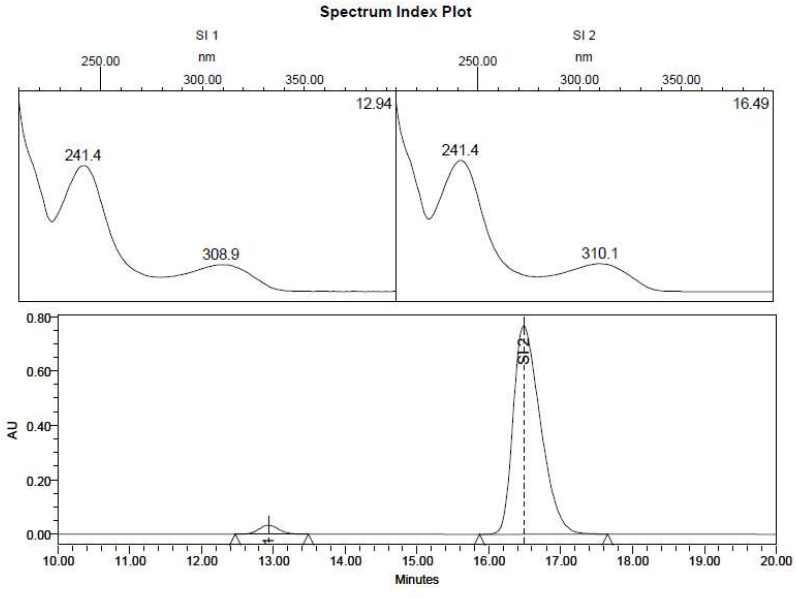

Peak Results

	Name	RT	% Area	Area	Height
1		12.929	3.04	632126	33083
2		16.484	96.96	20163593	767040

***N*-(4-methoxyphenyl)-1-(3,4-dimethoxyphenyl)ethylamine (6d):** Chiralcel OD-H, 30° C, *n*-hexane/2-propanol (90:10), flow 0.5 mL/min, t_1 = 27.7 min (*R*), t_2 = 31.9 min (*S*).

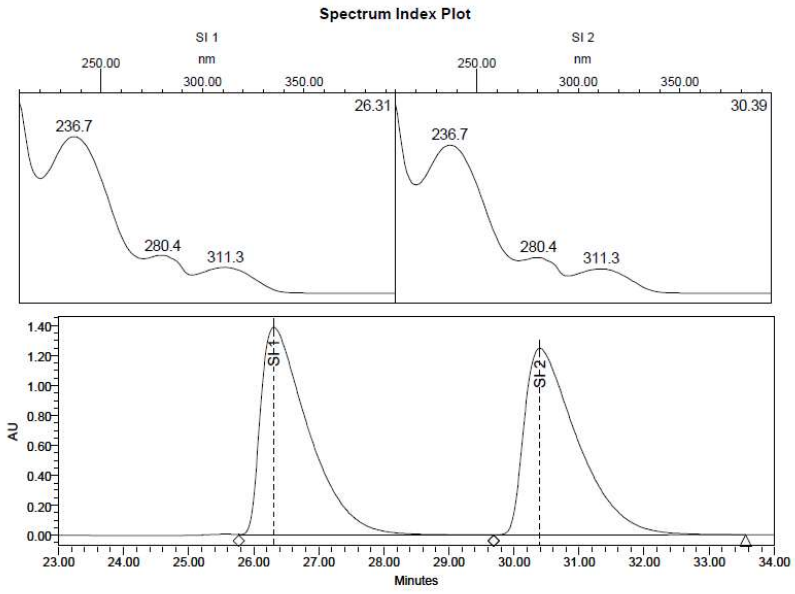

Peak Results

	Name	RT	% Area	Area	Height
1		26.310	50.09	70941829	1388202
2		30.397	49.91	70682490	1245411

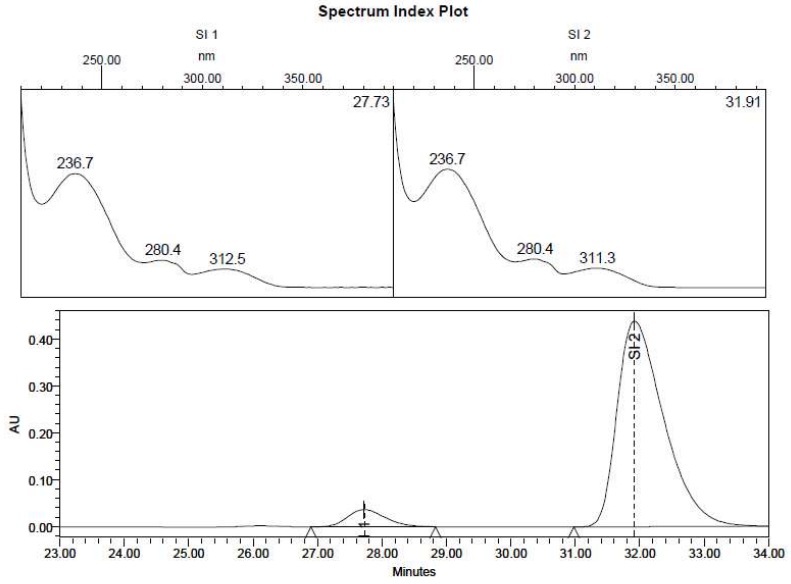

Peak Results

	Name	RT	% Area	Area	Height
1		27.722	6.32	1489898	36671
2		31.919	93.68	22081435	439010

***N*-(4-fluorophenyl)-1-phenylethylamine (6e):** Chiralcel OD-H, 30° C, *n*-hexane/2-propanol (98:2), flow 0.5 mL/min, t_1 = 15.2 min (*R*), t_2 = 17.5 min (*S*).

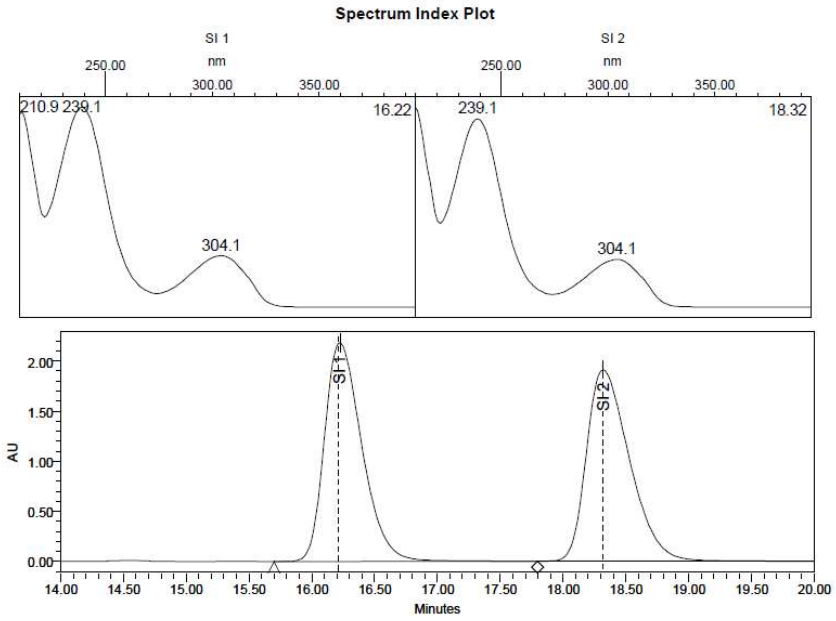

Peak Results

	Name	RT	% Area	Area	Height
1		16.222	49.80	45220562	2187208
2		18.319	50.20	45589910	1915218

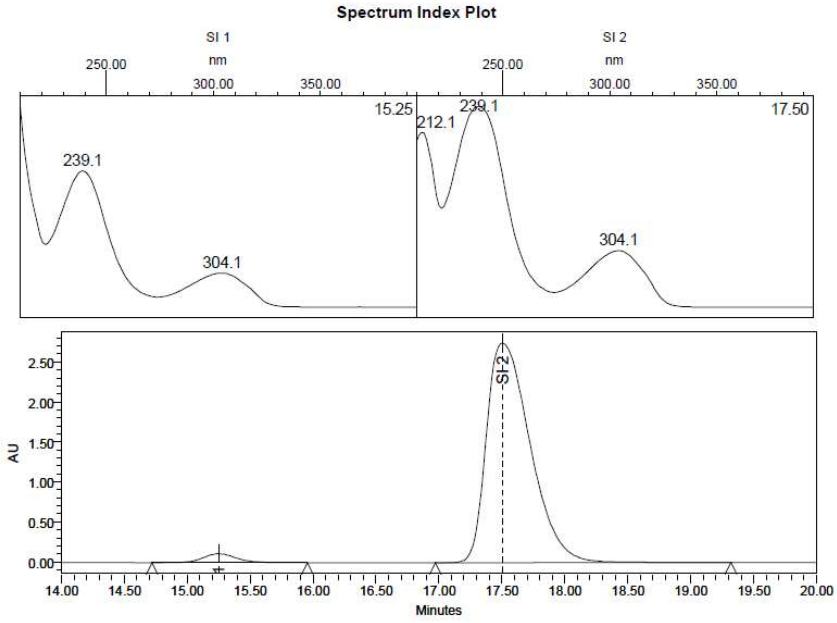

Peak Results

	Name	RT	% Area	Area	Height
1		15.249	2.93	2004181	111136
2		17.506	97.07	66334247	2744249

***N*-(3,5-dimethoxyphenyl)-1-phenylethylamine (6f):** Chiralcel OB-H, 30° C, *n*-hexane/2-propanol (99:1), flow 1.0 mL/min, t_1 = 37.2 min (*S*), t_2 = 54.8 min (*R*).

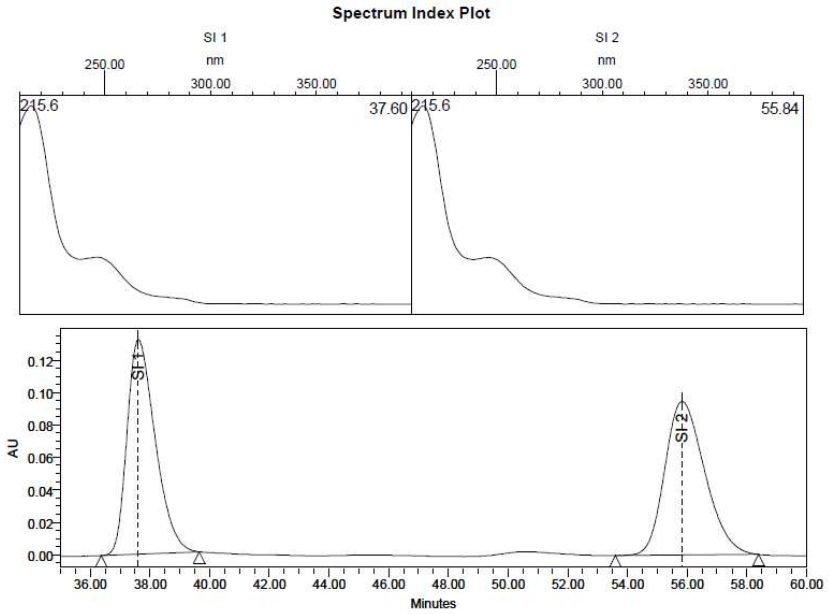

Peak Results

	Name	RT	% Area	Area	Height
1		37.610	49.65	8679624	132270
2		55.829	50.35	8800560	94637

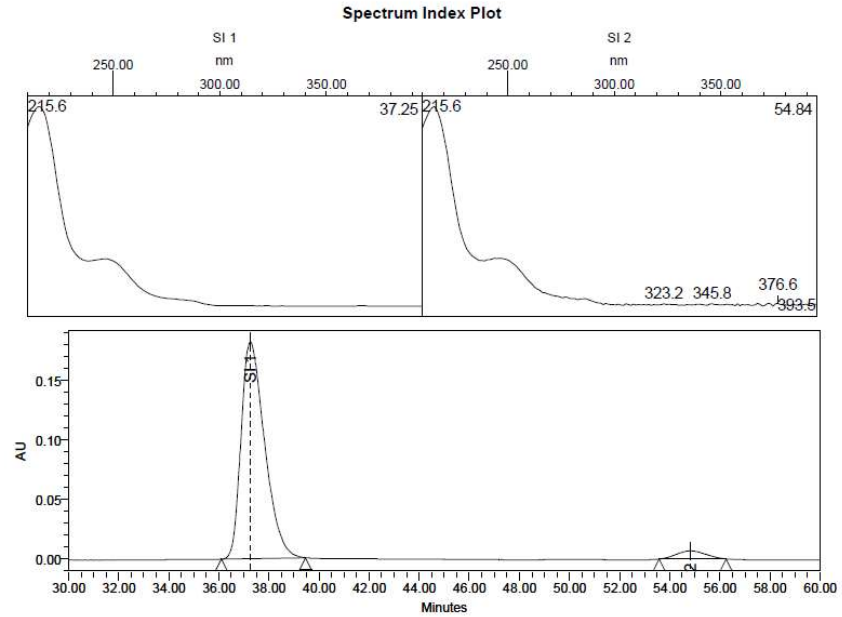

Peak Results

	Name	RT	% Area	Area	Height
1		37.254	95.59	11924598	182725
2		54.835	4.41	550473	6809

***N*-(4-methoxyphenyl)-1-phenylethylamine (6g):** Chiralcel AD-H, 30° C, *n*-hexane/2-propanol (99:1), flow 1.0 mL/min, t_1 = 12.8 min (*R*), t_2 = 14.0 min (*S*).

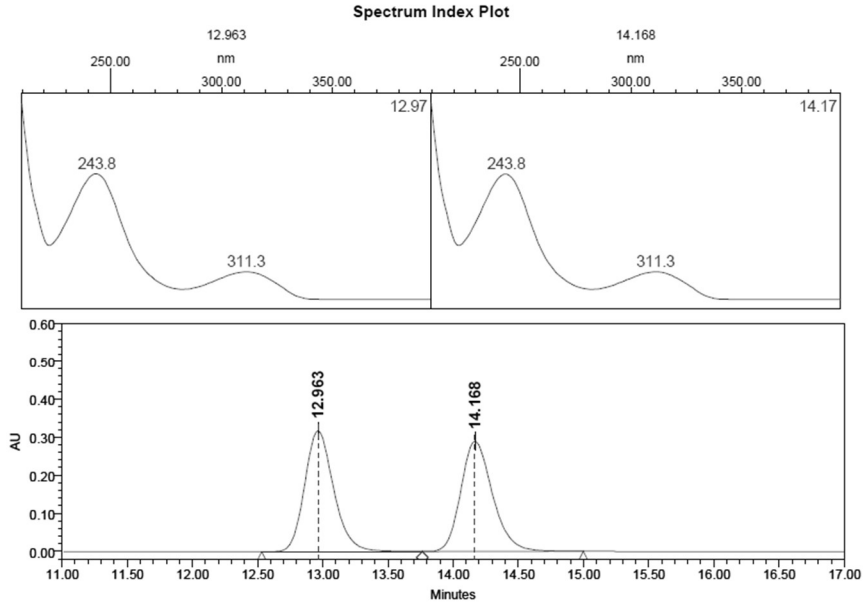

Peak Results

	RT	Area	% Area
1	12.963	4903461	50.09
2	14.168	4885891	49.91

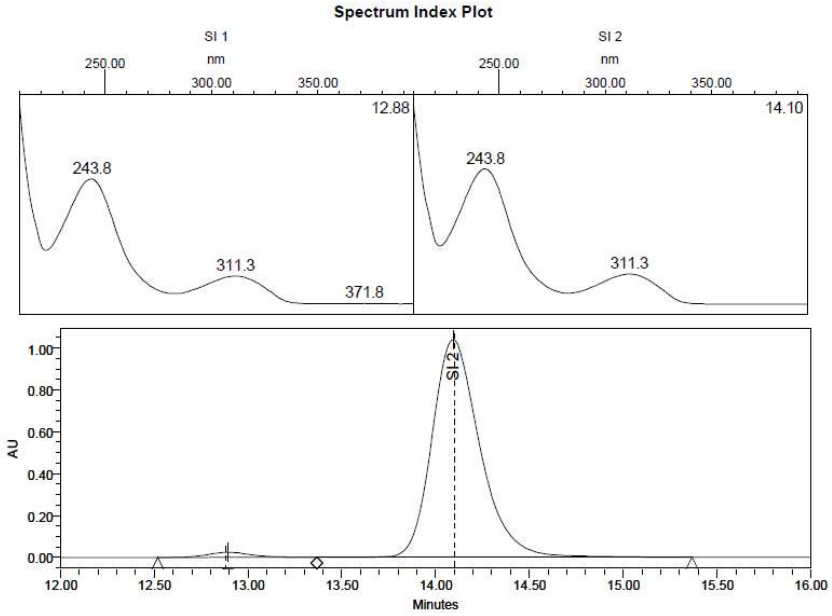

Peak Results

	Name	RT	% Area	Area	Height
1		12.891	2.03	382592	24212
2		14.093	97.97	18444318	1041253

***N*-(4-methoxyphenyl)-1-(3-methoxyphenyl)ethylamine (6h):** Chiralcel OD-H, 30° C, *n*-hexane/2-propanol (99:1), flow 1.0 mL/min, t_1 = 22.1 min (*R*), t_2 = 25.5 min (*S*).

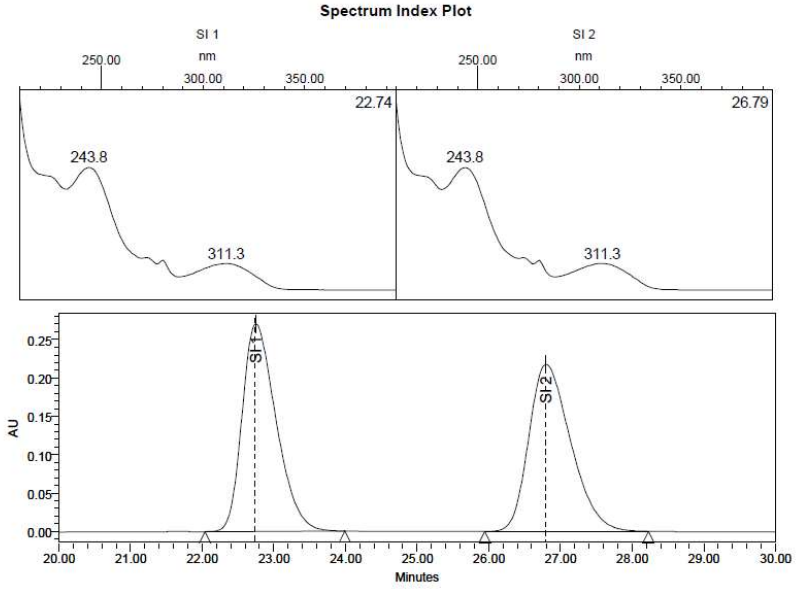

Peak Results

	Name	RT	% Area	Area	Height
1		22.750	50.18	8909573	270428
2		26.800	49.82	8845769	217628

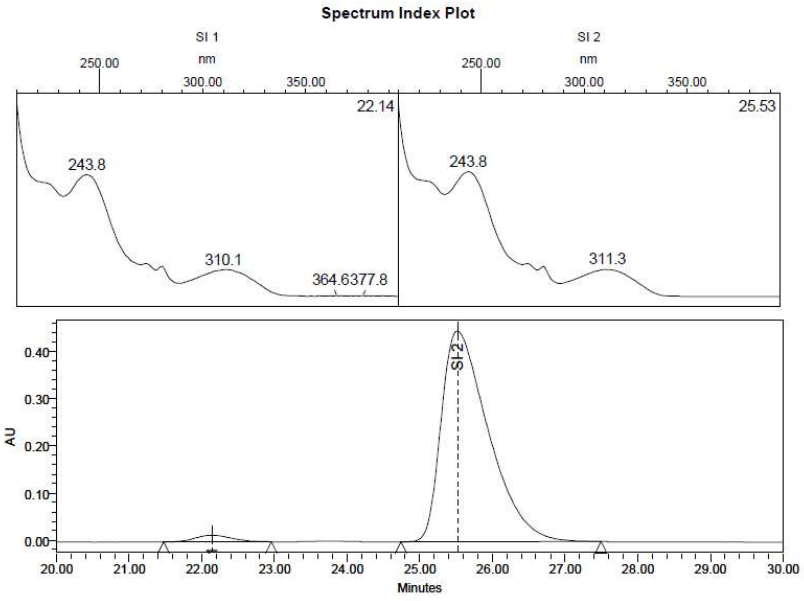

Peak Results

	Name	RT	% Area	Area	Height
1		22.142	2.34	483551	14103
2		25.518	97.66	20162183	446984

***N*-(4-methoxyphenyl)-1-(2-methylphenyl)ethylamine (6i):** Chiralcel OD-H, 30° C, *n*-hexane/2-propanol (99:1), flow 1.0 mL/min, t_1 = 8.3 min (*R*), t_2 = 9.5 min (*S*).

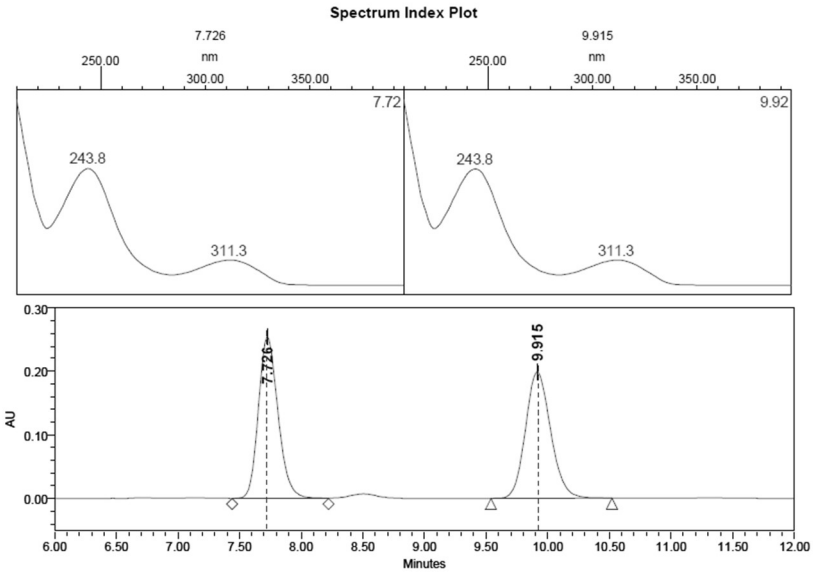

Peak Results

	RT	Area	% Area
1	7.726	2808424	50.06
2	9.915	2801894	49.94

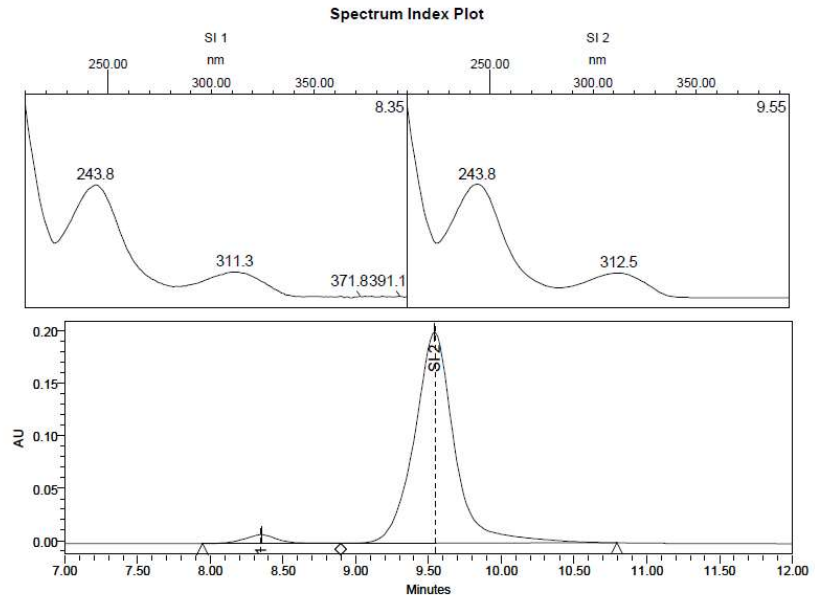

Peak Results

	Name	RT	% Area	Area	Height
1		8.348	3.25	129598	8281
2		9.541	96.75	3852378	201008

***N*-(4-methoxyphenyl)-1-(2-fluorophenyl)ethylamine (6j):** Chiralcel OD-H, 30° C, *n*-hexane/2-propanol (99:1), flow 1.0 mL/min, t_1 = 10.5 min (*R*), t_2 = 12.6 min (*S*).

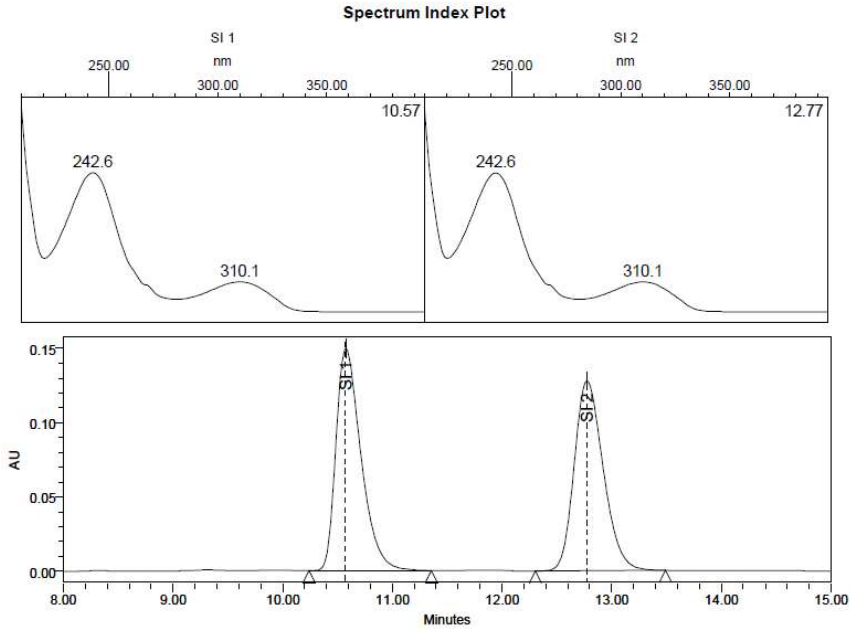

Peak Results

	Name	RT	% Area	Area	Height
1		10.576	50.18	2375250	149863
2		12.775	49.82	2358551	128047

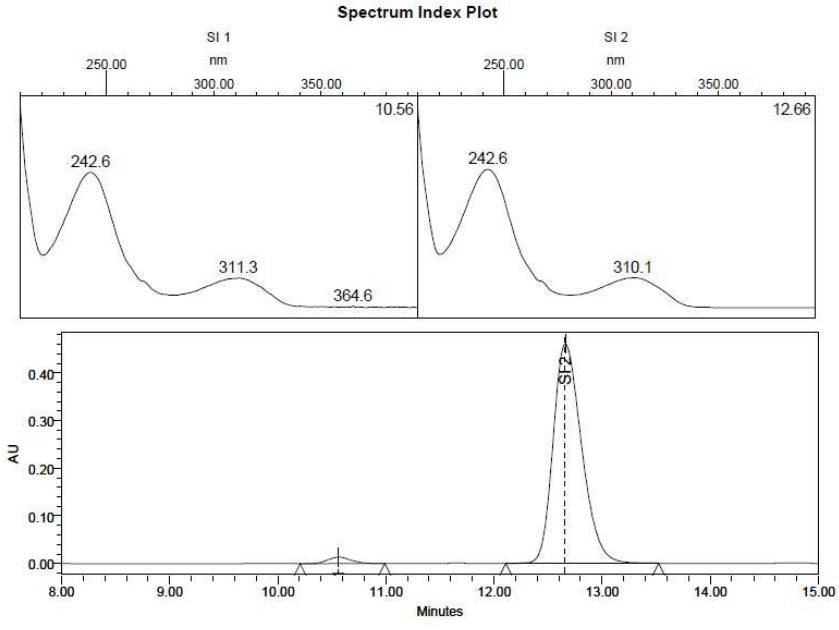

Peak Results

	Name	RT	% Area	Area	Height
1		10.562	2.30	198298	13441
2		12.660	97.70	8412955	461189

***N*-(4-methoxyphenyl)-1-(4-methylphenyl)ethylamine (6k):** Chiralcel OD-H, 30° C, *n*-hexane/2-propanol (99:1), flow 1.0 mL/min, t_1 = 11.6 min (*R*), t_2 = 13.1 min (*S*).

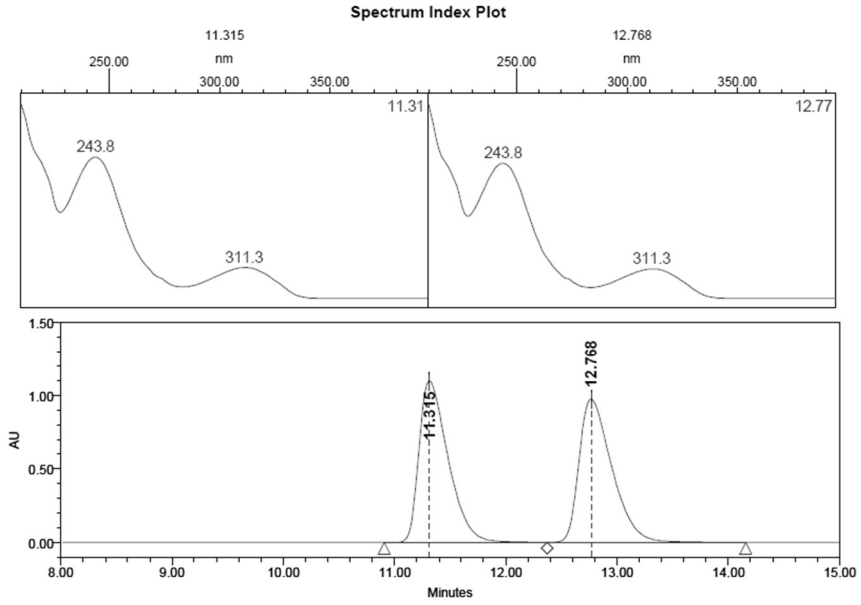

Peak Results

	RT	Area	% Area
1	11.315	19942722	49.98
2	12.768	19959419	50.02

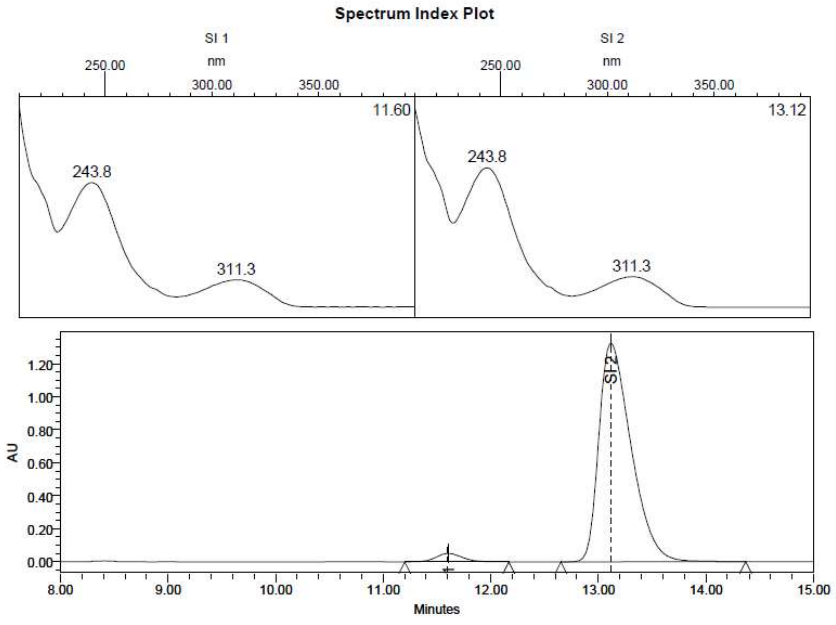

Peak Results

	Name	RT	% Area	Area	Height
1		11.605	2.98	841618	50358
2		13.117	97.02	27435467	1325196

***N*-phenyl-1-(4-chlorophenyl)ethylamine (6l):** Chiralcel OD-H, 30° C, *n*-hexane/2-propanol (99:1), flow 1.0 mL/min, t_1 = 16.5 min (*S*), t_2 = 20.6 min (*R*).

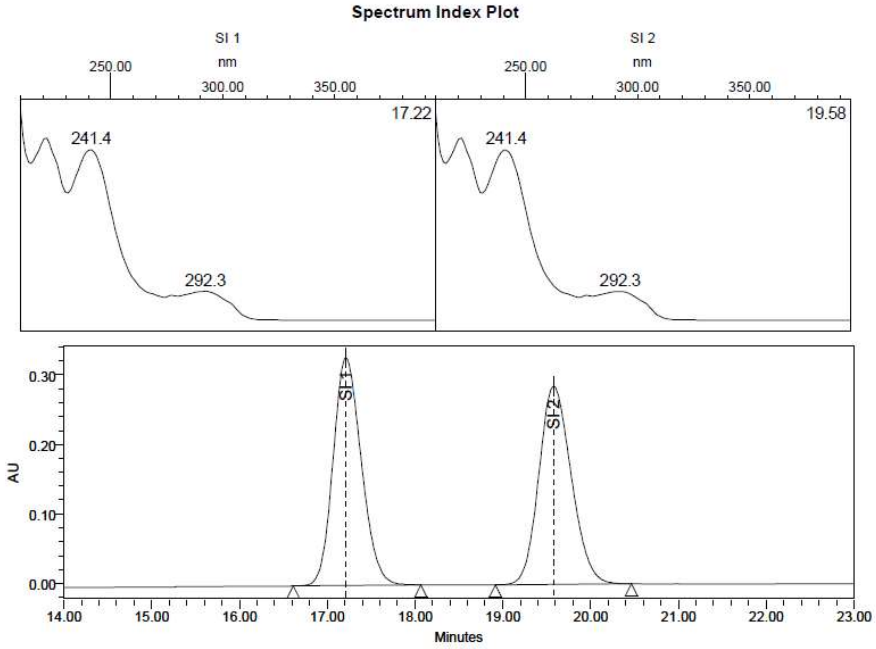

Peak Results

	Name	RT	% Area	Area	Height
1		17.213	50.03	7329124	327615
2		19.579	49.97	7321023	284960

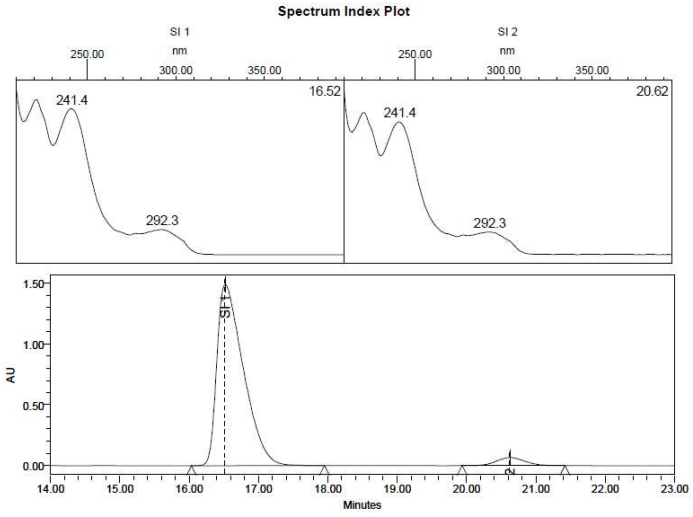

Peak Results

	Name	RT	% Area	Area	Height
1		16.524	95.47	39466190	1491298
2		20.627	4.53	1871410	66200

***N*-(4-methoxyphenyl)-1-(2-thienyl)ethylamine (6m):** Chiralcel OD-H, 30° C, *n*-hexane/2-propanol (99:1), flow 1.0 mL/min, t_1 = 17.2 min (*R*), t_2 = 19.1 min (*S*).

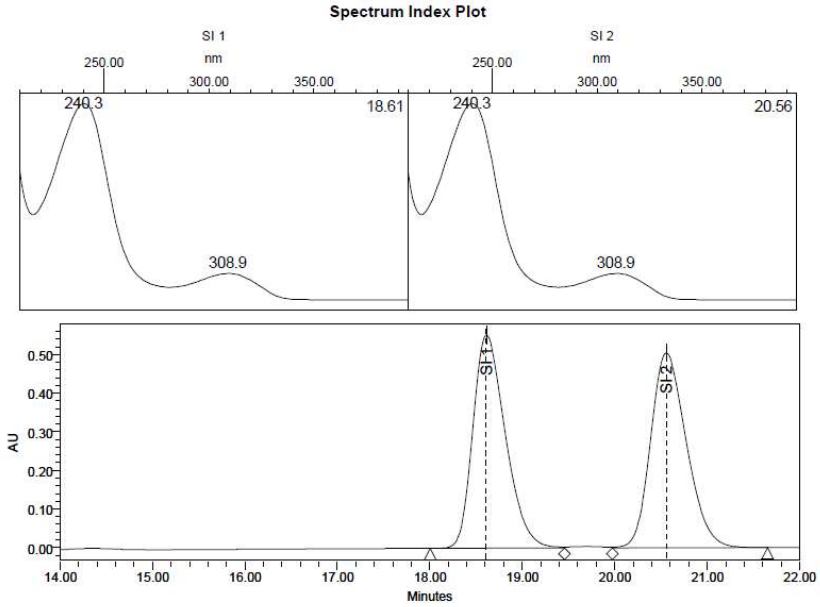

Peak Results

	Name	RT	% Area	Area	Height
1		18.612	49.87	13517055	553562
2		20.557	50.13	13589952	505770

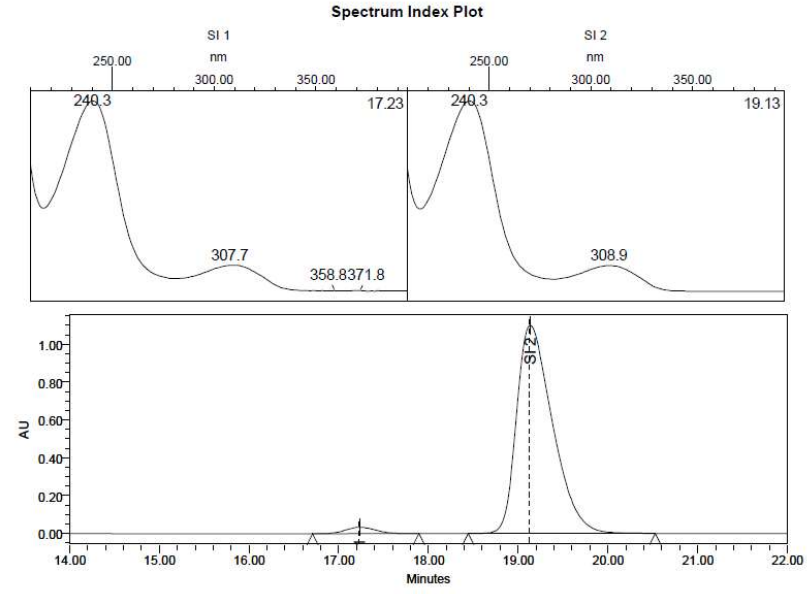

Peak Results

	Name	RT	% Area	Area	Height
1		17.233	2.43	760978	33515
2		19.134	97.57	30600116	1102306

***N*-(4-methoxyphenyl)-1-(1-naphthyl)ethylamine (6n):** Chiralcel OD-H, 30° C, *n*-hexane/2-propanol (99:1), flow 1.0 mL/min, t_1 = 22.9 min (*R*), t_2 = 31.7 min (*S*).

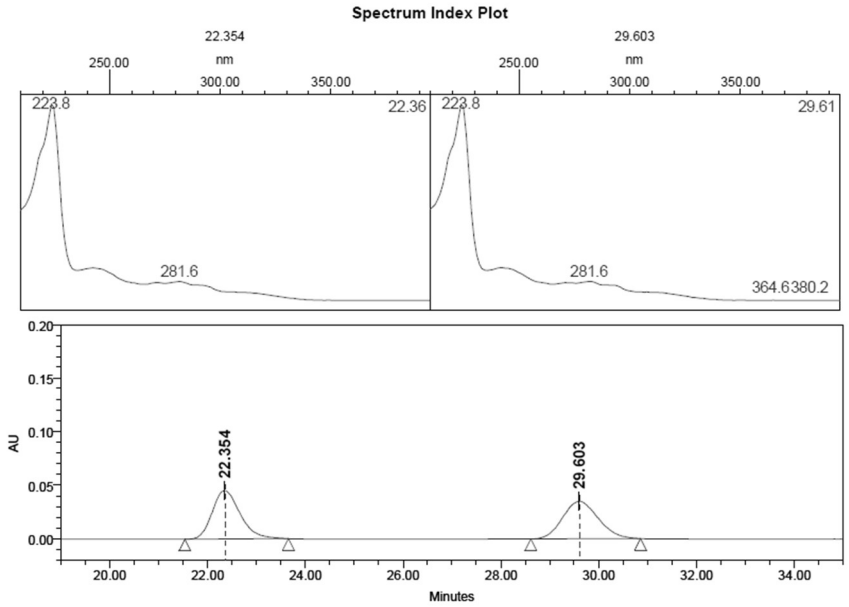

Peak Results

	RT	Area	% Area
1	22.354	1796249	50.51
2	29.603	1760014	49.49

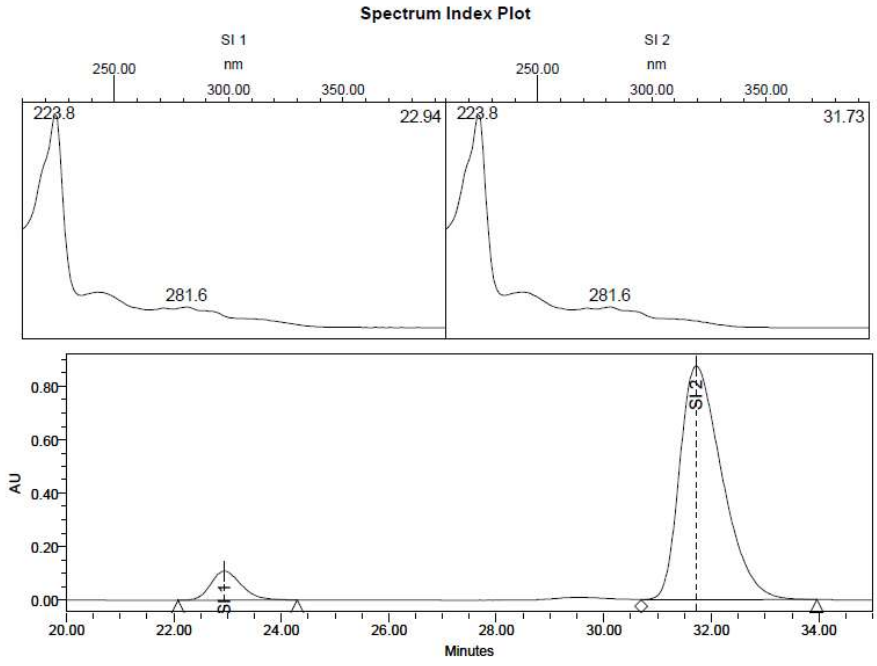

Peak Results

	Name	RT	% Area	Area	Height
1		22.939	8.14	4252422	108219
2		31.719	91.86	47983091	875500

***N*-(4-methoxyphenyl)-1-(2-naphthyl)ethylamine (6o):** Chiralcel OD-H, 30° C, *n*-hexane/2-propanol (99:1), flow 1.0 mL/min, t_1 = 23.6 min (*R*), t_2 = 28.7 min (*S*).

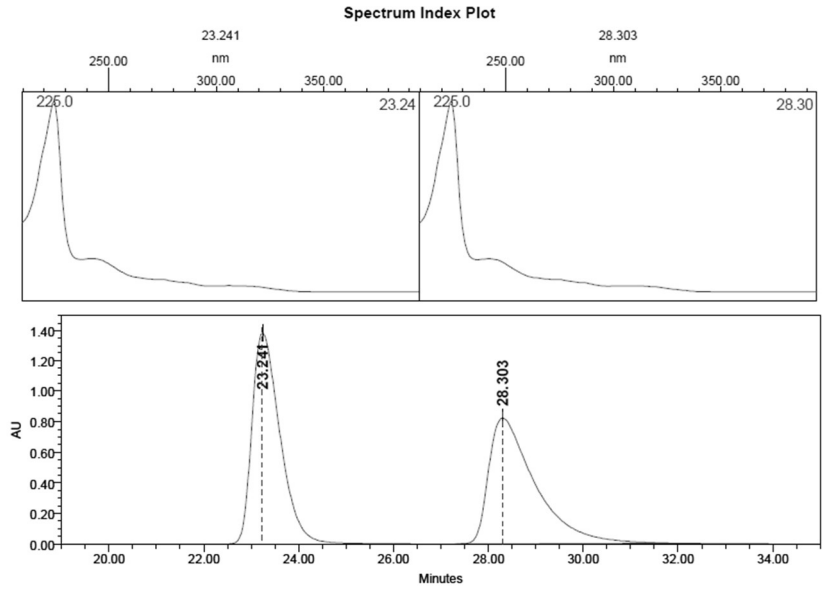

Peak Results

	RT	Area	% Area
1	23.241	56344071	50.15
2	28.303	56010524	49.85

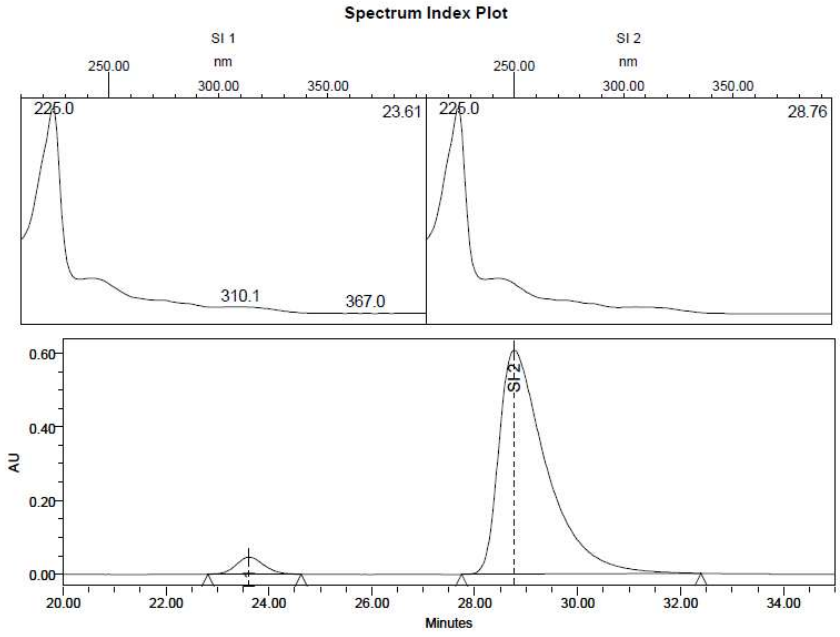

Peak Results

	Name	RT	% Area	Area	Height
1		23.615	4.20	1711960	45693
2		28.767	95.80	39010343	607798

***N*-(4-methoxyphenyl)-1-phenylpropylamine (6p):** Chiralcel OD-H, 30° C, *n*-hexane/2-propanol (99:1), flow 1.0 mL/min, t_1 = 10.7 min (*R*), t_2 = 11.0 min (*S*).

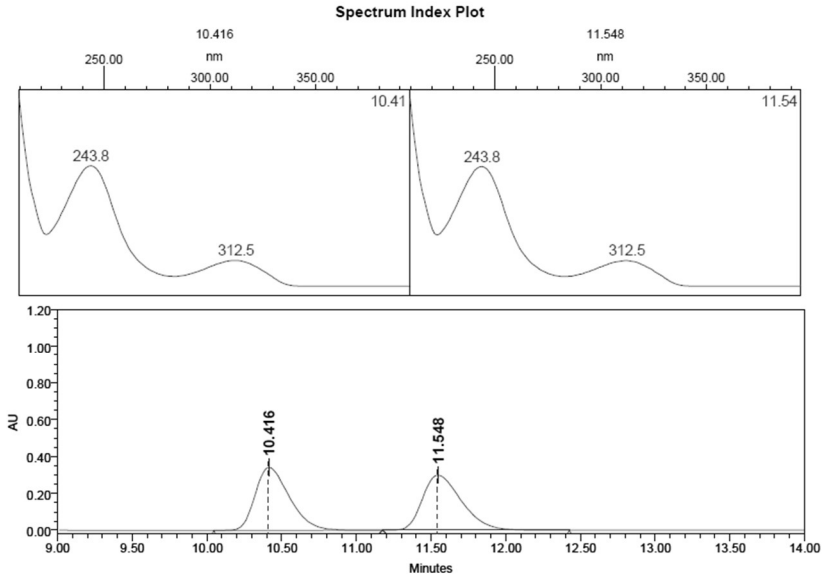

Peak Results

	RT	Area	% Area
1	10.416	5452003	49.99
2	11.548	5455051	50.01

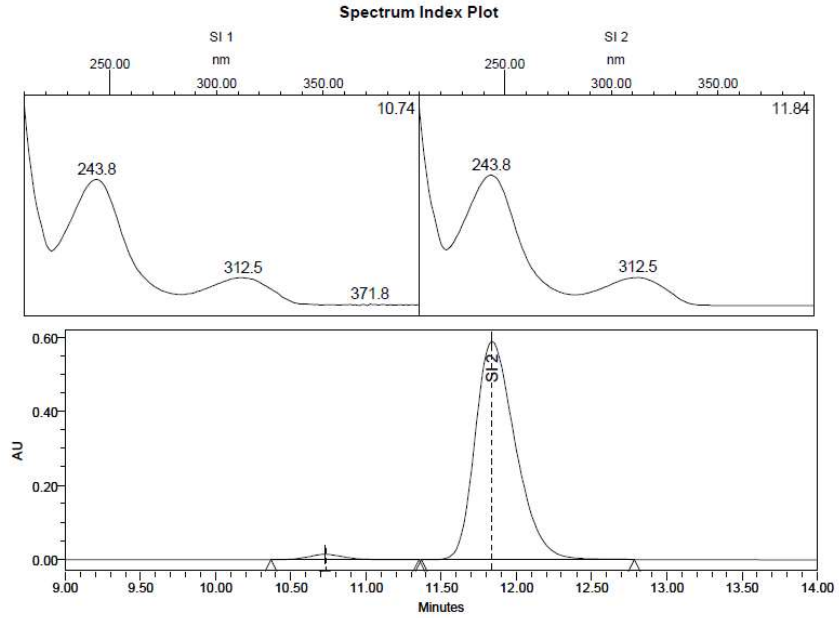

Peak Results

	Name	RT	% Area	Area	Height
1		10.728	2.01	225462	14161
2		11.838	97.99	10968665	591768